CZECH TECHNICAL UNIVERSITY IN PRAGUE

Faculty of Nuclear Science and Physical Engineering

Higgs Particle Masses in Supersymmetric Models of Electroweak Interactions

Diploma thesis

Author : Michal Malinský

Supervisor : Prof. RNDr. Jiří Hořejší, DrSc.

1998/99

I declare that I have written this work myself and used only the aforementioned literature. I agree with using this diploma thesis.

Contents

Preface

The Minimal Supersymmetric Standard Model (MSSM) provides one of the first realistic attempts to describe physics beyond the Standard Model. Although there is a huge amount of new fields and parameters in any SUSY-extended model, the MSSM reproduces all the succesful predictions of the original GWS theory with a very good accuracy. Moreover, the global $N = 1$ supersymmetry, being a new symmetry in addition to the original $SU(3)_c \otimes SU(2)_{\rm L} \otimes U(1)$ local gauge invariance, puts constraints on the Higgs sector of the model, which is rather indefinite in the nonsupersymmetric theories. In the case of MSSM this leads to the tree-level relation $m_h \leq m_Z|\cos 2\beta\,|$ which bounds the mass of the lightest Higgs scalar. For $\beta \ll \frac{\pi}{2}$ this bound would be in conflict with the present-day lower bound $m_h \geq 74.4$ GeV/c^2 arising from the LEP experiments [21]. However, radiative corrections modify the upper bound substantially.

Up to now there were many papers attempting to compute one-loop renormalised relations for the lightest Higgs boson mass (for example [4],[8],[10],[20] and many others) and also several partial two-loop results were already obtained [12].

In this work I have discussed some technical details of the relevant one-loop calculations that are not presented in current literature in sufficient detail. In particular, cancellation of ultraviolet divergences in the relation $m_h^2 + m_H^2 = m_A^2 + m_Z^2$ is demonstrated explicitly. In a similar spirit, I have shown that the one-loop radiative corrections to the MSSM neutral Goldstone boson propagator coming from the quark and superquark loops vanish, i.e. both the UV-divergent and the finite parts of the sum of corresponding one-loop graphs are zero. In the RGE approach I have generalised the schemes used by [20] and [6] for the β-function computation into an arbitrary R_ξ gauge.

The work is organized as follows: Chapter 1 contains a brief overview of the MSSM Higgs sector; with the help of the explicit form of the MSSM Higgs potential (derived in Appendix D) the Higgs spectrum is reviewed and the tree-level upper bound for the mass of the lightest Higgs scalar $m_h \leq m_Z|\cos 2\beta\,|$ is derived. Chapter 2 describes the renormalisation of the tree-level Higgs mass relation $m_h^2 + m_H^2 = m_A^2 + m_Z^2$. Chapter 3 is a supplementary part devoted to the one-loop Goldstone scalar self-energy which was not explicitly discussed in the literature yet. The problem of the lightest Higgs boson within MSSM is recalled in chapter 4 and reinvestigated using renormalisation group techniques. The rest of this work consists of four appendices containing computational details; dimensional regularisation of relevant integrals is performed in the Appendix A. Feynman rules for the MSSM Higgs sector are written down in the Appendix B. Appendix C contains a complete list of contributions of diagrams considered in chapter 2. To make this work more self-contained there is the Appendix D describing the basic MSSM structure at the end of the text. The references in the last section are nothing more than a list of *used* literature. For more comprehensive list see for example [17] or [12].

I would like to thank to my supervisor, Prof. Jiří Hořejší from the Nuclear Centre of the Charles University in Prague for his patience and encouragement throughout the writing of this work.

Michal Malinský

Notation, conventions

Constants:

g, g'	$SU(2)_L$ and $U(1)$ gauge couplings
λ	SM quartic Higgs coupling
h_f	Yukawa couplings
g_{XYZ}, g_{WXYZ}	general trilinear and quartic coupling constants
v_1, v_2	vacuum expectation values of Higgs fields
θ_W	Weinberg's (weak mixing) angle
α	MSSM Higgs sector ortogonalisation angle
β	MSSM Higgs VEVs proportionality angle
θ_t	supertop $L-R$ mixing angle
e	electric charge in units of positron charge
A_u,A_d,m_6,$m_{1\ldots3}$,μ	MSSM (soft) SUSY-breaking parameters
$M_{\rm L}$,$M_{\rm R}$,$M_{\rm U}$,$M_{\rm D}$,$M_{\rm Q}$	
f,f_1,f_2,M,M'	

Parameters:

ε, $d \equiv 4-2\varepsilon$	dimensional parameters
μ^2	regularisation parameter
ξ	gauge fixing parameter in R_ξ gauges
q, k	external and internal momenta of Feynman graphs

Fields, Superfields:

$\hat{H}_{1,2}$,$\hat{L}$,$\hat{R}$,$\hat{U}$,$\hat{D}$,$\hat{Q}$	Higgs, lepton and quark chiral superfields
$\hat{A}$,$\hat{B}$	vector superfields of gauge bosons
H,h,A,$H^\pm$,G^0,$G^\pm$	MSSM Higgs fields
t, $\tilde{t}_1$, $\tilde{t}_2$	top quark and two top squark (stop) fields
Z, $W^\pm$	$SU(2)_{\rm L} \otimes U(1)$ gauge bosons
λ^a, λ'	gauginos
F_X, D^a, D', W^α	auxiliary quantities
W	superpotential

Others:

$\mathrm{C}_{\rm UV}[.]$, $F[.]$	divergent and finite parts of considered diagrams
$\Pi_Z^{XY}(q)$, $\Pi^{\mu\nu}(q)$	self-energies, vacuum polarisation tensors
$D_\xi^{\mu\nu}(q)$	Feynman propagator of gauge bosons
T^a, $Y_{\rm W}$	isospin and weak hypercharge operators
μ, ν,...	Lorentz indices
α, $\dot{\alpha}$,...	spinorial indices
θ, $\bar{\theta}$	anticommuting superspace coordinates

We use $g^{\mu\nu} \equiv \mathrm{diag}\,(1,-1,-1,-1)$ metric tensor and the usual sumation convention. Sumation over undotted spinorial indices goes in the upper left-lower right direction. This and other conventions of 'spinor calculus' are those used in [17].

1 The Minimal Supersymmetric Standard Model

The Minimal Supersymmetric Extension of the Standard Model (also Minimal Supersymmetric Standard Model, MSSM) was formulated at the beginning of 1980s as a generalisation (and the first supersymmetric alternative) of the original GWS model of electroweak interactions. (In fact, the full Standard Model (and also the full MSSM) includes strong interactions too, but this work is devoted to the electroweak sector only.) Although the GWS theory was unprecedently succesful, there were several reasons to try to find a SUSY-improvement of it:

- There are many free parameters in the model; for example the mass of the Higgs scalar and the Higgs quartic self-coupling constant λ (one proportional to the other) remain in non-SUSY models unpredicted.

- SUSY is the first attempt to unify fermions with bosons; supersymmetry describes fermionic and bosonic fields as different components of one or several "superfields". This also seems to be very atractive from the philosophical point of view.

- Any additional symmetry improves the asymptotic behaviour of the theory; for example the quadratic ultraviolet divergences in the self-energy graphs coming from the matter loops are cancelled by the graphs involving loops of their superpartners; this mechanism is demonstrated explicitly in chapters 2 and 3.

The adjective 'minimal' in the name of MSSM means that the supersymmetrisation of the SM was done in a minimal way i.e. MSSM contains as few fields and free parameters as possible. Models that do not obey this condition are called non-minimal (NMSSM); we will not consider them because the number of new free parameters is usually not significantly compensated by any growth of their predictive power.

There are many excellent papers describing the MSSM construction, for example [4], [11], [14], [17] and others; more comprehensive list of references can be found in [17]. A brief overview of the MSSM structure is also included in Appendix D.

The main topic of this work is to reconsider some technical aspects of the Higgs sector of the MSSM (namely the mass of the lightest Higgs boson) at the one loop level of perturbation theory. First of all we look at the Higgs potential to recall the way in which the known relation $m_h \leq m_Z|\cos\beta\,|$ arises. After that we are going to derive several tree-level relations which will be useful later.

1.1 The MSSM Higgs sector and relation $m_h \leq m_Z|\cos 2\beta\,|$

As we will see in a moment the Higgs sector of the MSSM is much more complicated than in the original GWS model. There are five physical Higgs bosons (two neutral scalars h and H, one neutral pseudoscalar A and two charged scalars $H^\pm$) and three Goldstone modes (neutral pseudoscalar G^0 and two charged $G^\pm$). The main source of such a structure is the presence of *two* Higgs doublets in the theory [3]. Let us express them by means of eight real parameters:

$$H_1 = \frac{1}{\sqrt{2}}\begin{pmatrix} h_1 + ih_2 \\ h_3 + ih_4 \end{pmatrix}, \quad H_2 = \frac{1}{\sqrt{2}}\begin{pmatrix} h_5 + ih_6 \\ h_7 + ih_8 \end{pmatrix} \tag{1}$$

(The normalisation factor $(\sqrt{2})^{-1}$ is involved to ensure the correct normalisation of the kinetic terms.) Inserting (1) into the explicit expression for the Higgs potential derived at the end of Appendix D (395) we can rewrite $V_{\rm HIGGS}$ to the form

$$\begin{aligned} V_{\rm HIGGS} = & \frac{1}{2}\Big(m_1^2\sum_{i=1}^{4}h_i^2 + m_2^2\sum_{i=5}^{8}h_i^2\Big) - m_3^2\big(h_1h_7 + h_4h_6 - h_3h_5 - h_2h_8\big) + \\ & + \frac{1}{32}(g^2+g'^2)\Big(\sum_{i=1}^{4}h_i^2 - \sum_{i=5}^{8}h_i^2\Big)^2 + \frac{1}{8}g^2\big(h_1h_5 + h_2h_6 + h_3h_7 + h_4h_8\big)^2 + \\ & + \frac{1}{8}g^2\big(h_1h_6 + h_3h_8 - h_2h_5 - h_4h_7\big)^2 \end{aligned} \tag{2}$$

The asymmetric minimum is chosen so that

$$\langle H_1\rangle = \frac{1}{\sqrt{2}}\begin{pmatrix} v_1 \\ 0 \end{pmatrix}, \quad \langle H_2\rangle = \frac{1}{\sqrt{2}}\begin{pmatrix} 0 \\ v_2 \end{pmatrix} \tag{3}$$

where the quantities v_1 and v_2 are the so-called vacuum expectation values (VEVs). This particular choice of VEVs ensures the correct spontaneous symmetry breaking pattern, i.e. there are three broken generators of $SU(2)_{\rm L}\otimes U(1)$ corresponding to three massive vector bosons $Z, W^{\pm}$ and the charge $U(1)_{\rm Q}$ remains unbroken so the related gauge boson (photon) is massless. (Note that only the neutral components of doublets received VEVs; all the necessary quantum numbers are written in the Table 1. on page 68.) In this minimalisation point the potential fulfills the following relations

$$\left.\frac{\partial V_{\rm HIGGS}}{\partial h_1}\right|_{min} = m_1^2v_1 - m_3^2v_2 + \frac{1}{8}(g^2+g'^2)(v_1^2-v_2^2)v_1 = 0 \tag{4}$$

$$\left.\frac{\partial V_{\rm HIGGS}}{\partial h_7}\right|_{min} = m_2^2v_2 - m_3^2v_1 - \frac{1}{8}(g^2+g'^2)(v_1^2-v_2^2)v_2 = 0 \tag{5}$$

which will be useful later. Next, it is convenient to define a new parameter β

$$\tan\beta \equiv \frac{v_2}{v_1} \qquad \beta\in\Big[0,\frac{\pi}{2}\Big) \tag{6}$$

We are now ready to compute the corresponding Higgs sector mass-squared matrix M^2:

$$M_{ij}^2 \equiv \left.\frac{\partial^2 V_{\rm HIGGS}}{\partial h_i\partial h_j}\right|_{min} \tag{7}$$

It is huge but the computation is not too hard because of a simple structure of (3):

$$M^2 = \begin{pmatrix} M_{11} & 0 & 0 & 0 & 0 & 0 & M_{17} & 0 \\ 0 & M_{22} & 0 & 0 & 0 & 0 & 0 & M_{28} \\ 0 & 0 & M_{33} & 0 & M_{35} & 0 & 0 & 0 \\ 0 & 0 & 0 & M_{44} & 0 & M_{46} & 0 & 0 \\ 0 & 0 & M_{53} & 0 & M_{55} & 0 & 0 & 0 \\ 0 & 0 & 0 & M_{64} & 0 & M_{66} & 0 & 0 \\ M_{71} & 0 & 0 & 0 & 0 & 0 & M_{77} & 0 \\ 0 & M_{82} & 0 & 0 & 0 & 0 & 0 & M_{88} \end{pmatrix} \tag{8}$$

Due to the polynomial character of $V_{\rm HIGGS}$ this matrix is symmetric and its nonzero entries have the following form:

$$M_{11} \equiv m_1^2 + \frac{1}{8}(g^2+g'^2)(3v_1^2-v_2^2) \qquad M_{17} \equiv -m_3^2 - \frac{1}{4}(g^2+g'^2)v_1v_2$$

$$
\begin{aligned}
M_{22} &\equiv m_1^2 + \frac{1}{8}(g^2+g'^2)(v_1^2-v_2^2) & M_{28} &\equiv m_3^2 \\
M_{33} &\equiv m_1^2 + \frac{1}{8}g^2(v_1^2+v_2^2) + \frac{1}{8}g'^2(v_1^2-v_2^2) & M_{35} &\equiv m_3^2 + \frac{1}{4}g^2 v_1 v_2 \\
M_{44} &\equiv m_1^2 + \frac{1}{8}g^2(v_1^2+v_2^2) + \frac{1}{8}g'^2(v_1^2-v_2^2) & M_{46} &\equiv -m_3^2 - \frac{1}{4}g^2 v_1 v_2 \\
M_{55} &\equiv m_2^2 + \frac{1}{8}g^2(v_1^2+v_2^2) + \frac{1}{8}g'^2(v_1^2-v_2^2) & M_{77} &\equiv m_2^2 - \frac{1}{8}(g^2+g'^2)(v_1^2-3v_2^2) \\
M_{66} &\equiv m_2^2 + \frac{1}{8}g^2(v_1^2+v_2^2) + \frac{1}{8}g'^2(v_1^2-v_2^2) & M_{88} &\equiv m_2^2 - \frac{1}{8}(g^2+g'^2)(v_1^2-v_2^2)
\end{aligned}
\qquad (9)
$$

The mass-squared matrix (8) looks a little bit better in a specially reordered basis $H \equiv (h_1, h_7, h_2, h_8, h_3, h_5, h_4, h_6)$ because it is then block-diagonal:

$$
(M^2)_H = \begin{pmatrix} M_A^2 & 0 & 0 & 0 \\ 0 & M_B^2 & 0 & 0 \\ 0 & 0 & M_C^2 & 0 \\ 0 & 0 & 0 & M_D^2 \end{pmatrix} \qquad (10)
$$

with

$$
M_A^2 \equiv \begin{pmatrix} M_{11} & M_{17} \\ M_{71} & M_{77} \end{pmatrix} \qquad M_B^2 \equiv \begin{pmatrix} M_{22} & M_{28} \\ M_{82} & M_{88} \end{pmatrix}
$$
$$
M_C^2 \equiv \begin{pmatrix} M_{33} & M_{35} \\ M_{53} & M_{55} \end{pmatrix} \qquad M_D^2 \equiv \begin{pmatrix} M_{44} & M_{46} \\ M_{64} & M_{66} \end{pmatrix} \qquad (11)
$$

Diagonalisation of matrix (10) is then equivalent to the simultaneous diagonalisation of four 2×2 matrices $M_A^2 \ldots M_D^2$. Note that matrices M_A^2 and M_B^2 describe masses of neutral physical states because they operate in spaces of the neutral components h_1,h_2,h_7 and h_8 while M_C^2 and M_D^2 correspond to the charged sector.

In this work we will not deal with the charged Higgs or Goldstone fields so in the following text we aim on the M_A^2 and M_B^2 only. Let us start with the neutral pseudoscalar sector, i.e. with M_B^2.

I. Neutral pseudoscalar sector: Let us rewrite M_B^2 explicitly. Using (4),(5) and (9) we obtain

$$
M_B^2 = \frac{m_3^2}{v_1 v_2} \begin{pmatrix} v_2^2 & v_1 v_2 \\ v_1 v_2 & v_1^2 \end{pmatrix} \qquad (12)
$$

This matrix is singular ($\det M_B^2 = 0$) and has two eigenvalues:

$$
m_{G^0}^2 = 0 \qquad \text{and} \qquad m_A^2 = \frac{m_3^2}{v_1 v_2}(v_1^2 + v_2^2) \qquad (13)
$$

The notation should be self-explanatory: G^0 is the neutral Goldstone pseudoscalar and A is the usual name of the (only) massive neutral MSSM pseudoscalar.

II. Neutral scalar sector: Let us again first write down the M_A^2 matrix. With the help of (4),(5) and (9) we get

$$
M_A^2 = \begin{pmatrix} m_3^2 v_2 v_1^{-1} + \frac{1}{4}(g^2+g'^2)v_1^2 & -m_3^2 - \frac{1}{4}(g^2+g'^2)v_1 v_2 \\ -m_3^2 - \frac{1}{4}(g^2+g'^2)v_1 v_2 & m_3^2 v_1 v_2^{-1} + \frac{1}{4}(g^2+g'^2)v_2^2 \end{pmatrix} \equiv \begin{pmatrix} A & B \\ B & C \end{pmatrix} \qquad (14)
$$

The eigenvalues $\lambda_{1,2}$ of this matrix, which are identified with squared masses of the corresponding particles, are solutions of the characteristic equation $\det(M_B^2 - \lambda) = 0$:

$$\lambda_{1,2} = \frac{1}{2}\left[A + C \pm \sqrt{(A+C)^2 - 4(AC - B^2)}\right] \tag{15}$$

Having the eigenvalues we can easily get the associated eigenvectors $x_{1,2}$; for $B \neq 0$ they are

$$x_{1,2} = N_{1,2}\begin{pmatrix} 1 \\ (2B)^{-1}\left[-(A-C) \pm \sqrt{(A-C)^2 + 4B^2}\right] \end{pmatrix} \tag{16}$$

Here $N_{1,2}$ are some (unimportant) normalisation constants. From this we can obtain the mixing angle α defined as an angle between vectors $(1,0)$ and x_1 (counterclockwise), i.e. the following relation holds

$$\tan\alpha = \frac{-(A-C) \pm \sqrt{(A-C)^2 + 4B^2}}{2B} \tag{17}$$

To evaluate the eigenvalues (15), note first that

$$A + C = \left[\frac{m_3^2}{v_1 v_2} + \frac{1}{4}(g^2 + g'^2)\right](v_1^2 + v_2^2) = m_A^2 + m_Z^2 \tag{18}$$

Here we have used (13) and $m_Z^2 = \frac{1}{4}(g^2 + g'^2)(v_1^2 + v_2^2)$ (which is the MSSM equivalent of the known GWS relation). Similarly (14) implies

$$AC - B^2 = \left[\frac{1}{4}\left(g^2 + g'^2\right)\left(v_1^2 + v_2^2\right)\right]\left[\frac{m_3^2}{v_1 v_2}\left(v_1^2 + v_2^2\right)\right]\left(\frac{v_1^2 - v_2^2}{v_1^2 + v_2^2}\right)^2 \tag{19}$$

The terms in square brackets again correspond to the masses m_A^2 and m_Z^2. The remaining part can be recast in a more compact form using (6). Then

$$AC - B^2 = m_A^2 m_Z^2 \cos^2 2\beta \tag{20}$$

Inserting now (18) and (20) into (15) we get the masses of the Higgs scalars h (corresponding to the minus sign in (15) and therefore lighter) and H:

$$m_{H,h}^2 = \frac{1}{2}\left[m_A^2 + m_Z^2 \pm \sqrt{(m_A^2 + m_Z^2)^2 - 4m_A^2 m_Z^2 \cos^2 2\beta}\right] \tag{21}$$

The mass of h is bounded; we can see it from its first derivative with respect to m_A^2:

$$\frac{\partial m_h^2}{\partial m_A^2} = \frac{1}{2}\left\{1 - \frac{m_A^2 + m_Z^2 - 2m_Z^2 \cos^2 2\beta}{\left[(m_A^2 + m_Z^2)^2 - 4m_A^2 m_Z^2 \cos^2 2\beta\right]^{\frac{1}{2}}}\right\} \tag{22}$$

which is still positive, i.e. m_h^2 grows with m_A^2 growing. The upper bound is then

$$\lim_{m_A^2 \to \infty} \frac{1}{2}\left[m_A^2 + m_Z^2 \pm \sqrt{(m_A^2 + m_Z^2)^2 - 4m_A^2 m_Z^2 \cos^2 2\beta}\right] = m_Z^2 \cos^2 2\beta \tag{23}$$

This means that the tree-level mass of the lightest Higgs scalar h is smaller than the mass of the Z boson.

$$m_h \leq m_Z |\cos 2\beta| \tag{24}$$

At first sight this prediction would be problematic if there is no experimental evidence of any Higgs state bellow the weak scale ≈ 90 GeV. (Note that recent measurements give the lower bound to the mass of the lightest MSSM Higgs at the level 74.4 GeV/c^2, see [21].) But it would not exclude the MSSM from the game because this relation provides only a tree-level prediction which can (and really does) receive large corrections from the higher orders of perturbation theory. This will be shown in detail in this work:

- In the first part (chapters 2 and 3) we perform a direct diagrammatic computation of the one-loop correction to the tree-level relation

$$m_h^2 + m_H^2 = m_A^2 + m_Z^2 \tag{25}$$

  (this is a consequence of (21)) which will allow us to see that the Higgs scalar sector receives a large contribution of order $\frac{m_t^4}{m_Z^2}$ where m_t denotes the top-quark mass.

- In the second part, the mass of the lightest Higgs boson h is calculated indirectly using the renormalisation group method (chapter 4).

To be able to perform the first step of this program we will need to derive one additional relation among the Higgs sector parameters, which has not been given explicitly in the literature. Using (17), we can state

$$\sin 2\alpha = \frac{2B}{\sqrt{(A-C)^2 + 4B^2}} = \left(\frac{m_h^2 + m_H^2}{m_h^2 - m_H^2}\right) \sin 2\beta \tag{26}$$

$$\cos 2\alpha = \frac{A-C}{\sqrt{(A-C)^2 + 4B^2}} = \left(\frac{m_A^2 - m_Z^2}{m_h^2 - m_H^2}\right) \cos 2\beta \tag{27}$$

Here we have utilised definitions (6) and (14). Now, the previous relations together with (25) imply

$$\frac{1}{2}\left[\left(m_h^2 + m_H^2 - m_A^2 - m_Z^2\right) + \left(m_h^2 - m_H^2\right)\cos 2\alpha - \left(m_A^2 - m_Z^2\right)\cos 2\beta\right] = 0 \tag{28}$$

Simplifying the left-hand side we obtain

$$m_h^2 \cos^2\alpha + m_H^2 \sin^2\alpha - m_A^2 \cos^2\beta - m_Z^2 \sin^2\beta = 0 \tag{29}$$

This relation will be very handy later on.

2 Renormalisation of the Higgs boson masses

In this section we perform a partial one-loop renormalisation of the tree-level relation

$$m_h^2 + m_H^2 - m_A^2 - m_Z^2 = 0 \tag{30}$$

The word 'partial' should express the fact, that we do not consider all the possible one-loop graphs but only a special subset of them: graphs involving one top quark and top squark (supertop) loop. There are several reasons for doing this:

- There are no significant contributions from the gaugino-higgsino and IVB sectors of the MSSM (see for example [8])
- Contributions coming from the matter-fields turns out to be proportional to the mass of corresponding fermion and the heaviest known fermionic field is the top quark

2.1 Definition of renormalization parameters

The main part of the following computation will be performed in the unitary gauge; this particular choice reduces the number of diagrams to be considered and simplifies the renormalisation scheme. The only disadvantage of this is the fact that the computation scheme is a little bit more complicated than for example in R_ξ gauges (see [4]), because no cancellation within the tadpole sector occurs. The diagrams to be computed are listed and regularised in Appendix A. (There are also several graphs including the neutral Goldstone pseudoscalar G which will be useful mainly in the next section.) Let us now start with definitions of renormalization constants.

I. Renormalized (pseudo)scalar masses:
The renormalized masses $m_X$of (pseudo)scalars h,H and A are defined genericly by

$$(1 + \delta Z_X)\, m_{XB}^2 = m_X^2 + \delta m_X^2 \tag{31}$$

where the renormalisation constants (coming from the counterterm Lagrangian) correspond to the counter-graph

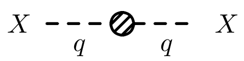

$$\sim \qquad i\left(\delta Z_X q^2 - \delta m_X^2\right) \tag{32}$$

Next, let us denote the sum of all (relevant) OPI graphs by $-i\Pi_X(q) = \sum -i\Pi_X^Y(q)$. Then the two-point OPI Green functions can be written in the form

$$i\Gamma_X^{(2)}(q,-q) = q^2 - m_X^2 - i\Pi_X(q) + i\left(\delta Z_X q^2 - \delta m_X^2\right) + \text{higher order} \tag{33}$$

We adopt the so-called *on-shell* renormalisation scheme in which all the external momenta (q's) are evaluated on the mass-shell i.e. $q^2 = m_X^2$ where m_X^2 denotes the square of the mass of the considered particle. In this scheme we use the following renormalisation conditions

$$\Gamma_X^{(2)}(q,-q) = 0 \quad , \qquad \frac{\partial \Gamma_X^{(2)}}{\partial q^2}(q,-q) = 1 \qquad \text{at} \quad q^2 = m_X^2 \tag{34}$$

This particular choice implies

$$\delta Z_X = 0 + \text{higher order}\,; \qquad \delta m_X^2 = -\Pi_X\left(q^2 = m_X^2\right) + \text{higher order} \tag{35}$$

The physical mass m_X can then be expressed (using (31) and (35)) as

$$m_X^2 = m_{BX}^2 + \Pi_X(q^2 = m_X^2) + \text{higher order} \tag{36}$$

II. Renormalized Z-boson mass:
Let us denote the sum of all the (Z) 'vacuum polarisation graphs' by $-i\Pi_Z^{\mu\nu}(q)$. This quantity renormalizes the Z-boson mass to a new value (see [16],[2])

$$m_Z^2 = m_{ZB}^2 - A_Z(q^2 = m_Z^2) + \text{higher order} \tag{37}$$

(we have again used the on-shell conditions) where $A_Z(q^2)$ is defined by

$$\Pi_Z^{\mu\nu}(q^2) \equiv A_Z(q^2)g^{\mu\nu} + B_Z(q^2)q^\mu q^\nu$$

(i.e. corresponds to the coefficient of the transverse part of $\Pi_Z^{\mu\nu}$). Having defined renormalised quantities we can recast the relation (30) in the renormalised form

$$m_h^2 + m_H^2 - m_A^2 - m_Z^2 = \Delta + \text{higher order} \tag{38}$$

where

$$\Delta \equiv \Pi_h(q^2 = m_h^2) + \Pi_H(q^2 = m_H^2) - \Pi_A(q^2 = m_A^2) + A_Z(q^2 = m_Z^2) \tag{39}$$

This is the main relation of this section. In the following section we are going to evaluate Π_h, Π_H, Π_A and A_Z in the one-loop approximation.

2.2 Compensation of ultraviolet divergences

The topic of this subsection is to show the explicit total compensation of UV divergences in renormalisation of the tree-level relation $m_h^2 + m_H^2 = m_A^2 + m_Z^2$. The only quantities that we are going to work with now are the ultraviolet divergent parts of the graphs evaluated in Appendix C. We will denote them $\mathrm{C_{UV}}[\Pi_C^{AB}]$. (The sub- and superscripts have the same (and perhaps intuitive) meaning as in the Appendix.)

The whole calculation is performed in the unitary gauge which causes absence of the Goldstone boson in the theory. (Renormalisation of the MSSM Higgs sector with unphysical Goldstone bosons in other gauges can be found for instance in [4].) There will be a special section devoted to the neutral MSSM Goldstone boson in the next chapter. A summation over the quark colours is omitted because it contributes only by an overall factor $N_c = 3$ which is not important now but will be necessary later to obtain the correct expression for the finite part.

2.2.1 UV divergences in graphs involving t-loops

Let us start with the divergences descending from the graphs involving one top-quark loop. At the beginning we use results (283), (285) and (287) to compute the total contribution of the first three graphs of the subgroup (C.1):

$$\mathrm{C_{UV}}[\Pi_h^{tt}] + \mathrm{C_{UV}}[\Pi_H^{tt}] - \mathrm{C_{UV}}[\Pi_A^{tt}] = \frac{g^2 m_t^2}{16\pi^2 m_W^2 \sin^2\beta} \times \tag{40}$$

$$\times \left[\cos^2\alpha \left(3m_t^2 - \frac{m_h^2}{2}\right) + \sin^2\alpha \left(3m_t^2 - \frac{m_H^2}{2}\right) + \cos^2\beta \left(-m_t^2 + \frac{m_A^2}{2}\right)\right] =$$

$$= \frac{g^2 m_t^2}{16\pi^2 m_W^2 \sin^2\beta} \left[3m_t^2 - m_t^2\cos^2\beta + \frac{1}{2}\left(-m_h^2\cos^2\alpha - m_H^2\sin^2\alpha + m_A^2\cos^2\beta\right)\right]$$

Next, the tadpoles (298) and (302) give

$$-\mathrm{C}_{\mathrm{UV}}[\Pi_A^{ht}] - \mathrm{C}_{\mathrm{UV}}[\Pi_A^{Ht}] = -\frac{g^2 m_t^4}{16\pi^2 m_W^2} \tag{41}$$

This term together with the factor proportional to $m_t^2\cos^2\beta$ in (40) partially compensates the factor $3m_t^2$ above.

Let us now write down the divergence coming from the graph (288), which will allow us to compensate another part of (40):

$$\mathrm{C}_{\mathrm{UV}}[A_Z^{tt}] = \frac{g^2 m_Z^2}{16\pi^2 m_W^2}\left[-\frac{m_t^2}{2} + \frac{2}{3} m_Z^2 (X^2+Y^2)\right] =$$

$$= -\frac{g^2 m_t^2 m_Z^2}{32\pi^2 m_W^2} + \frac{g^2 m_Z^4}{24\pi^2 m_W^2}(X^2+Y^2) \tag{42}$$

Now we collect the three parts (40), (41) and (42) and obtain the total divergence from the graphs involving one top-quark loop:

$$\mathbf{C_t} \equiv \mathrm{C}_{\mathrm{UV}}[\Pi_h^{tt}] + \mathrm{C}_{\mathrm{UV}}[\Pi_H^{tt}] - \mathrm{C}_{\mathrm{UV}}[\Pi_A^{tt}] - \mathrm{C}_{\mathrm{UV}}[\Pi_A^{ht}] - \mathrm{C}_{\mathrm{UV}}[\Pi_A^{Ht}] + \mathrm{C}_{\mathrm{UV}}[A_Z^{tt}] =$$

$$= \frac{g^2 m_t^4}{8\pi^2 m_W^2 \sin^2\beta} - \frac{g^2 m_t^2 m_Z^2}{16\pi^2 m_W^2} + \frac{g^2 m_Z^4}{24\pi^2 m_W^2}(X^2+Y^2) \tag{43}$$

Here ve have used the previously derived relation (29).

2.2.2 UV divergences in graphs with one s-top loop

The amount of graphs to be covered in this subsection is much larger than in the previous part and also the computations are longer so we will divide this subsection into several paragraphs corresponding to the hierarchy of the Appendix (C.2).

I. Graphs dependent on external momenta involving h, H and A

The main property of the contributions investigated in (C.2) is the fact that the total divergence coming from the graphs (310) - (322) is the sum of squares of the couplings

$$\begin{aligned} {}^{(1)} \quad &\equiv \mathrm{C}_{\mathrm{UV}}[\Pi_h^{\tilde t_1\tilde t_1}] + \mathrm{C}_{\mathrm{UV}}[\Pi_h^{\tilde t_2\tilde t_2}] + \mathrm{C}_{\mathrm{UV}}[\Pi_h^{\tilde t_1\tilde t_2}] + \\ &+ \mathrm{C}_{\mathrm{UV}}[\Pi_H^{\tilde t_1\tilde t_1}] + \mathrm{C}_{\mathrm{UV}}[\Pi_H^{\tilde t_2\tilde t_2}] + \mathrm{C}_{\mathrm{UV}}[\Pi_H^{\tilde t_2\tilde t_2}] - \mathrm{C}_{\mathrm{UV}}[\Pi_A^{\tilde t_1\tilde t_2}] = \\ &= \frac{1}{16\pi^2}\left(g^2_{h\tilde t_1\tilde t_1} + g^2_{h\tilde t_2\tilde t_2} + 2g^2_{h\tilde t_1\tilde t_2} + g^2_{H\tilde t_1\tilde t_1} + g^2_{H\tilde t_2\tilde t_2} + 2g^2_{H\tilde t_2\tilde t_2} + 2g^2_{A\tilde t_1\tilde t_2}\right) \end{aligned} \tag{44}$$

(Note that the + sign of the $g^2_{A\tilde t_1\tilde t_2}$ factor comes from antisymmetry of the vertex.) Although the structure of the couplings above is very complicated, the final result is not so ugly; we are going to discuss it by parts:

I.a. Terms proportional to m_t^4: Such terms come only from the squares of $g_{h\tilde t_1\tilde t_1}$,$g_{h\tilde t_2\tilde t_2}$,$g_{H\tilde t_1\tilde t_1}$ and $g_{H\tilde t_2\tilde t_2}$ and it is trivial to sum them up with the result

$$-\frac{g^2 m_t^4}{8\pi^2 m_W^2 \sin^2\beta} \tag{45}$$

I.b. Terms containing squares of $A_t m_6$ and μ: Here we have to sum up contributions from all the couplings above with the result:

$$\frac{g^2 m_t^2}{32\pi^2 m_W^2 \sin^2\beta}[-(A_t m_6 \cos\alpha - \mu \sin\alpha)^2 - (A_t m_6 \sin\alpha + \mu\cos\alpha)^2 + +(A_t m_6 \cos\beta - \mu\sin\beta)^2] = -\frac{g^2 m_t^2}{32\pi^2 m_W^2 \sin^2\beta}(A_t m_6 \sin\beta + \mu\cos\beta)^2 \quad (46)$$

(Performing our computation in R_ξ-gauges we would obtain zero because of presence of the Goldstone boson contribution.)

I.c. Terms containing squares of X and Y: The contributions of this type arise again from the first six terms only. The result has the form

$$-\frac{g^2 m_Z^2}{16\pi^2 \cos^2\theta_W}[(X\cos^2\theta_t + Y\sin^2\theta_t)^2 + (X\sin^2\theta_t + Y\cos^2\theta_t)^2 + +2(-X\sin^2\theta_t \cos^2\theta_t + Y\cos^2\theta_t \sin^2\theta_t)^2] = -\frac{g^2 m_Z^2}{16\pi^2\cos^2\theta_W}(X^2 + Y^2) \quad (47)$$

I.d. Mixed terms proportional to $m_t m_Z$: These terms are combinations of the first and third parts of the couplings (238)-(245). Fortunately they cancel one another; for example the part proportional to $(A_t m_6 \cos\alpha - \mu\sin\alpha)$ (coming from the couplings including h only):

$$\frac{g^2 m_t m_Z^2}{16\pi^2 m_W^2 \sin\beta}(A_t m_6 \cos\alpha - \mu\sin\alpha)\sin(\alpha+\beta)\times \times\left[\sin 2\theta_t (X\cos^2\theta_t + Y\sin^2\theta_t - X\sin^2\theta_t - Y\cos^2\theta_t) + +2\cos 2\theta_t(-X\sin\theta_t\cos\theta_t + Y\sin\theta_t\cos\theta_t)\right] = 0 \quad (48)$$

In a similar way we can show the same property of the terms involving $(A_t m_6 \sin\alpha + \mu\cos\alpha)$ coming from the graphs with H.

I.e. Mixed terms proportional to $\frac{m_t^3}{m_Z}$: These terms give zero because of the structure of couplings (238)-(243).

I.f. Mixed terms proportional to m_t^2: The total contribution is a mixture of the first and second terms of couplings (238)-(243)

$$\frac{g^2 m_t^2 m_Z}{8\pi^2 m_W \cos\theta_t \sin\beta}\{(X+Y)[\cos\alpha\sin(\alpha+\beta) - \sin\alpha\cos(\alpha+\beta)]\} = \frac{g^2 m_t^2 m_Z^2}{16\pi^2 m_W^2} \quad (49)$$

Here we have used relations $X + Y = \frac{1}{2}$ and $m_W = m_Z \cos\theta_W$.

Now we are ready to collect all the partial results (45),(46),(47) and (49) to write down the total divergence

$$\mathbf{C_{st}}^{(1)} = -\frac{g^2 m_t^4}{8\pi^2 m_W^2 \sin^2\beta} - \frac{g^2 m_t^2}{32\pi^2 m_W^2 \sin^2\beta}(A_t m_6 \sin\beta + \mu\cos\beta)^2 + +\frac{g^2 m_t^2 m_Z^2}{16\pi^2 m_W^2} - \frac{g^2 m_Z^4}{16\pi^2 m_W^2}(X^2 + Y^2) \quad (50)$$

II. Self energy graphs dependent on external momenta for Z-boson: There are three such graphs in the Appendix C - (327), (329) and (331). The divergent part of their total contribution is

$$\mathbf{C_{st}}^{(2)} \equiv \mathrm{C_{UV}}[A_Z^{\tilde{t}_1\tilde{t}_1}] + \mathrm{C_{UV}}[A_Z^{\tilde{t}_2\tilde{t}_2}] + \mathrm{C_{UV}}[A_Z^{\tilde{t}_1\tilde{t}_2}] = \tag{51}$$

$$\frac{g^2 m_Z^4}{48\pi^2 m_W^2}\Big[\left(-X\cos^2\theta_t\ + Y\sin^2\theta_t\,\right)^2 + \left(-X\sin^2\theta_t\ + Y\cos^2\theta_t\,\right)^2 +$$

$$+2\left(X\sin\theta_t\cos\theta_t\ + Y\sin\theta_t\cos\theta_t\,\right)^2\Big] -$$

$$-\frac{g^2 m_Z^2 m_{\tilde{t}_1}^2}{8\pi^2 m_W^2}[\left(-X\cos^2\theta_t\ + Y\sin^2\theta_t\,\right)^2 + \left(X\sin\theta_t\cos\theta_t\ + Y\sin\theta_t\cos\theta_t\,\right)^2]-$$

$$-\frac{g^2 m_Z^2 m_{\tilde{t}_2}^2}{8\pi^2 m_W^2}[\left(-X\sin^2\theta_t\ + Y\cos^2\theta_t\,\right)^2 + \left(X\sin\theta_t\cos\theta_t\ + Y\sin\theta_t\cos\theta_t\,\right)^2]$$

which can be easily simplified to the form

$$\mathbf{C_{st}}^{(2)} = \frac{g^2 m_Z^4}{48\pi^2 m_W^2}(X^2+Y^2) - \tag{52}$$

$$-\frac{g^2 m_Z^2}{8\pi^2 m_W^2}[m_{\tilde{t}_1}^2\left(X^2\cos^2\theta_t\ + Y^2\sin^2\theta_t\,\right) + m_{\tilde{t}_2}^2\left(X^2\sin^2\theta_t\ + Y^2\cos^2\theta_t\,\right)]$$

III. UV divergences in tadpole graphs involving super-tops:
Performing our computation in the unitary gauge we have to involve four tadpole graphs (332)-(338). The sum of divergent parts of these graphs will be denoted by $\mathbf{C_{st}}^{(3)}$ i.e.

$$\mathbf{C_{st}}^{(3)} = -\mathrm{C_{UV}}[\Pi_A^{h\tilde{t}_1}] - \mathrm{C_{UV}}[\Pi_A^{h\tilde{t}_2}] - \mathrm{C_{UV}}[\Pi_A^{H\tilde{t}_1}] - \mathrm{C_{UV}}[\Pi_A^{H\tilde{t}_2}] \tag{53}$$

(Note that the minus sign is caused by the fact that the mass m_A^2 occurs in the right-hand side of the renormalized relation.) Let us again divide the total contribution into several parts:

III.a. Terms proportional to $m_{\tilde{t}_1}^2$: Summing up divergences of the tadpoles with $\tilde{t}_1$-loop gives

$$-\mathrm{C_{UV}}[\Pi_A^{h\tilde{t}_1}] - \mathrm{C_{UV}}[\Pi_A^{H\tilde{t}_1}] = \frac{g^2 m_{\tilde{t}_1}^2}{32\pi^2 m_W}\times$$

$$\times\Bigg\{\Bigg[\frac{m_Z^2}{m_W}\sin(\alpha+\beta)\left(X\cos^2\theta_t\ + Y\sin^2\theta_t\,\right) - \frac{m_t^2\cos\alpha}{m_W\sin\beta} -$$

$$-\frac{m_t}{2m_W\sin\beta}\left(A_t m_6\cos\alpha\ - \mu\sin\alpha\,\right)\sin2\theta_t\Bigg]\sin(\alpha-\beta) +$$

$$+\Bigg[\frac{m_Z^2}{m_W}\cos(\alpha+\beta)\left(X\cos^2\theta_t\ + Y\sin^2\theta_t\,\right) + \frac{m_t^2\sin\alpha}{m_W\sin\beta} +$$

$$+\frac{m_t}{2m_W\sin\beta}\left(A_t m_6\sin\alpha\ + \mu\cos\alpha\,\right)\sin2\theta_t\Bigg]\cos(\alpha-\beta)\Bigg\} =$$

$$= \frac{g^2 m_Z^2 m_{\tilde{t}_1}^2}{32\pi^2 m_W^2}\left(X\cos^2\theta_t\ + Y\sin^2\theta_t\,\right)\cos2\beta + \frac{g^2 m_t^2 m_{\tilde{t}_1}^2}{32\pi^2 m_W^2} + \tag{54}$$

$$+\frac{g^2 m_t m_{\tilde{t}_1}^2}{64\pi^2 m_W^2\sin\beta}\left(A_t m_6\sin\beta\ + \mu\cos\beta\,\right)\sin2\theta_t$$

III.b. Terms proportional to $m^2_{\tilde{t}_2}$: Similarly we can obtain the result for the tadpole graphs with one $\tilde{t}_2$-loop:

$$-\mathrm{C}_{\mathrm{UV}}[\Pi_A^{h\tilde{t}_2}] - \mathrm{C}_{\mathrm{UV}}[\Pi_A^{H\tilde{t}_2}] =$$

$$= \frac{g^2 m_Z^2 m_{\tilde{t}_2}^2}{32\pi^2 m_W^2}\left(X\sin^2\theta_t + Y\cos^2\theta_t\right)\cos 2\beta + \frac{g^2 m_t^2 m_{\tilde{t}_2}^2}{32\pi^2 m_W^2} - \tag{55}$$

$$-\frac{g^2 m_t m_{\tilde{t}_2}^2}{64\pi^2 m_W^2 \sin\beta}\left(A_t m_6 \sin\beta + \mu\cos\beta\right)\sin 2\theta_t$$

Collecting now (54) and (55) and utilising

$$(m^2_{\tilde{t}_1} - m^2_{\tilde{t}_2})\sin\beta\sin 2\theta_t = 2m_t\left(A_t m_6\sin\beta + \mu\cos\beta\right) \tag{56}$$

(for derivation see for example the discussion of the small supertop mixing on page 15) allows us to conclude

$$\mathbf{C_{st}}^{(3)} = \frac{g^2 m_t^2}{32\pi^2 m_W^2}(m^2_{\tilde{t}_1} + m^2_{\tilde{t}_2}) + \frac{g^2 m_t^2}{32\pi^2 m_W^2 \sin^2\beta}\left(A_t m_6\sin\beta + \mu\cos\beta\right)^2 + \tag{57}$$

$$+\frac{g^2 m_Z^2}{32\pi^2 m_W^2}\cos 2\beta\, [m^2_{\tilde{t}_1}\left(X\cos^2\theta_t + Y\sin^2\theta_t\right) + m^2_{\tilde{t}_2}\left(X\sin^2\theta_t + Y\cos^2\theta_t\right)]$$

IV. UV divergences in the seagull graphs containing super-top loops
The total divergence arising from the seagulls (345) - (353) is defined by

$$\mathbf{C_{st}}^{(4)} = \mathrm{C}_{\mathrm{UV}}[\Pi_h^{\tilde{t}_1}] + \mathrm{C}_{\mathrm{UV}}[\Pi_h^{\tilde{t}_2}] + \mathrm{C}_{\mathrm{UV}}[\Pi_H^{\tilde{t}_1}] + \mathrm{C}_{\mathrm{UV}}[\Pi_H^{\tilde{t}_2}] -$$

$$-\mathrm{C}_{\mathrm{UV}}[\Pi_A^{\tilde{t}_1}] - \mathrm{C}_{\mathrm{UV}}[\Pi_A^{\tilde{t}_2}] + \mathrm{C}_{\mathrm{UV}}[A_Z^{\tilde{t}_1}] + \mathrm{C}_{\mathrm{UV}}[A_Z^{\tilde{t}_2}] \tag{58}$$

Let us first deal with the graphs involving Higgs bosons h, H and A (not G because of the gauge fixing).

IV.a. Divergences in the seagull graphs with h, H and A: The structure of divergences of these graphs is simply proportional to the quartic couplings so it is easy to sum up all the contributing terms. From (345)-(351) we obtain

$$\mathrm{C}_{\mathrm{UV}}[\Pi_h^{\tilde{t}_1}] + \mathrm{C}_{\mathrm{UV}}[\Pi_h^{\tilde{t}_2}] + \mathrm{C}_{\mathrm{UV}}[\Pi_H^{\tilde{t}_1}] + \mathrm{C}_{\mathrm{UV}}[\Pi_H^{\tilde{t}_2}] = \frac{g^2 m_t^2}{32\pi^2 m_W^2 \sin^2\beta}(m^2_{\tilde{t}_1} + m^2_{\tilde{t}_2}) \tag{59}$$

and

$$-\mathrm{C}_{\mathrm{UV}}[\Pi_A^{\tilde{t}_1}] - \mathrm{C}_{\mathrm{UV}}[\Pi_A^{\tilde{t}_2}] = \frac{g^2 m_t^2}{32\pi^2 m_W^2}\tan^2\beta\,(m^2_{\tilde{t}_1} + m^2_{\tilde{t}_2}) - \tag{60}$$

$$-\frac{g^2 m_Z^2}{32\pi^2 m_W^2}\cos 2\beta\left[m^2_{\tilde{t}_1}\left(X\cos^2\theta_t + Y\sin^2\theta_t\right) + m^2_{\tilde{t}_2}\left(X\sin^2\theta_t + Y\cos^2\theta_t\right)\right]$$

IV.b. Divergences in the seagull graphs with Z: There are two contributions from (352) and (353) in the form

$$\mathrm{C}_{\mathrm{UV}}[A_Z^{\tilde{t}_1}] + \mathrm{C}_{\mathrm{UV}}[A_Z^{\tilde{t}_2}] =$$

$$= \frac{g^2 m_Z^2}{8\pi^2 m_W^2}\left[m^2_{\tilde{t}_1}\left(X^2\cos^2\theta_t + Y^2\sin^2\theta_t\right) + m^2_{\tilde{t}_2}\left(X^2\sin^2\theta_t + Y^2\cos^2\theta_t\right)\right] \tag{61}$$

We can collect now the results (59),(60) and (61) to obtain the complete ultraviolet divergence coming from the seagull sector:

$$\mathbf{C_{st}}^{(4)} = -\frac{1}{32\pi^2}\frac{g^2 m_t^2}{m_W^2}(m_{\tilde{t}_1}^2 + m_{\tilde{t}_2}^2) -$$

$$-\frac{g^2 m_Z^2}{32\pi^2 m_W^2}\cos 2\beta \left[m_{\tilde{t}_1}^2 \left(X\cos^2\theta_t + Y\sin^2\theta_t\right) + m_{\tilde{t}_2}^2 \left(X\sin^2\theta_t + Y\cos^2\theta_t\right)\right] +$$

$$+\frac{g^2 m_Z^2}{8\pi^2 M_W^2}\left[m_{\tilde{t}_1}^2 \left(X^2\cos^2\theta_t + Y^2\sin^2\theta_t\right) + m_{\tilde{t}_2}^2 \left(X^2\sin^2\theta_t + Y^2\cos^2\theta_t\right)\right] \tag{62}$$

2.2.3 Compensation mechanism

Having extracted all the divergences in the previous section it is now easy to see that the sum of them is zero. The first two terms in $\mathbf{C_t}$ (43) cancel with the first and the third terms of $\mathbf{C_{st}}^{(1)}$ (50). The last term of $\mathbf{C_t}$ is removed by the last in $\mathbf{C_{st}}^{(1)}$ together with the first in $\mathbf{C_{st}}^{(2)}$ (52). The second term in $\mathbf{C_{st}}^{(1)}$ is subtracted by the second term in $\mathbf{C_{st}}^{(3)}$ (57).The last term in $\mathbf{C_{st}}^{(2)}$ is removed by the last term of $\mathbf{C_{st}}^{(4)}$ (62). Finally the first and the third terms of $\mathbf{C_{st}}^{(3)}$ cancel with the rest of $\mathbf{C_{st}}^{(4)}$. This can be written in the form

$$\mathbf{C_t} + \mathbf{C_{st}}^{(1)} + \mathbf{C_{st}}^{(2)} + \mathbf{C_{st}}^{(3)} + \mathbf{C_{st}}^{(4)} = 0 \tag{63}$$

The structure of the compensation mechanism is clearly gauge-dependent. For example in R_ξ-gauges there are more diagrams to be investigated but the mechanism of divergence compensation is less complicated. Including graphs with the Goldstone bosons would cause:

- total compensation of the tadpole graphs (not only divergences)
- more transparent compensation of divergences in the seagull sector

2.3 Finite part

In this section we are going to investigate the finite parts of diagrams discussed in the previous section. Having proven the full cancellation of divergences coming from those graphs we are ready to demonstrate the overall regularisation constant independence of the finite part although it is very hard to see it from the (very long) sum of relevant expressions.

2.3.1 Regularisation constant independence

The proof of the previous statement is nothing but recalling the structure of expressions obtained performing dimensional regularisation procedure (see Appendix A). For any considered integral we have got an expression of the general form

$$\text{Int.} \to stg. \left(\frac{D}{4\pi\mu^2}\right)^{-\varepsilon} \Gamma(n-\varepsilon) \tag{64}$$

(The term *stg.* denotes some overall constant or expression which does not affect the structure in the brackets) This is expanded in the form (using (175) and (177))

$$\text{Int.} \overset{\text{DR}}{\sim} stg. \left[1 - \varepsilon \ln\left(\frac{D}{4\pi\mu^2}\right) + O(\varepsilon^2)\right] \frac{(-1)^n}{n!}\left[\frac{1}{\varepsilon} + \psi_1(n+1) + O(\varepsilon)\right] \tag{65}$$

and such expression is simplified to the final result (neglecting the factor $O(\varepsilon)$ in the limit $\varepsilon \to 0$). Assuming that all the mass parameters in the expansion above are expressed in terms of some fixed mass unit M, we can divide the logarithm (its argumend is now supposed to be dimensionless) into two pieces and recast the previous relation in the form

$$\text{Int.} \overset{\text{DR}}{\sim} stg.\frac{(-1)^n}{n!}\left[\mathrm{C_{UV}} + \ln\mu^2 + \psi_1(n+1) + \gamma_{\mathrm{E}} - \ln D\right] \tag{66}$$

Then we couple the factor $\ln\mu^2$ to the divergence symbol $\mathrm{C_{UV}}$ and define a new C'_{UV}, which is removed from the total correction Δ in the same way as the original $\mathrm{C_{UV}}$. This proves the regularisation parameter independence of the finite part of Δ.

2.3.2 Computation of the leading term

As was stated before we can fix the particular value of the regularisation parameter μ; let us take $\mu = 1$ (in chosen mass units). Inspecting the finite parts of diagrams calculated in Appendix C we can catalogize them into several groups with different overall mass factors. Although it seems that the most important should be the terms proportional to the squares of the supertop masses $m^2_{\tilde{t}_1}$ and $m^2_{\tilde{t}_2}$ it will be shown that this is true only in the special case of significant mixing in the squark sector. If none or only a negligible mixing in the supertop sector occurs it turns out that the most important term is proportional to $\frac{m_t^4}{m_Z^2}$.

In the whole discussion we are going to use several assumptions:

- The masses of squarks and the top mass are much bigger than the other masses involved in the computation - $m_{\tilde{t}_1}, m_{\tilde{t}_2}, m_t \gg m_W, m_A, m_H, m_h$)
- The off-diagonal entries in the $\tilde{t}_L - \tilde{t}_R$ mass-matrix are not too large i.e. there is no significant mixing in the supertop sector. This condition can be translated into the mathematical form $A_t m_6, \mu\mathrm{cot}\beta \ll m_t$.

To see this connection explicitly, let us recall the form of the supertop mass-squared matrix (see for example [4]):

$$M^2_{\tilde{t}} = \begin{pmatrix} A & B \\ B & C \end{pmatrix} \tag{67}$$

where

$$\begin{aligned} A &= M^2_{\mathrm{Q}} + m^2_Z \mathrm{cos}2\beta\, X + m^2_t \\ B &= m_t\,(A_t m_6 + \mu\mathrm{cot}\beta\,) \\ C &= M^2_{\mathrm{U}} + m^2_Z \mathrm{cos}2\beta\, Y + m^2_t \end{aligned}$$

(the matrix entries come from the superpotential and $\mathcal{L}_{\mathrm{SM}}$, see page 69). The condition of small mixing is evidently equivalent to the negligibility of the non-diagonal entries, i.e. $B \ll A, C$. To be more precise, the problem of eigenvalues is the same (and the notation too) as in the exercise (15) - (17) from the first chapter. The mixing angle θ_t can be obtained from

$$\mathrm{sin}2\theta_t = \frac{2B}{\sqrt{(A-C)^2 + 4B^2}} = \frac{2B}{(\lambda_1 - \lambda_2)} \tag{68}$$

where $\lambda_{1,2}$ are the eigenvalues of (67); here we have used relations (26) and (15). These eigenvalues are interpreted as the (tree-level) squared masses of the supertops, so we can write

$$\sin 2\theta_t = \frac{2m_t\,(A_t m_6 + \mu \cot\beta\,)}{m^2_{\tilde{t}_1} - m^2_{\tilde{t}_2}} \tag{69}$$

which is quite useful, see for example (56).

None of the conditions above is fully experimentally founded but we use them only to show that up to now there exist at least a corner in the parametrical space for which a large one-loop correction in the Higgs sector can occur. It is believed that this is indeed true in a slightly bigger domain than only in several special cases.

The first condition is relevant for (almost) the whole (experimentaly admitable) area of the MSSM parametrical space with the only exception when m_A is very massive. But the mass m_A often appears together with the factor $\cos\beta$, which suppresses its eventual big value very well; note that we work mostly in the $\beta \to \frac{\pi}{2}$ regime. The second condition is more speculative but this seems to be true for all the squarks species except possibly supertop (see [4]).

Let us start with the explicit computation of the leading correction to the tree-level MSSM relation $m_h^2 + m_H^2 = m_A^2 + m_Z^2$. It will be performed in the unitary gauge (to reduce the number of relevant diagrams). We start with the possibly most important terms proportional to the mass parameters of the maximal magnitude and continue with the other less and less important. This procedure will be cut on the level of terms proportional to m_Z^2 and smaller because of the assumptions $m_t, m_{\tilde{t}_1}, m_{\tilde{t}_2} \gg m_Z$. (In [15] the recent values of m_t, m_W and m_Z are $m_t = 180 \pm 12$ GeV, $m_W = 80.33 \pm 0.15$ GeV and $m_Z = 91.187 \pm 0.007$ GeV so $m_t^4/m_W^2 \gg m_Z^2$.)

I. Terms proportional to $m^2_{\tilde{t}_1}$ and $m^2_{\tilde{t}_2}$:

Terms of this type come generally from graphs with one supertop loop and in this paragraph we focus our attention mostly on them. We are going to use many result of the supplementary section 3, because a lot of computations performed in detail there can be utilised here because of the coupling relations

$$\begin{aligned} g_{hAA} + g_{hGG} &= 0 \\ g_{HAA} + g_{HGG} &= 0 \end{aligned} \tag{70}$$

$$g_{hh\tilde{t}_1\tilde{t}_1} + g_{HH\tilde{t}_1\tilde{t}_1} - g_{AA\tilde{t}_1\tilde{t}_1} - g_{GG\tilde{t}_1\tilde{t}_1} + g_{hh\tilde{t}_2\tilde{t}_2} + g_{HH\tilde{t}_2\tilde{t}_2} - g_{AA\tilde{t}_2\tilde{t}_2} - g_{GG\tilde{t}_2\tilde{t}_2} = 0$$

Let us denote by $F[\Pi]$ (with appropriate indices) the finite parts of all the investigated graphs. The sum of all contrinutions that are proportional to squares of supertop masses is then

$$\begin{aligned} F_{\tilde{t}_1\tilde{t}_2} \equiv\; & F[A_Z^{\tilde{t}_1\tilde{t}_1}] + F[A_Z^{\tilde{t}_2\tilde{t}_2}] + F[A_Z^{\tilde{t}_1\tilde{t}_2}] + \\ & + F[\Pi_h^{h\tilde{t}_1}] + F[\Pi_H^{h\tilde{t}_1}] - F[\Pi_A^{h\tilde{t}_1}] + F[A_Z^{h\tilde{t}_1}] + \\ & + F[\Pi_h^{h\tilde{t}_2}] + F[\Pi_H^{h\tilde{t}_2}] - F[\Pi_A^{h\tilde{t}_2}] + F[A_Z^{h\tilde{t}_2}] + \\ & + F[\Pi_h^{H\tilde{t}_1}] + F[\Pi_H^{H\tilde{t}_1}] - F[\Pi_A^{H\tilde{t}_1}] + F[A_Z^{H\tilde{t}_1}] + \end{aligned}$$

$$
\begin{aligned}
&+F[\Pi_h^{H\tilde t_2}]+F[\Pi_H^{H\tilde t_2}]-F[\Pi_A^{H\tilde t_2}]+F[A_Z^{H\tilde t_2}]+\\
&+F[\Pi_h^{\tilde t_1}]+F[\Pi_H^{\tilde t_1}]-F[\Pi_A^{\tilde t_1}]+F[A_Z^{\tilde t_1}]+\\
&+F[\Pi_h^{\tilde t_2}]+F[\Pi_H^{\tilde t_2}]-F[\Pi_A^{\tilde t_2}]+F[A_Z^{\tilde t_2}]+
\end{aligned} \tag{71}
$$

Note that we do not involve graphs (310)-(323) because they are not explicitly $m_{\tilde t}^2$ dependent; they will be included in the next paragraph. From relations (280) we can remove all the tadpole diagrams contributing to the h,H and Z propagators:

$$
\begin{aligned}
F[\Pi_h^{h\tilde t_1}]+F[\Pi_H^{h\tilde t_1}]+F[A_Z^{h\tilde t_1}] &= 0\\
F[\Pi_h^{h\tilde t_2}]+F[\Pi_H^{h\tilde t_2}]+F[A_Z^{h\tilde t_2}] &= 0\\
F[\Pi_h^{H\tilde t_1}]+F[\Pi_H^{H\tilde t_1}]+F[A_Z^{H\tilde t_1}] &= 0\\
F[\Pi_h^{H\tilde t_2}]+F[\Pi_H^{H\tilde t_2}]+F[A_Z^{H\tilde t_2}] &= 0
\end{aligned}
$$

Moreover, the tadpole contributions to the propagator of A can be easily obtained from those computed for the Goldstone boson in chapter 3; using (70) we get

$$
\begin{aligned}
F[\Pi_A^{h\tilde t_1}] &= -F[\Pi_G^{h\tilde t_1}]\\
F[\Pi_A^{h\tilde t_2}] &= -F[\Pi_G^{h\tilde t_2}]\\
F[\Pi_A^{h\tilde t_1}] &= -F[\Pi_G^{h\tilde t_1}]\\
F[\Pi_A^{h\tilde t_2}] &= -F[\Pi_G^{h\tilde t_2}]
\end{aligned}
$$

A similar situation occurs for the seagull graphs. Using the last relation in (70) we get

$$
F[\Pi_h^{\tilde t_1}]+F[\Pi_H^{\tilde t_1}]-F[\Pi_A^{\tilde t_1}]+F[\Pi_h^{\tilde t_2}]+F[\Pi_H^{\tilde t_2}]-F[\Pi_A^{\tilde t_2}] \;=\; F[\Pi_G^{\tilde t_1}]+F[\Pi_G^{\tilde t_1}]
$$

The previous results allow us to simplify (71) to the form

$$
\begin{aligned}
F_{\tilde t_1\tilde t_2} \;=\;& F[A_Z^{\tilde t_1\tilde t_1}]+F[A_Z^{\tilde t_2\tilde t_2}]+F[A_Z^{\tilde t_1\tilde t_2}]+F[A_Z^{\tilde t_1}]+F[A_Z^{\tilde t_2}]+\\
&+F[\Pi_G^{h\tilde t_1}]+F[\Pi_G^{h\tilde t_2}]+F[\Pi_G^{H\tilde t_1}]+F[\Pi_G^{H\tilde t_2}]+F[\Pi_G^{\tilde t_1}]+F[\Pi_G^{\tilde t_1}]
\end{aligned} \tag{72}
$$

As we can see from the relation (103) which contains the last six terms, (72) can be rewritten in the form

$$
F_{\tilde t_1\tilde t_2} \;=\; F[A_Z^{\tilde t_1\tilde t_1}]+F[A_Z^{\tilde t_2\tilde t_2}]+F[A_Z^{\tilde t_1\tilde t_2}]+F[A_Z^{\tilde t_1}]+F[A_Z^{\tilde t_2}]-F[\Pi_G^{\tilde t_1\tilde t_2}] \tag{73}
$$

Now we use the results of the explicit diagrammatic computation in Appendix C to obtain

$$
\begin{aligned}
F_{\tilde t_1\tilde t_2} = \frac{3g^2m_Z^2}{16\pi^2m_W^2}\Big\{&2\left(X^2\cos^2\theta_t+Y^2\sin^2\theta_t\right)m_{\tilde t_1}^2\left(1-\ln m_{\tilde t_1}^2\right)+\\
&+2\left(X^2\sin^2\theta_t+Y^2\cos^2\theta_t\right)m_{\tilde t_2}^2\left(1-\ln m_{\tilde t_2}^2\right)-\\
&-\left(-X\cos^2\theta_t+Y\sin^2\theta_t\right)^2\left[2m_{\tilde t_1}^2-\frac{m_Z^2}{3}-2\int_0^1 \mathrm{d}x D_{m_Z}^{\tilde t_1\tilde t_1}(x)\ln D_{m_Z}^{\tilde t_1\tilde t_1}(x)\right]-\\
&-\left(-X\sin^2\theta_t+Y\cos^2\theta_t\right)^2\left[2m_{\tilde t_2}^2-\frac{m_Z^2}{3}-2\int_0^1 \mathrm{d}x D_{m_Z}^{\tilde t_2\tilde t_2}(x)\ln D_{m_Z}^{\tilde t_2\tilde t_2}(x)\right]-\\
&-2\left(X\sin\theta_t\cos\theta_t+Y\sin\theta_t\cos\theta_t\right)^2\times\\
&\times\left[m_{\tilde t_1}^2+m_{\tilde t_2}^2-\frac{m_Z^2}{3}-2\int_0^1 \mathrm{d}x D_{m_Z}^{\tilde t_1\tilde t_2}(x)\ln D_{m_Z}^{\tilde t_1\tilde t_2}(x)\right]\Big\}-
\end{aligned}
$$

$$-\frac{3g^2m_t^2}{32\pi^2m_W^2\sin^2\beta}\,(A_tm_6\sin\beta\,+\mu\cos\beta\,)^2\int_0^1 \mathrm{d}x\ln D_0^{\tilde{t}_1\tilde{t}_2}(x) \qquad (74)$$

(Here we have performed the summation over the quark colours which produces an overall factor $N_c = 3$.) Now it can be easily checked that the factors proportional to $m_{\tilde{t}_1}^2$ and $m_{\tilde{t}_2}^2$ cancel (of course, there still remains a strong dependence on them in the functions $D(x)$): Note first that the last term does not explicitly contain any overall factor of order $m_{\tilde{t}}^2$ and we will see that it can be neglected because it is much smaller (due to the presence of the off-diagonal terms A_tm_6 and μ which are assumed to be negligible, see assumptions on previous pages) compared to the term proportional to $\frac{m_t^4}{m_W^2}$ which is discussed in the next paragraph. Similarly the factor coming from m_Z^2 terms.

Let us now discuss the rest of (74). The assumption of small mixing in the supertop sector (i.e. $\theta_t \approx 0$) allows us to put $\sin\theta_t \approx 0$ and $\cos\theta_t \approx 1$. This practically removes the term in the sixth line of (74). The sum of the remaining terms proportional to $m_{\tilde{t}_1}$ is also very small because of the relation

$$D_{m_Z}^{\tilde{t}_1\tilde{t}_1}(x) = m_{\tilde{t}_1}^2 - m_Z^2x(1-x) \qquad (75)$$

which implies

$$\ln D_{m_Z}^{\tilde{t}_1\tilde{t}_1}(x) = \ln m_{\tilde{t}_1}^2 + \ln\left[1-\frac{m_Z^2}{m_{\tilde{t}_1}^2}x(1-x)\right] = \ln m_{\tilde{t}_1}^2 - \frac{m_Z^2}{m_{\tilde{t}_1}^2}x(1-x) + O\left(\frac{m_Z^4}{m_{\tilde{t}_1}^4}\right) \qquad (76)$$

Similar discussion holds in the same way for the terms with $m_{\tilde{t}_2}$.

Now it is already easy to see that the terms proportional to $m_{\tilde{t}}^2\ln m_{\tilde{t}}^2$ exactly cancel and the remaining terms are (at least) of order m_Z^2 and therefore can be neglected too. We can now make an important conclusion:

- In the case of the small mixing in the supertop sector there is no large contribution to the tree-level relation $m_h^2 + m_H^2 = m_A^2 + m_Z^2$ of order $m_{\tilde{t}_1}^2$ (or $m_{\tilde{t}_2}^2$) coming from the diagrams with one supertop loop.

If any significant stop mixing occurs the investigated diagrams might produce a large negative contribution (see [4]). Note again, that we are looking for the situation of a large possitive correction (to allow the lightest Higgs boson to be out of the directly observable area) and that is why we omit discussions of such phenomena - these terms simply cannot solve our problem.

II. Terms proportional to m_t^2:

We have seen in the previous paragraph that the contribution proportional to the square of the largest used mass scale $m_{\tilde{t}}$ is (atleast in the case of a small mixing in the stop sector) negligible compared to the factor $\frac{m_t^4}{m_W^2}$. The terms producing contribution proportional to this scale descent from two sources:

- all the diagrams involving top quark loop are proportional to m_t^2
- there is a large number of graphs with one stop loop belonging to this group because of m_t factor in the relevant couplings ($g_{h\tilde{t}\tilde{t}}$,...); for example the logarithmicly divergent graphs (i.e. these with the superficial degree of divergence equal to 0) involving one supertop loop. Note that the mass of the "looping particle" in such graphs is *not*

factorized out during the regularisation procedure so the only mass dependence comes from the trilinear coupling constant.

First we are going to deal with the terms proportional to $\frac{m_t^4}{m_W^2}$ only; they should (having thrown away the $m_{\tilde{t}}^2$ dependence) make up the largest contribution to Δ. After that we will discuss in few words the nonaccuracy of such a leading term approximation.

Contribution proportional to $\frac{m_t^4}{m_W^2}$; derivation of the leading term

As in the previous paragraphs we first inspect the huge set of diagrams of Appendix C (their finite parts) for any terms proportional to $\frac{m_t^4}{m_W^2}$. They can be found in diagrams (282),(284),(286),(288), (298),(302) (graphs involving top loops), (310),(312),(316) and (318) (diagrams with supertop loops).

Let us write down the relevant expressions (denoted by $F[\Pi]_4$ to express the fact that we extract only the most important part of $F[\Pi]$) coming from these diagrams; their sum will be denoted by Δ_4:

$$\Delta_4 \equiv F[\Pi_h^{tt}]_4 + F[\Pi_H^{tt}]_4 - F[\Pi_A^{tt}]_4 - F[\Pi_A^{ht}]_4 - F[\Pi_A^{ht}]_4 + F[A_Z^{tt}]_4 + \tag{77}$$
$$+F[\Pi_h^{\tilde{t}_1\tilde{t}_1}]_4 + F[\Pi_h^{\tilde{t}_2\tilde{t}_2}]_4 + F[\Pi_H^{\tilde{t}_1\tilde{t}_1}]_4 + F[\Pi_H^{\tilde{t}_2\tilde{t}_2}]_4$$

First we deal with the diagrams involving one top-quark loop; evaluating all the external momenta on-shell we obtain

$$\Delta_4^t = \frac{3g^2 m_t^2 \cos^2\alpha}{16\pi^2 m_W^2 \sin^2\beta} \left\{ \left(m_t^2 - \frac{m_h^2}{6} \right) + \int_0^1 \mathrm{d}x \ln D_{m_h}^{tt}(x) \left[-3m_t^2 + 3m_h^2 x(1-x) \right] \right\} +$$
$$+\frac{3g^2 m_t^2 \sin^2\alpha}{16\pi^2 m_W^2 \sin^2\beta} \left\{ \left(m_t^2 - \frac{m_H^2}{6} \right) + \int_0^1 \mathrm{d}x \ln D_{m_H}^{tt}(x) \left[-3m_t^2 + 3m_H^2 x(1-x) \right] \right\} +$$
$$+\frac{3g^2 m_t^2 \cos^2\beta}{16\pi^2 m_W^2 \sin^2\beta} \left\{ -\left(m_t^2 - \frac{m_A^2}{6} \right) + \int_0^1 \mathrm{d}x \ln D_{m_A}^{tt}(x) \left[m_t^2 - 3m_A^2 x(1-x) \right] \right\} +$$
$$+\frac{3g^2 m_Z^2}{16\pi^2 m_W^2} \left\{ \int_0^1 \mathrm{d}x \ln D_{m_Z}^{tt}(x) \frac{m_t^2}{2} + 4m_Z^2 \int_0^1 \mathrm{d}x \ln D_{m_Z}^{tt}(x)(X^2+Y^2)x(1-x) \right\} -$$
$$-\frac{3g^2 m_t^4}{16\pi^2 m_W^2} \left(1 - \ln m_t^2 \right) \tag{78}$$

(The origin of the first four lines can be guessed from the indices of D functions, the last term comes from the tadpole graphs (298),(302).) Let us investigate this expression more precisely:

- the term in the fourth line can be neglected because its first part is of order m_t^2 and the rest even of m_Z^2 so it is (with error level about 10%) negligible compared to the others
- the terms in brackets proportional to the scalar masses that are unknown and maybe large (in the case of m_A^2) can be recast using the relation

  $$m_h^2 \cos^2\alpha + m_H^2 \sin^2\alpha - m_A^2 \cos^2\beta = m_Z^2 \sin^2\beta$$

  which reduces them to some negligible factor

- the terms in integrands proportional to the scalar masses can also be removed, because the two light scalars h and H are expected to have masses at the m_Z scale and the m_A^2 is suppressed by the overall factor $\cos^2\beta$ for β close to $\frac{\pi}{2}$ (which is the only experimentally acceptable domain of this parameter)
- the terms m_t^2 standing alone in the brackets exactly cancel

The only important factors (for our purposes) in Δ_4^t are then:

$$\Delta_4^t \approx \frac{3g^2m_t^4}{16\pi^2m_W^2\sin^2\beta}\left\{-3\cos^2\alpha\int_0^1 \mathrm{d}x\ln D_{m_h}^{tt}(x) - 3\sin^2\alpha\int_0^1 \mathrm{d}x\ln D_{m_H}^{tt}(x) + \right.$$
$$\left. + \cos^2\beta\int_0^1 \mathrm{d}x\ln D_{m_A}^{tt}(x) + \sin^2\beta\ln m_t^2\right\} \tag{79}$$

The second line of (77) i.e. the contribution of diagrams involving stop loop (denoted by $\Delta_4^{\tilde{t}}$) can be written in the form

$$\Delta_4^{\tilde{t}} = \frac{3}{16\pi^2}\left\{\left[\frac{gm_Z}{\cos\theta_W}\sin(\alpha+\beta)\left(X\cos^2\theta_t + Y\sin^2\theta_t\right) - \frac{gm_t^2\cos\alpha}{m_W\sin\beta} - \right.\right.$$
$$\left. -\frac{gm_t\sin2\theta_t}{2m_W\sin\beta}\left(A_tm_6\cos\alpha - \mu\sin\alpha\right)\right]^2\int_0^1 \mathrm{d}x\ln D_{m_h}^{\tilde{t}_1\tilde{t}_1}(x) +$$
$$+\left[\frac{gm_Z}{\cos\theta_W}\sin(\alpha+\beta)\left(X\sin^2\theta_t + Y\cos^2\theta_t\right) - \frac{gm_t^2\cos\alpha}{m_W\sin\beta} + \right. \tag{80}$$
$$\left. +\frac{gm_t\sin2\theta_t}{2m_W\sin\beta}\left(A_tm_6\cos\alpha - \mu\sin\alpha\right)\right]^2\int_0^1 \mathrm{d}x\ln D_{m_h}^{\tilde{t}_2\tilde{t}_2}(x) +$$
$$+\left[-\frac{gm_Z}{\cos\theta_W}\cos(\alpha+\beta)\left(X\cos^2\theta_t + Y\sin^2\theta_t\right) - \frac{gm_t^2\sin\alpha}{m_W\sin\beta} - \right. \tag{81}$$
$$\left. -\frac{gm_t\sin2\theta_t}{2m_W\sin\beta}\left(A_tm_6\sin\alpha + \mu\cos\alpha\right)\right]^2\int_0^1 \mathrm{d}x\ln D_{m_H}^{\tilde{t}_1\tilde{t}_1}(x) +$$
$$+\left[-\frac{gm_Z}{\cos\theta_W}\cos(\alpha+\beta)\left(X\sin^2\theta_t + Y\cos^2\theta_t\right) - \frac{gm_t^2\sin\alpha}{m_W\sin\beta} + \right. \tag{82}$$
$$\left.\left. +\frac{gm_t\sin2\theta_t}{2m_W\sin\beta}\left(A_tm_6\sin\alpha + \mu\cos\alpha\right)\right]^2\int_0^1 \mathrm{d}x\ln D_{m_H}^{\tilde{t}_2\tilde{t}_2}(x)\right\}$$

We have again several reasons to omit a lot of terms above:

- the only part relevant to further computation is in fact the sum of squares of the terms proportional to $\frac{gm_t^2}{m_W\sin\beta}$
- the other terms are negligible because they contain the off-diagonal terms of the supertop mass squared matrix (A_tm_6 and μ), that are assumed to be small compared to the m_t scale, or factors proportional to m_Z.

The only remaining factors are the following:

$$\Delta_4^{\tilde{t}} \approx \frac{3g^2m_t^4}{16\pi^2m_W^2\sin^2\beta}\left\{\cos^2\alpha\left[\int_0^1 \mathrm{d}x\ln D_{m_h}^{\tilde{t}_1\tilde{t}_1}(x) + \int_0^1 \mathrm{d}x\ln D_{m_h}^{\tilde{t}_2\tilde{t}_2}(x)\right] + \right.$$
$$\left. + \sin^2\alpha\left[\int_0^1 \mathrm{d}x\ln D_{m_H}^{\tilde{t}_1\tilde{t}_1}(x) + \int_0^1 \mathrm{d}x\ln D_{m_H}^{\tilde{t}_2\tilde{t}_2}(x)\right]\right\} \tag{83}$$

Inspecting the remaining diagrams of Appendix C we can state that there is no other possibility to obtain any contribution of order $\frac{m_t^4}{m_W^2}$ so the set of diagrams considered up to now is complete in this sense. Knowing this we are ready to conclude our long computation; to obtain the final result we must sum up the main contributions (79) and (83). It is convenient to express it in a more elegant way. To do this we utilise the relation

$$\ln D_m^{XX}(x) = \ln M_X^2 + \ln\left[1 - \frac{m^2}{M_X^2}x(1-x)\right] \approx \ln M_X^2 - \frac{m^2}{M_X^2}x(1-x) \tag{84}$$

which is valid for some mass scale M_X high enough to suppress the other masses like m_Z, m_h, m_H and m_A generally denoted by m. (To be more precise the term proportional to $\frac{m_A^2}{m_t^2}$ could be large but as in the previous case it is suppressed by $\cos^2\beta$). Using the logarithmic part only we can write down the final approximate form of the leading term:

$$\Delta_4 \equiv \Delta_4^t + \Delta_4^{\tilde{t}} \approx \frac{3g^2 m_t^4}{16\pi^2 m_W^2 \sin^2\beta}\left\{-2\ln m_t^2 + \ln m_{\tilde{t}_1}^2 + \ln m_{\tilde{t}_2}^2\right\} =$$

$$= \frac{3g^2 m_t^4}{16\pi^2 m_W^2 \sin^2\beta}\ln\left(\frac{m_{\tilde{t}_1}^2 m_{\tilde{t}_2}^2}{m_t^4}\right) \tag{85}$$

This is the main result of the whole computation. It tells that the original tree-level relation (30) can be recast, when including the leading logarithmic one-loop corrections, in the form

$$m_h^2 + m_H^2 = m_A^2 + m_Z^2 + \frac{3g^2 m_t^4}{16\pi^2 m_W^2 \sin^2\beta}\ln\left(\frac{m_{\tilde{t}_1}^2 m_{\tilde{t}_2}^2}{m_t^4}\right) \tag{86}$$

This relation agree with the results presented in the literature ([4], [8]).

Note that the relative error of the approximations used to derive the previous relation does not exceed values about 10%. It comes mainly from the fact that we have completely neglected all the terms of order m_t^2 and lower. Next, the form of the leading term (85) is invalid in case that any significant mixing in the stop sector occurs.

3 One-loop self-energy of the MSSM neutral Goldstone boson

The topic of this section is to show the total cancellation of the MSSM neutral Goldstone boson self-energy graphs with one quark or squark loop, i.e. both its divergences and the finite parts. Although this is expected to be true there is, up to my knowledge, no explicit one-loop diagrammatic calculation in the literature so this work should fill the existing gap.

I restrict myself on the top-quark (and squark) sector only because the generalisation to other flavours is straightforward and can be obtained from the results for tops and supertops. Moreover the diagrams involving Higgs bosons used for the previous purposes are practically identical with the diagrams relevant to this problem. We omit completely the other sectors (lepton, gaugino and higgsino) of the model. The reason is simply the fact that we have already evaluated all the necessary Feynman diagrams in the Appendix C so it is convenient to use them also in this supplementary section.

Let us start with the computation. Recall that there are 20 diagrams to be considered in general - all the diagrams in Appendix C containing Goldstone boson G. Not to expand this section too much we are going to use several results from the previous sections, mainly the expressions for divergences of the graphs containing A because of the relations (280), which help us for example in the cases of the tadpole graphs.

3.1 UV divergent part of the Goldstone boson self-energy

The total sum of divergences descending from the graphs including neutral Goldstone boson G will be defined by

$$\mathbf{C_G} \equiv \mathrm{C}_{\mathrm{UV}}[\Pi_G^{tt}] + \mathrm{C}_{\mathrm{UV}}[\Pi_G^{ht}] + \mathrm{C}_{\mathrm{UV}}[\Pi_G^{Ht}] + \mathrm{C}_{\mathrm{UV}}[\Pi_G^{\tilde{t}_1\tilde{t}_2}] + \mathrm{C}_{\mathrm{UV}}[\Pi_G^{h\tilde{t}_1}] + \mathrm{C}_{\mathrm{UV}}[\Pi_G^{h\tilde{t}_2}] + \\ + \mathrm{C}_{\mathrm{UV}}[\Pi_G^{H\tilde{t}_1}] + \mathrm{C}_{\mathrm{UV}}[\Pi_G^{H\tilde{t}_2}] + \mathrm{C}_{\mathrm{UV}}[\Pi_G^{\tilde{t}_1}] + \mathrm{C}_{\mathrm{UV}}[\Pi_G^{\tilde{t}_2}] \qquad (87)$$

I. Divergences coming from the tadpole graphs
Let us start with the divergences coming from the tadpole graphs. Up to the minus sign coming from (280) they are identical with the divergences calculated in subsections (2.2.1) and (2.2.2) so we can write them down immediately.

I.a. Tadpoles involving t-loop: Using relations (41) and (280) we get

$$\mathrm{C}_{\mathrm{UV}}[\Pi_G^{ht}] + \mathrm{C}_{\mathrm{UV}}[\Pi_G^{Ht}] = -\frac{g^2 m_t^4}{16\pi^2 m_W^2} \qquad (88)$$

I.b. Tadpoles involving st-loop: In the same way from (57) and (280) follows

$$\mathrm{C}_{\mathrm{UV}}[\Pi_G^{h\tilde{t}_1}] + \mathrm{C}_{\mathrm{UV}}[\Pi_G^{h\tilde{t}_2}] + \mathrm{C}_{\mathrm{UV}}[\Pi_G^{H\tilde{t}_1}] + \mathrm{C}_{\mathrm{UV}}[\Pi_G^{H\tilde{t}_2}] = \\ = \frac{g^2 m_t^2}{32\pi^2 m_W^2}(m_{\tilde{t}_1}^2 + m_{\tilde{t}_2}^2) + \frac{g^2 m_t^2}{32\pi^2 m_W^2 \sin^2\beta}\left(A_t m_6 \sin\beta + \mu\cos\beta\right)^2 + \qquad (89) \\ + \frac{g^2 m_Z^2}{32\pi^2 m_W^2}\cos 2\beta\,[m_{\tilde{t}_1}^2\left(X\cos^2\theta_t + Y\sin^2\theta_t\right) + m_{\tilde{t}_2}^2\left(X\sin^2\theta_t + Y\cos^2\theta_t\right)]$$

II. Seagull graphs: The relation (262) allows us to use again the already computed quantities (59) and (60) to conclude

$$\mathrm{C_{UV}}[\Pi_G^{\tilde{t}_1}] + \mathrm{C_{UV}}[\Pi_G^{\tilde{t}_2}] = -\frac{g^2 m_t^2}{32\pi^2 m_W^2}(m_{\tilde{t}_1}^2 + m_{\tilde{t}_2}^2) - \tag{90}$$

$$-\frac{g^2}{32\pi^2 \cos^2\theta_W}\cos 2\beta \left[m_{\tilde{t}_1}^2\left(X\cos^2\theta_t + Y\sin^2\theta_t\right) + m_{\tilde{t}_2}^2\left(X\sin^2\theta_t + Y\cos^2\theta_t\right)\right]$$

III. Graphs dependent on external momenta: The last two graphs with the neutral Goldstone boson are (296) and (324). In the on-shell scheme the external momenta of the Goldstone boson are evaluated in the point $q^2 = 0$ so the contribution coming from these graphs is

$$\mathrm{C_{UV}}[\Pi_G^{tt}] + \mathrm{C_{UV}}[\Pi_G^{\tilde{t}_1\tilde{t}_2}] = \frac{g^2 m_t^4}{16\pi^2 m_W^2} - \frac{g^2 m_t^2}{32\pi^2 m_W^2 \sin^2\beta}\left(A_t m_6 \sin\beta + \mu\cos\beta\right)^2 \tag{91}$$

We are now ready to sum up all the divergences (89),(90) and (91) and conclude

$$\mathbf{C_G} = 0 \tag{92}$$

i.e. the ultraviolet divergences of the Goldstone boson self-energy graphs exactly cancel.

3.2 Finite parts

Having shown the total compensation of divergences in the Goldstone two-point OPI Green function we can state that the finite part of this function does not depend on the regularisation parameter μ and simplify it by fixing $\mu = 1$ (mass unit). As in the previous sections we are going to denote the finite part of the regularized expression corresponding to some Feynman graph by $F[\Pi_G^{XY}]$. We will sum up all the contributions computed in the Appendix C to obtain $\mathbf{F_G}$, which is defined by

$$\mathbf{F_G} \equiv F[\Pi_G^{tt}] + F[\Pi_G^{ht}] + F[\Pi_G^{Ht}] + F[\Pi_G^{\tilde{t}_1\tilde{t}_2}] + F[\Pi_G^{h\tilde{t}_1}] + F[\Pi_G^{h\tilde{t}_2}] +$$

$$+ F[\Pi_G^{H\tilde{t}_1}] + F[\Pi_G^{H\tilde{t}_2}] + F[\Pi_G^{\tilde{t}_1}] + F[\Pi_G^{\tilde{t}_2}] \tag{93}$$

Let us start with

I. Diagrams containing top quark loop: The total contribution proportional to m_t^2 cancels in the same way as the corresponding divergences in (3.1), because the only difference between the divergent and the finite parts is the presence of the overall factor

$$1 - \int_0^1 \mathrm{d}x D_0^{tt}(x) = 1 - \ln m_t^2 \tag{94}$$

in $F[.]$ instead of $\mathrm{C_{UV}}$ in $\mathrm{C_{UV}}[.]$ so

$$F[\Pi_G^{tt}] + F[\Pi_G^{ht}] + F[\Pi_G^{Ht}] = 0 \tag{95}$$

II. Diagrams containing supertop loop: Here the situation is not so clear as in the previous case. The reason is that it is not generally possible to extract any common overall factor from the considered diagrams and use the same argument as above, because $F[\Pi_G^{\tilde{t}_1\tilde{t}_2}]$ is proportional to $\int_0^1 \mathrm{d}x D_0^{\tilde{t}_1\tilde{t}_2}(x)$. Fortunately it is the only problem here; a lot of factors get compensated in the usual way in full correspondence with the compensation of divergences. For example the terms

$$F[\Pi_G^{\tilde{t}_1}] = -\frac{g^2}{32\pi^2 m_W^2} m_{\tilde{t}_1}^2 \left[m_t^2 + m_Z^2 \cos 2\beta \left(X\cos^2\theta_t + Y\sin^2\theta_t\right)\right]\left(1 - \ln m_{\tilde{t}_1}^2\right) \tag{96}$$

$$F[\Pi_G^{\tilde{t}_2}] = -\frac{g^2}{32\pi^2 m_W^2} m_{\tilde{t}_2}^2 \left[m_t^2 + m_Z^2 \cos 2\beta \left(X\sin^2\theta_t + Y\cos^2\theta_t\right)\right]\left(1 - \ln m_{\tilde{t}_2}^2\right) \tag{97}$$

coming from the seagull graphs (59) and (60) are compensated almost completely by the factors coming from the tadpole sector

$$F[\Pi_G^{h\tilde{t}_1}] + F[\Pi_G^{H\tilde{t}_1}] = \left\{\frac{g^2 m_t \sin 2\theta_t}{64\pi^2 m_W^2 \sin^2\beta} m_{\tilde{t}_1}^2 \left(A_t m_6 \sin\beta + \mu\cos\beta\right) + \right. \tag{98}$$

$$\left. + \frac{g^2}{32\pi^2 m_W^2} m_{\tilde{t}_1}^2 \left[m_t^2 + m_Z^2 \cos 2\beta \left(X\cos^2\theta_t + Y\sin^2\theta_t\right)\right]\right\}\left(1 - \ln m_{\tilde{t}_1}^2\right)$$

and

$$F[\Pi_G^{h\tilde{t}_2}] + F[\Pi_G^{H\tilde{t}_2}] = \left\{-\frac{g^2 m_t \sin 2\theta_t}{64\pi^2 m_W^2 \sin^2\beta} m_{\tilde{t}_2}^2 \left(A_t m_6 \sin\beta + \mu\cos\beta\right) + \right. \tag{99}$$

$$\left. + \frac{g^2}{32\pi^2 m_W^2} m_{\tilde{t}_2}^2 \left[m_t^2 + m_Z^2 \cos 2\beta \left(X\sin^2\theta_t + Y\cos^2\theta_t\right)\right]\right\}\left(1 - \ln m_{\tilde{t}_2}^2\right)$$

The remaining part proportional to $(A_t m_6 \sin\beta + \mu\cos\beta)^2$ must be somehow removed by the problematic term

$$F[\Pi_G^{\tilde{t}_1\tilde{t}_2}] = \frac{g^2 m_t^2}{32\pi^2 m_W^2 \sin^2\beta} \left(A_t m_6 \sin\beta + \mu\cos\beta\right)^2 \int_0^1 \mathrm{d}x \ln D_0^{\tilde{t}_1\tilde{t}_2}(x) \tag{100}$$

But it is so because $D_0^{\tilde{t}_1\tilde{t}_2}(x) = m_{\tilde{t}_1}^2 x + m_{\tilde{t}_2}^2(1-x)$ and the integral can be handled by substituting $y \equiv m_{\tilde{t}_2}^2 + (m_{\tilde{t}_2}^2 - m_{\tilde{t}_2}^2)x$ and using a partial integration

$$\int_0^1 \mathrm{d}x \ln[m_{\tilde{t}_1}^2 x + m_{\tilde{t}_2}^2(1-x)] = \frac{1}{m_{\tilde{t}_1}^2 - m_{\tilde{t}_2}^2} \int_{m_{\tilde{t}_2}^2}^{m_{\tilde{t}_1}^2} \mathrm{d}y \ln y = \tag{101}$$

$$= \frac{1}{m_{\tilde{t}_1}^2 - m_{\tilde{t}_2}^2} \left[y\ln y - y\right]_{m_{\tilde{t}_2}^2}^{m_{\tilde{t}_1}^2} = \frac{1}{m_{\tilde{t}_1}^2 - m_{\tilde{t}_2}^2}\left[m_{\tilde{t}_1}^2\left(\ln m_{\tilde{t}_1}^2 - 1\right) - m_{\tilde{t}_2}^2\left(\ln m_{\tilde{t}_2}^2 - 1\right)\right]$$

Using this and (56) we can rewrite (100) into the form

$$F[\Pi_G^{\tilde{t}_1\tilde{t}_2}] = \frac{g^2 m_t \sin 2\theta_t}{64\pi^2 m_W^2 \sin^2\beta} \left(A_t m_6 \sin\beta + \mu\cos\beta\right) \times$$

$$\times \left[m_{\tilde{t}_1}^2\left(\ln m_{\tilde{t}_1}^2 - 1\right) - m_{\tilde{t}_2}^2\left(\ln m_{\tilde{t}_2}^2 - 1\right)\right] \tag{102}$$

It is easy to see that this expression exactly cancels the remaining terms from (98) and (99). We can then conclude

$$F[\Pi_G^{\tilde{t}_1\tilde{t}_2}] + F[\Pi_G^{h\tilde{t}_1}] + F[\Pi_G^{h\tilde{t}_2}] + F[\Pi_G^{H\tilde{t}_1}] + F[\Pi_G^{H\tilde{t}_2}] + F[\Pi_G^{\tilde{t}_1}] + F[\Pi_G^{\tilde{t}_2}] = 0 \tag{103}$$

which implies

$$\mathbf{F_G} = 0 \tag{104}$$

It means that (the quark and superquark parts of) the one-loop selfenergy of the neutral Goldstone scalar within the MSSM is zero, as was expected. To make this section more useful and self-contained it would be nice to compute the full MSSM neutral Goldstone boson one-loop two-particle OPI Green function which is out of the scope of this work.

4 Renormalisation group approach

In this chapter we investigate the (lightest) MSSM Higgs boson mass using the RGE techniques. This mass is shown to be proportional to the corresponding Higgs quartic self-coupling λ similarly as in the GWS model. The following subsection describes how to obtain GWS model as an effective limit of MSSM in region $\beta \to \frac{\pi}{2}$ (note that this is the only possibility to obtain the renormalized m_H significantly above m_Z), which simplifies computation performed in the next part of this chapter.

4.1 GWS model as an effective $\beta \to \frac{\pi}{2}$ theory

First thing to be stated is the fact, that in the $\beta \to \frac{\pi}{2}$ limit the neutral pseudoscalar A decouples from the theory; it is because its mass is proportional to $\frac{1}{v_1}$ which becomes infinite (see (13)). This means, that the bound (23) is saturated so $m_h \to m_Z$ in such a case. Relation (21) then implies decoupling of H. Moreover, from the relation (26) we see that $\beta \to \frac{\pi}{2}$ gives $\alpha \to 0$. These relations affect the effective structure of the Higgs sector. If we diagonalized the whole Higgs sector in chapter 1, we would obtain the following relation between the original doublets H_1 and H_2 and their physical content, i.e. h,H,A,$H^{\pm}$,G^0 and $G^{\pm}$:

$$H_1 = \begin{pmatrix} \sqrt{2}^{-1}\left(v_1 + H\cos\alpha - h\sin\alpha + iG^0\cos\beta + iA\sin\beta\right) \\ H^-\sin\beta + G^-\cos\beta \end{pmatrix} \tag{105}$$

$$H_2 = \begin{pmatrix} H^+\cos\beta - G^+\sin\beta \\ \sqrt{2}^{-1}\left(v_2 + H\sin\alpha + h\cos\alpha - iG^0\sin\beta + iA\cos\beta\right) \end{pmatrix} \tag{106}$$

Putting now $\beta = \frac{\pi}{2}$ and $\alpha = 0$, the doublet H_2 becomes

$$H_2 = \begin{pmatrix} -G^+ \\ \sqrt{2}^{-1}\left(v_2 + h - iG^0\right) \end{pmatrix} \tag{107}$$

which is (up to a minus sign of Goldstones) the same as in the GWS model in formulation [2], which we utilise in the next section. (Note that this difference does not affect the scheme used below, because the total number of Goldstones in vertices of all the considered diagrams is even.) Moreover, the interactions with the other non-SUSY fields have also the same form. In the effective low-energy approximation (i.e. with all the superheavy fields excluded) the lightest Higgs boson h can be identified with the usual GWS Higgs.

4.2 Derivation of β-function for the GWS Higgs quartic self-coupling λ

In this section we are going to derive the explicit form of the beta function $\beta_{\hat{\lambda}}$ in the GWS standard model (using formulation and notation of [2]). This object stands on the right-hand side of a differential equation for the running coupling constant $\bar{\lambda}$, which is (for our purposes) the most important quantity within the considered renormalisation group technique (see [2],[16])). To be able to compute $\beta_{\hat{\lambda}}$ we first have to renormalize the Higgs sector of the theory, i.e. define the renormalisation constants and compute the corresponding counterterms. It is then straightforward to derive the beta-function out of the results of the previous step.

4.2.1 Renormalisation of the GWS Higgs sector

We start with the GWS Higgs boson bare Lagrangian

$$\mathcal{L}^B_{\text{HIGGS}} = (D_\mu \phi_B)^\dagger (D^\mu \phi_B) - m_B^2 \phi_B^\dagger \phi_B - \frac{1}{4}\lambda_B (\phi_B^\dagger \phi_B)^2 \tag{108}$$

where

$$\phi \equiv \begin{pmatrix} G_B^+ \\ \frac{1}{\sqrt{2}}(v_B + H_B + G_B^0) \end{pmatrix} \tag{109}$$

Expanding the expression (108) with the help of (109) we obtain

$$\mathcal{L}^B_{\text{HIGGS}} = \frac{1}{2}\partial_\mu H_B \partial^\mu H_B - \frac{1}{16}\lambda_B H_B^4 + \dots \tag{110}$$

The terms denoted by ... are not important now. This bare Lagrangian is then expressed in the form

$$\mathcal{L}^B_{\text{HIGGS}} = \mathcal{L}_{\text{HIGGS}} + \delta\mathcal{L}_{\text{HIGGS}} \tag{111}$$

where

$$\mathcal{L}_{\text{HIGGS}} = \frac{1}{2}\partial_\mu H \partial^\mu H - \frac{1}{16}\lambda H^4 + \dots \tag{112}$$

and the counterterm-Lagrangian

$$\delta\mathcal{L}_{\text{HIGGS}} = \Delta Z_H \frac{1}{2}\partial_\mu H \partial^\mu H - \frac{1}{16}\delta\lambda H^4 + \dots \tag{113}$$

The wave-function renormalization constant is defined by

$$H_B = \sqrt{Z_H} H \tag{114}$$

and can be expressed in terms of ΔZ_H like $Z_H = 1 + \Delta Z_H$. The counterterm $\delta\lambda$ is related to the bare quantities by

$$\lambda_B Z_H^2 = \lambda + \delta\lambda \tag{115}$$

It is usual to factorize λ out of $\delta\lambda$ as $\delta\lambda = \lambda K_\lambda$. This allows us to rewrite (115) in the final form

$$\lambda_B = \lambda(1 + K_\lambda) Z_H^{-2} \tag{116}$$

Having computed both the K_λ and ΔZ_H we will calculate $\beta_{\hat{\lambda}}$ as a logarithmic derivative of λ from (116) (holding λ_B constant)

$$\beta_{\hat{\lambda}} = \mu \frac{\partial \hat{\lambda}}{\partial \mu} \tag{117}$$

(The exact connection between λ and $\hat{\lambda}$ will be defined later.)

4.2.2 Calculation of the renormalisation constants ΔZ_H and K_λ

The constants ΔZ_H and K_λ play the role of parameters describing the additional interactions coming from the counterterm-Lagrangian (113) which generates the following Feynman rules (including symmetry factors corresponding to the permutations of external dashed lines):

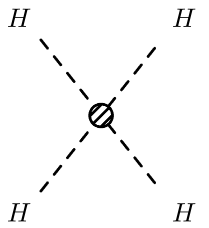

$$\sim \quad -\frac{3}{2} i\lambda K_\lambda \tag{118}$$

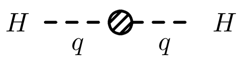

$$\sim \quad i(\Delta Z_H q^2 - \delta m^2) \tag{119}$$

The term δm^2 corresponds to the mass renormalisation and is not important for further discussion so we drop it out.

We shall compute the two- and four-particle OPI-Green functions $\Gamma^{(2)}(q,-q)$ and $\Gamma^{(4)}(q_1,q_2,q_3,q_4)$. These quantities should be finite in any renormalisation scheme. All the possible divergences must be therefore absorbed into the renormalisation constants. We will work in the so-called minimal subtraction (MS) scheme in which only the divergent parts of relevant Feynman diagrams are cancelled by the definition of counterterms. (Note that the particular choice of a renormalisation scheme can not affect the resulting one-loop beta-function and the MS scheme is chosen for simplicity.)

We are going to compute all the quantities at the one-loop level of the perturbation theory. The whole calculation will be performed in a general R_ξ gauge; we fix this gauge because:

- The vector boson propagator in ultraviolet region decreases as $\frac{1}{k^2}$ (it is *not* so in the unitary gauge) which causes that several one-loop OPI-diagrams involving gauge bosons are convergent and therefore do not contribute to the counterterm K_λ (in the unitary gauge they would be highly divergent); examples of such diagrams are

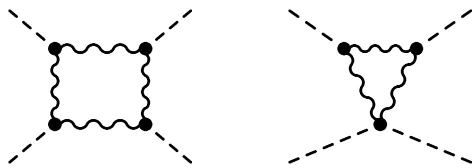

(120)

  with (R_ξ) superficial degrees of divergence -2 and -1.

- Up to my knowledge there is no explicit discussion of the gauge parameter independence of the one-loop $\beta_{\hat{\lambda}}$ function in the literature and it is quite interesting to inspect it in details

We are now ready to investigate the set of all the divergent one-loop OPI Feynman graphs contributing to K_λ and ΔZ_H. There are six types of relevant diagrams in the first and two types in the second cathegory

- Diagrams contributing to the pure vertex renormalisation K_λ:

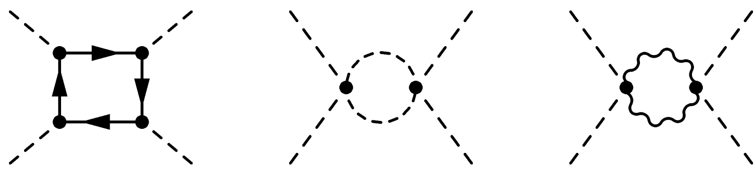

(121)

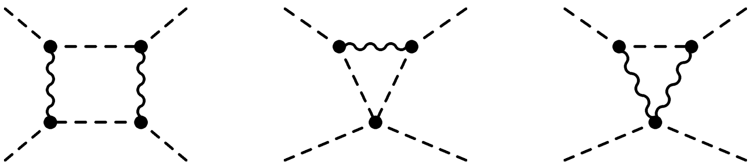

(122)

The lines with arrows in the first type denotes all the fermions of the theory, every external line describes the Higgs boson, the internal dashed lines correspond to the Goldstone bosons (in the second diagram also to the Higgses). Any internal wavy line denotes the gauge bosons W and Z.

- Diagrams contributing to the renormalisation of the wave function Z_H:

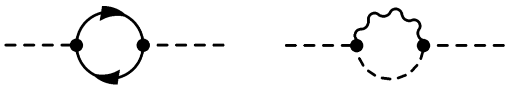

(123)

The first loop again corresponds to all possible fermions and the second contains one Goldstone and one vector bosons. Note that there are no diagrams with pure vector-boson loops contributing to ΔZ_H because the coupling constant of VVH vertex is proportional to masses of the vector-bosons so the regularised integral is logarithmically divergent and its singularity can not contain any external momenta dependent term. The same holds also for graphs containing the Faddeev-Popov ghosts.

The whole computation will be performed in dimension $d \equiv 4 - 2\varepsilon$ and all the diagrams above will be regularised by using standard dimensional regularisation procedure. Let us first recall the relevant interaction Lagrangian in dimension d. Note that the dimensionalities (in units of mass) of fields in this case are

$$[\phi] = \frac{d}{2} - 1, \qquad [V] = \frac{d}{2} - 1, \qquad [f] = \frac{d-1}{2} \tag{124}$$

(The ϕ, V and f are generic symbols for Higgs and Goldstone bosons, vector bosons and fermions respectively.) Hence the relevant coupling must be redefined (to keep the dimension of Lagrangian to be d) to the form

- Yukawa term describing interactions of fermions with the Higgs scalars:

$$\mathcal{L}^{(4)}_{Hff} \equiv -\frac{1}{\sqrt{2}} h_f \bar{f} f H \to \mathcal{L}^{(d)}_{Hff} \equiv -\mu^{\varepsilon} \frac{1}{\sqrt{2}} \hat{h}_f \bar{f} f H \quad (\text{where} \quad \hat{h}_f \equiv h_f \mu^{-\varepsilon}) \tag{125}$$

(the hat is used to express the fact that the coupling $\hat{h}_f$ is dimensionless; note that the original h_f has no longer this nice property and that is why we write down the Lagrangian in terms of 'hatted' parameters). Similarly for the other couplings.

- Quartic interactions of Higgs and Goldstone bosons:

$$\begin{aligned} \mathcal{L}^{(4)}_{\phi} &\equiv -\frac{1}{16}\lambda H^4 - \frac{1}{8}\lambda {G^0}^2 H^2 - \frac{1}{4}\lambda G^+ G^- H^2 \to \quad (\text{using} \quad \hat{\lambda} \equiv \lambda \mu^{-2\varepsilon}) \\ \mathcal{L}^{(d)}_{\phi} &\equiv -\mu^{2\varepsilon}\frac{1}{16}\hat{\lambda} H^4 - \mu^{2\varepsilon}\frac{1}{8}\hat{\lambda} {G^0}^2 H^2 - \mu^{2\varepsilon}\frac{1}{4}\hat{\lambda} G^+ G^- H^2 \end{aligned} \tag{126}$$

- Quartic interactions of Higgs and vector bosons:

$$\begin{aligned} \mathcal{L}^{(4)}_{HHVV} &\equiv \frac{1}{8}(g^2 + {g'}^2) Z_\mu Z^\mu H^2 + \frac{1}{4} g^2 W^-_\mu W^{+\mu} H^2 \to \quad (\hat{g}^2 = g^2 \mu^{-2\varepsilon}) \\ \mathcal{L}^{(d)}_{HHVV} &\equiv \mu^{2\varepsilon}\frac{1}{8}(\hat{g}^2 + {\hat{g}'}^2) Z_\mu Z^\mu H^2 + \mu^{2\varepsilon}\frac{1}{4}\hat{g}^2 W^-_\mu W^{+\mu} H^2 \end{aligned} \tag{127}$$

- Trilinear coupling of Higgs, Goldstone and vector bosons:

$$\begin{aligned}\mathcal{L}^{(4)}_{HGV} &\equiv g(H\overset{\leftrightarrow}{\partial^{\mu}}G^{+}W^{-}_{\mu} + \text{h.c.}) + \frac{1}{2}\sqrt{g^2+g'^2}H\overset{\leftrightarrow}{\partial^{\mu}}G^{0}Z_{\mu} \rightarrow \\ \mathcal{L}^{(d)}_{HGV} &\equiv \mu^{\varepsilon}\hat{g}(H\overset{\leftrightarrow}{\partial^{\mu}}G^{+}W^{-}_{\mu} + \text{h.c.}) + \mu^{\varepsilon}\frac{1}{2}\sqrt{\hat{g}^2+\hat{g}'^2}H\overset{\leftrightarrow}{\partial^{\mu}}G^{0}Z_{\mu} \qquad (128)\end{aligned}$$

Now we are in a position to carry out an explicit computation of the relevant diagrams.

I. Vertex renormalisation parameter K_λ

Let us start with the first diagram in (121). Using (125) we can write down

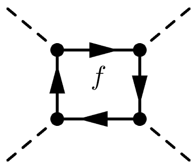

$$\equiv C_{h_f^4} \sim \sum_f N_{cf}\mu^{2\varepsilon}(-1)\left(i\frac{\hat{h}_f}{\sqrt{2}}\right)^4 \frac{\mathrm{n_c}}{4!}\times \qquad (129)$$

$$\times \,\mathrm{Tr}\int\frac{d^dk}{(2\pi)^d}\frac{i^4\mu^{2\varepsilon}}{(\not{k}-m_f)(\not{k}+\not{q}_2-m_f)(\not{k}+\not{q}_2+\not{q}_3-m_f)(\not{k}+\not{q}_2+\not{q}_3+\not{q}_4-m_f)}$$

Here the constant $\mathrm{n_c} = 144$ counts all the possible contractions leading to the OPI graphs of this type and N_{cf} is the colour factor of the considered fermion field, i.e. $N_{cq} = 3$ for quarks and $N_{cl} = 1$ for leptons. External momenta $q_1 \dots q_4$ are denoted clockwise. The integral is regularised in the appendix A (224). Using this result we can rewrite the last expression in the form

$$C_{h_f^4} \overset{\text{DR}}{\sim} -6\sum_f N_{cf}\hat{h}_f^4\mu^{2\epsilon}\frac{i}{16\pi^2\varepsilon} + \text{finite} \qquad (130)$$

Next, there are three diagrams of the second type in (121); with the help of (126) we obtain

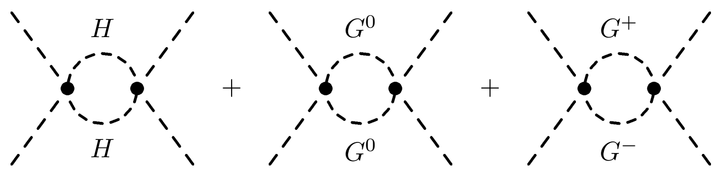

$$\equiv C^a_{\lambda^2} + C^b_{\lambda^2} + C^c_{\lambda^2} \qquad (131)$$

where

$$\begin{aligned}C^a_{\lambda^2} &= \left(-i\frac{\hat{\lambda}}{16}\right)^2\mu^{2\varepsilon}\frac{\mathrm{n}^a_c}{2}\int\frac{d^dk}{(2\pi)^d}\frac{i^2}{(k^2-m_H^2)[(k-q)^2-m_H^2]} \\ C^b_{\lambda^2} &= \left(-i\frac{\hat{\lambda}}{8}\right)^2\mu^{2\varepsilon}\frac{\mathrm{n}^b_c}{2}\int\frac{d^dk}{(2\pi)^d}\frac{i^2}{(k^2-\xi m_Z^2)[(k-q)^2-\xi m_Z^2]} \\ C^c_{\lambda^2} &= \left(-i\frac{\hat{\lambda}}{4}\right)^2\mu^{2\varepsilon}\frac{\mathrm{n}^c_c}{2}\int\frac{d^dk}{(2\pi)^d}\frac{i^2}{(k^2-\xi m_W^2)[(k-q)^2-\xi m_W^2]} \qquad (132)\end{aligned}$$

It can be easily checked that the numbers of relevant contractions are the following: $\mathrm{n}^a_c = 24\times 36$, $\mathrm{n}^b_c = 24\times 2$ and $\mathrm{n}^c_c = 24$. The integrals of the same type as in (132) are regularised in (187). Extracting only the part proportional to $\frac{1}{\varepsilon}$ we can conclude

$$\begin{aligned}C^a_{\lambda^2} &\overset{\text{DR}}{\sim} \frac{27}{8}\mu^{2\varepsilon}\hat{\lambda}^2\frac{i}{16\pi^2\varepsilon} + \text{finite} \\ C^b_{\lambda^2} &\overset{\text{DR}}{\sim} \frac{3}{8}\mu^{2\varepsilon}\hat{\lambda}^2\frac{i}{16\pi^2\varepsilon} + \text{finite} \\ C^c_{\lambda^2} &\overset{\text{DR}}{\sim} \frac{3}{4}\mu^{2\varepsilon}\hat{\lambda}^2\frac{i}{16\pi^2\varepsilon} + \text{finite} \qquad (133)\end{aligned}$$

which together gives

$$C_{\lambda^2} \equiv C^a_{\lambda^2} + C^b_{\lambda^2} + C^c_{\lambda^2} = \frac{9}{2}\mu^{2\varepsilon}\hat{\lambda}^2 \frac{i}{16\pi^2\varepsilon} + \text{finite} \tag{134}$$

The next type of diagrams contributing to the parameter K_λ are the following (the third type in (121)):

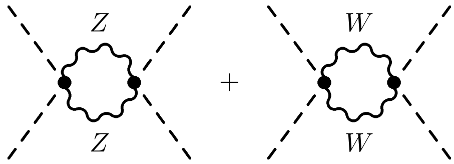

$$+ \quad \equiv C^a_{g^4} + C^b_{g^4} \tag{135}$$

where

$$\begin{aligned} C^a_{g^4} &= \left[-\frac{i}{8}(\hat{g}^2 + \hat{g}'^2)\right]^2 \frac{\mathrm{n}^a_c}{2}\mu^{4\varepsilon}\int \frac{\mathrm{d}^d k}{(2\pi)^d} g_{\mu\rho} g_{\nu\sigma} D^{\mu\nu}_{\xi,Z}(k) D^{\rho\sigma}_{\xi,Z}(k-q) \\ C^b_{g^4} &= \left(-\frac{i}{4}\hat{g}^2\right)^2 \frac{\mathrm{n}^b_c}{2}\mu^{4\varepsilon}\int \frac{\mathrm{d}^d k}{(2\pi)^d} g_{\mu\rho} g_{\nu\sigma} D^{\mu\nu}_{\xi,W}(k) D^{\rho\sigma}_{\xi,W}(k-q) \end{aligned} \tag{136}$$

Here we have denoted by $D_{\xi,X}(k)$ the Feynman propagator of the intermediate vector boson X in the R_ξ gauge, namely

$$D^{\mu\nu}_{\xi,X}(k) \equiv -i\left[\frac{g^{\mu\nu} - (1-\xi)k^\mu k^\nu (k^2 - \xi m_X^2)^{-1}}{k^2 - m_X^2 + i\varepsilon}\right] \tag{137}$$

Moreover, q is the sum of the external momenta incoming to the left vertex. The numbers of appropriate contractions can be easily computed with results $\mathrm{n}^a_c = 48$ and $\mathrm{n}^b_c = 24$. The explicit regularisation is quite long and tedious but standard, so we omit it; the results are

$$\begin{aligned} C^a_{g^4} &\overset{\text{DR}}{\sim} \frac{3}{8}(\hat{g}^2 + \hat{g}'^2)^2 \mu^{2\varepsilon}\frac{(3+\xi^2)i}{16\pi^2\varepsilon} + \text{finite} \\ C^b_{g^4} &\overset{\text{DR}}{\sim} \frac{3}{4}\hat{g}^4 \mu^{2\varepsilon}\frac{(3+\xi^2)i}{16\pi^2\varepsilon} + \text{finite} \end{aligned} \tag{138}$$

There are three more types of diagrams to be considered. Note that all of them are UV-finite within the Landau gauge. Regularisations are again not performed because they are even more complex (but simple in principle) to be shown in detail. Let us write down the results (the divergent parts only):

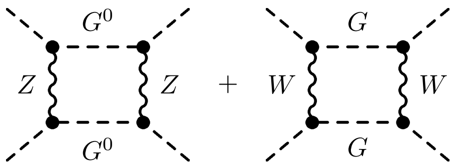

$$+ \quad \overset{\text{DR}}{\sim} \frac{3}{8}\left[2\hat{g}^4 + \left(\hat{g}^2 + \hat{g}'^2\right)^2\right]\frac{\mu^{2\varepsilon}\xi^2 i}{16\pi^2\varepsilon} \tag{139}$$

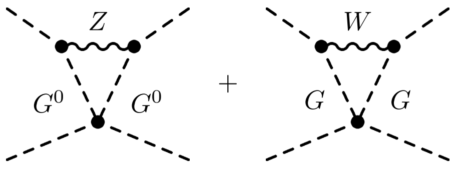

$$+ \quad \overset{\text{DR}}{\sim} -\frac{3}{4}\left[2\hat{g}^2 + \left(\hat{g}^2 + \hat{g}'^2\right)\right]\hat{\lambda}\frac{\mu^{2\varepsilon}\xi i}{16\pi^2\varepsilon} \tag{140}$$

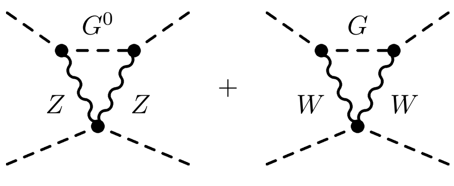

$$+ \quad \overset{\text{DR}}{\sim} -\frac{3}{4}\left[2\hat{g}^4 + \left(\hat{g}^2 + \hat{g}'^2\right)^2\right]\frac{\mu^{2\varepsilon}\xi^2 i}{16\pi^2\varepsilon} \tag{141}$$

Suming up the previous relations we obtain

$$(138) + (139) + (140) + (141) = \left\{ \frac{9}{8} \left[(\hat{g}^2 + \hat{g}'^2)^2 + 2\hat{g}^4 \right] - \frac{3}{4} \left(3\hat{g}^2 + \hat{g}'^2 \right) \hat{\lambda}\xi \right\} \frac{i\mu^{2\varepsilon}}{16\pi^2\varepsilon}$$

It is now easy to compute the renormalisation constant K_λ. Diagrams (129),(131) and (135) together with the counterterm (118) (transformed to d dimensions) are the only that could contribute to the divergent part of the four-particle OPI-Green function

$$\begin{aligned} \Gamma^{(4)}(q_1, q_2, q_3, q_4) \; &= \; \mu^{2\epsilon} \frac{i}{16\pi^2\varepsilon} \Big\{ -6 \sum_f N_{cf} \hat{h}_f^4 + \frac{9}{2}\hat{\lambda}^2 + \frac{9}{8} \left[(\hat{g}^2 + \hat{g}'^2)^2 + 2\hat{g}^4 \right] - \\ &- \frac{3}{4} \left(3\hat{g}^2 + \hat{g}'^2 \right) \hat{\lambda}\xi \Big\} - i\frac{3}{2}\mu^{2\varepsilon}\hat{\lambda}K_\lambda + \text{finite} \end{aligned} \tag{142}$$

This Green function should be finite in any renormalisation scheme. It can be ensured by the particular choice of the counterterm

$$K_\lambda = \frac{1}{16\pi^2\varepsilon} \Big\{ -4\hat{\lambda}^{-1} \sum_f N_{cf} \hat{h}_f^4 + 3\hat{\lambda} + \frac{3}{4}\hat{\lambda}^{-1} \left[(\hat{g}^2 + \hat{g}'^2)^2 + 2\hat{g}^4 \right] - \frac{1}{2} \left(3\hat{g}^2 + \hat{g}'^2 \right) \xi \Big\} \tag{143}$$

(this definition corresponds to the so-called MS-scheme but the resulting RGE does not depend on its concrete choice and we use this scheme only for the sake of simplicity).

II. Higgs boson wave function renormalisation constant ΔZ_H

The types of diagrams necessary for ΔZ_H computation are those written in (123). The first of them:

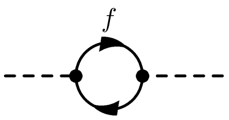

$$\equiv \quad C_{h_f^2} \quad \sim \quad \sum_f N_{cf} \left(i\frac{\hat{h}_f}{\sqrt{2}} \right)^2 (-1) \times \tag{144}$$

$$\times \, \mathrm{Tr} \int \frac{d^d k}{(2\pi)^d} \frac{\mu^{2\varepsilon} i^2}{(\not{k} - m_f)(\not{k} - \not{q} - m_f)} \tag{145}$$

Regularisation of the above integral is performed in the Appendix A (see (204) for $A = C = 1$, $B = D = 0$ and $m = m_f$) and the result sounds

$$C_{h_f^2} \overset{\text{DR}}{\sim} -\sum_f N_{cf} 2\hat{h}_f^2 \frac{i}{16\pi^2\varepsilon} \left(3m_f^2 - \frac{q^2}{2} \right) + \text{finite} \tag{146}$$

The last diagrams to be considered here are the following:

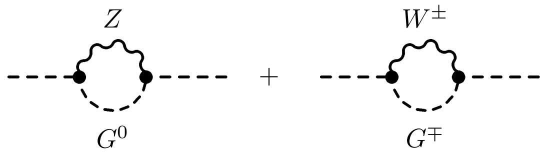

$$\equiv \quad C_{g^2}^a + 2C_{g^2}^b \tag{147}$$

where

$$\begin{aligned} C_{g^2}^a \;&=\; \frac{1}{4}(\hat{g}^2 + \hat{g}'^2)\mu^{2\varepsilon} \int \frac{d^d k}{(2\pi)^d} \frac{i(k+q)_\mu(-k-q)_\nu D_{\xi,Z}^{\mu\nu}(k-q)}{k^2 - \xi m_Z^2} \\ C_{g^2}^b \;&=\; \frac{1}{4}\hat{g}^2\mu^{2\varepsilon} \int \frac{d^d k}{(2\pi)^d} \frac{i(k+q)_\mu(-k-q)_\nu D_{\xi,W}^{\mu\nu}(k-q)}{k^2 - \xi m_W^2} \end{aligned} \tag{148}$$

Looking at (230) in the Appendix A we can conclude (the 'stg.' denotes the part of divergence that does not affect wave function renormalisation constant i.e. does not depend on the external momenta q)

$$\begin{aligned} C^a_{g^2} &\overset{\mathrm{DR}}{\sim} -\frac{1}{4}(\hat{g}^2+\hat{g}'^2)\frac{(3-\xi)i}{16\pi^2\varepsilon}q^2+\text{stg.}+\text{finite} \\ 2C^b_{g^2} &\overset{\mathrm{DR}}{\sim} -\frac{1}{2}\hat{g}^2\frac{(3-\xi)i}{16\pi^2\varepsilon}q^2+\text{stg.}+\text{finite} \end{aligned} \tag{149}$$

Collecting the previous results we can conclude

$$C_{g^2} \equiv C^a_{g^2}+2C^b_{g^2} \overset{\mathrm{DR}}{\sim} -\frac{3-\xi}{4}\frac{i}{16\pi^2\varepsilon}(3\hat{g}^2+\hat{g}'^2)q^2+\text{stg.}+\text{finite} \tag{150}$$

We are now ready to construct the corresponding one-loop two-particle OPI Green function. Suming up contributions (146) and (150) together with the counterterm (120) we can write

$$\Gamma^{(2)}(q,-q) = \frac{i}{16\pi^2\varepsilon}\Big[\sum_f N_{cf}\hat{h}^2_f - \frac{3-\xi}{4}(3\hat{g}^2+\hat{g}'^2)\Big]q^2 + i\Delta Z_H q^2+\text{stg.}+\text{finite} \tag{151}$$

As in the previous case this Green function should be finite in any renormalisation scheme. In the MS-scheme this corresponds to the following definition of the wave-function renormalisation constant:

$$\Delta Z_H = \frac{1}{16\pi^2\varepsilon}\Big[-\sum_f N_{cf}\hat{h}^2_f + \frac{3-\xi}{4}(3\hat{g}^2+\hat{g}'^2)\Big] \tag{152}$$

Derivation of the $\beta_{\hat{\lambda}}$-function

Now we have prepared all the necessary ingredients to write down the $\beta_{\hat{\lambda}}$-function defined by

$$\beta_{\hat{\lambda}} = \mu\frac{\partial\hat{\lambda}}{\partial\mu} \tag{153}$$

Recalling the relation $\hat{\lambda}=\lambda\mu^{-2\varepsilon}$ one gets

$$\mu\frac{\partial\hat{\lambda}}{\partial\mu} = \mu^{-2\varepsilon+1}\frac{\partial\lambda}{\partial\mu} - 2\varepsilon\hat{\lambda} \tag{154}$$

To evaluate it we express λ_B from (116) in terms of the renormalisation parameters and expand it to the first order

$$\lambda_B = \lambda(1+K_\lambda)Z_H^{-2} = \lambda(1+K_\lambda-2\Delta Z_H)+\text{higher order terms} \tag{155}$$

Differentiating both sides with respect to μ (holding λ_B constant and neglecting the higher order contributions) we get

$$\frac{\partial\lambda}{\partial\mu}(1+K_\lambda-2\Delta Z_H)+\lambda\left(\frac{\partial K_\lambda}{\partial\mu}-2\frac{\partial\Delta Z_H}{\partial\mu}\right)=0 \tag{156}$$

which can be (with the same accuracy) recast in the form

$$\frac{\partial\lambda}{\partial\mu} = \lambda\left(-\frac{\partial K_\lambda}{\partial\mu}+2\frac{\partial\Delta Z_H}{\partial\mu}\right) \tag{157}$$

Now, the derivatives on the right-hand side can be obtained from (143) and (152):

$$\begin{aligned} \frac{\partial K_\lambda}{\partial\mu} &= -2\varepsilon\mu^{-1}K_\lambda+\text{higher order terms} \\ \frac{\partial\Delta Z_H}{\partial\mu} &= -2\varepsilon\mu^{-1}\Delta Z_H+\text{higher order terms} \end{aligned} \tag{158}$$

Collecting (153),(154) and (158) we can rewrite the $\beta_{\hat{\lambda}}$-function in the form

$$\beta_{\hat{\lambda}} = \hat{\lambda}\varepsilon\,(2K_\lambda - 4\Delta Z_H) - 2\varepsilon\hat{\lambda} \tag{159}$$

Substituting for K_λ and ΔZ_H from (143) and (152) and neglecting the last term proportional to ε we conclude

$$\beta_{\hat{\lambda}} = \frac{1}{16\pi^2}\Big\{-8\sum_f N_{cf}\hat{h}_f^4 + 6\hat{\lambda}^2 + \frac{3}{2}\left[(\hat{g}^2+\hat{g}'^2)^2 + 2\hat{g}^4\right] + \\ + 4\hat{\lambda}\sum_f N_{cf}\hat{h}_f^2 - 3\hat{\lambda}(3\hat{g}^2+\hat{g}'^2)\Big\} \tag{160}$$

(Note that although both the K_λ and ΔZ_H depend on the gauge-fixing parameter ξ, the final expression is ξ-independent.) This is the most important result of this subsection. It can be easily checked that the equation (160) is in agreement with results given previously in the literature (without any derivation in [20] or [10] or within the Landau gauge in [6]).

Discussion of the $\beta_{\hat{\lambda}}$ function

Now we are going to discuss the relative importance of the terms in (160); this information will be useful in the next section where we try to find at least an approximate value of the running coupling at the weak scale.

Values of the couplings h_f, g, g' and λ can be estimated from the relations with the (tree level) masses of the corresponding particles. Using

$$h_f^2 = \frac{2m_f^2}{v^2}, \qquad \lambda = \frac{2m_H^2}{v^2}, \qquad g^2 + g'^2 = \frac{4m_Z^2}{v^2} \qquad \text{and} \qquad g^2 = \frac{4m_W^2}{v^2} \tag{161}$$

we can state, that the most important factor comes from the Yukawa coupling for the top-quark (with mass about 175 Gev). Relative values of the other terms in $\beta_{\hat{\lambda}}$ compared to the $-24h_t^4$ term (with one exception only - the term $12\lambda h_t$) do not exceed about 3%, as can be seen from the tables

mass parameter	m_t	m_H	m_Z^2	m_W^2
approximate value	175 GeV	$\sim$ 100 GeV	91 GeV	82 Gev
corresponding coupling	h_t^2	λ	$g^2+g'^2$	g^2
approximate value	~ 1	~ 0.3	~ 0.5	~ 0.4

term	approximate value	relative to $24h_t^4$
$24h_t^4$	24	1
$6\lambda^2$	0.5	2%
$\frac{3}{2}(\hat{g}^2+\hat{g}'^2)^2$	0.4	1.5 %
$3\hat{g}^4$	0.5	2%
$12\lambda h_t^2$	3.6	15%
$6\lambda g^2$	0.7	3%
$3\lambda(g^2+g'^2)$	0.4	2%

In the following subsection we attempt to solve a differential equation for the *running coupling constant* $\bar{\lambda}$ which describes the evolution of λ as a function of the subtraction scale μ.

4.3 The running coupling constant $\bar{\lambda}$ and the Higgs mass

The quantity called *running coupling constant* $\bar{\lambda}$ is defined in terms of the previously computed $\beta_{\hat{\lambda}}$ (160) function by the equation (see for example [2])

$$\mu \frac{\mathrm{d}\bar{\lambda}(\mu)}{\mathrm{d}\mu} = \beta_{\hat{\lambda}}[\bar{\lambda}(\mu), \ldots] \tag{162}$$

Although the parameters denoted by $\ldots$ (h_f,g and g') in general fulfill similar differential equations so they are also some functions of μ, we assume [20] that they do not change too rapidly in the region 100 GeV $\sim m_{\mathrm{SUSY}}$ and can be approximated by constants. Moreover, the tables above inform us about the relative importance of the terms in (160). We can see that the right hand side of (162) can be (with sufficient accuracy about 3%) approximated by the terms containing Yukawa coupling of the top quark h_t only. This is an improvement of disscusion presented in [20], where the only considered term is the leading factor $-24h_t^4$. Doing this, we obtain

$$\mu \frac{\mathrm{d}\bar{\lambda}(\mu)}{\mathrm{d}\mu} = \frac{1}{16\pi^2}\left[-24h_t^4 + 12h_t^2\bar{\lambda}(\mu)\right] \tag{163}$$

We will solve this equation with the initial condition $\lambda(m_{\mathrm{SUSY}}) = \frac{1}{2}(g^2 + g'^2)$ which in fact connects the 'effective' non-supersymmetric theory (GSW standard model) with the MSSM ([10],[20]). Solution of the previous equation is trivial (note its separability) and fulfills the (algebraic) equation (obtained by integration)

$$\ln\left[\frac{a + b\bar{\lambda}(\mu)}{a + b\lambda(m_{\mathrm{SUSY}})}\right] = b\ln\left(\frac{\mu}{m_{\mathrm{SUSY}}}\right) \qquad \text{with} \quad a \equiv -\frac{24h_t^4}{16\pi^2} \quad \text{and} \quad b \equiv \frac{12h_t^2}{16\pi^2} \tag{164}$$

(note that $b \ll 1$). Removing logarithms and expanding the right-hand side

$$\left(\frac{\mu}{m_{\mathrm{SUSY}}}\right)^b \doteq 1 + b\ln\left(\frac{\mu}{m_{\mathrm{SUSY}}}\right) \tag{165}$$

we obtain

$$\bar{\lambda}(\mu) \doteq \lambda(m_{\mathrm{SUSY}}) + a\ln\left(\frac{\mu}{m_{\mathrm{SUSY}}}\right) + b\lambda(m_{\mathrm{SUSY}})\ln\left(\frac{\mu}{m_{\mathrm{SUSY}}}\right) \tag{166}$$

Evaluating this expression we get (utilising $m_Z^2 = \frac{1}{4}(g^2 + g'^2)v^2$)

$$\frac{1}{2}\bar{\lambda}(\mu) \doteq \frac{m_Z^2}{v^2} + \frac{3h_t^4}{16\pi^2}\ln\left(\frac{m_{\mathrm{SUSY}}^4}{\mu^4}\right) - \frac{3h_t^2}{16\pi^2}\frac{m_Z^2}{v^2}\ln\left(\frac{m_{\mathrm{SUSY}}^4}{\mu^4}\right) \tag{167}$$

Using now (see [10],[20])

$$m_h^2 = \frac{1}{2}\lambda(m_h^2)v^2(m_h^2), \qquad m_W^2 = \frac{1}{4}g^2v^2 \qquad \text{and} \qquad h_f = \sqrt{2}\frac{m_f}{v} \tag{168}$$

we can conclude

$$m_h^2 \doteq m_Z^2 + \frac{3m_t^4g^2}{16\pi^2m_W^2}\ln\left(\frac{m_{\mathrm{SUSY}}^4}{m_h^4}\right) - \frac{3m_t^2g^2}{32\pi^2m_W^2}m_Z^2\ln\left(\frac{m_{\mathrm{SUSY}}^4}{m_h^4}\right) \tag{169}$$

The first positive term corresponds to the result of [20], the second (negative) is an improvement of magnitude about 15% .

The result (169) allows us to state, that the tree-level 'effective' relation $m_h \to m_Z$ (which provides an upper bound for m_h) receives a large positive one loop correction. Numerically, for $m_{\mathrm{SUSY}} \sim 1 - 100$ TeV the new upper bound (169) constraints the Higgs mass by the values about $130 - 190$ GeV, which is (up to now) experimentally acceptable.

Conclusion

This work should provide a rather detailed review of the Higgs boson spectrum within the Minimal Supersymmetric Standard Model (MSSM) at the level of one-loop radiative corrections. The unsatisfactory tree-level mass bound for the lightest Higgs scalar mass was recast using two methods: an explicite diagramatic calculation and a renormalisation group approach. We use the usual dimensional regularisation procedure to handle the ultraviolet divergences coming from the Feynman diagrams containing loops. The text consists of four main parts:

In the first chapter we have recalled the tree-level MSSM Higgs boson spectrum and the known upper bound for the lightest MSSM Higgs scalar $m_h \leq m_Z|\cos 2\beta|$. Several other relations that usually are not given in the literature were derived for later convenience.

In the second chapter we discuss the renormalisation of the the tree-level relation $m_h^2 + m_H^2 = m_A^2 + m_Z^2$ by performing a (restricted) diagrammatic calculation. The important feature of the calculation is the fact that the divergent parts of the corresponding counterterms exactly cancel. We have adopted the usual on-shell renormalisation scheme which allowed us to use many tree-level relations among the MSSM parameters derived in the first part. The only significant contribution comes from the top-supertop sector of the theory. (The unitary gauge is fixed so that the number of relevant diagrams is reduced; note that there are still 28 remaining graphs which are catalogized and regularised in Appendix A). We have recovered the well known large positive correction to the Higgs masses proportional to $\frac{m_t^4}{m_Z^2}$ To compute the leading logarithmic approximation we have neglected all the terms of magnitudes $\frac{m_t^3}{m_Z}$ and smaller. (The expected large contributions proportional to $m_{\tilde{t}}^2$ coming from the graphs involving stop loops turns to be negligible in the case of a small mixing in the squark sector, see [4].) These results are in agreement with the relations obtained earlier by various authors ([4],[8],[9]). The explicite mechanism of divergence cancellation (which does not appear in the literature) is exhibited in detail within the mentioned unitary gauge. Some further comments on the situation in R_ξ gauges are included.

In the third chapter we examine the MSSM neutral Goldstone boson self-energy at the one-loop level. We restrict ourselves on the graphs coming from the top and supertop sector only. The expected cancellation of one-loop self-energy contributions is confirmed. Up to my knowledge there is no such an explicit computation in the literature. Both in this and in the previous chapters we use the fact that many diagrams contributing to the Goldstone boson propagator can be easily obtained from diagrams for the MSSM pseudoscalar A and vice versa.

The connection between the MSSM and the original Standard Model is briefly reviewed at the beginning of the fourth chapter. From this point of view the GWS Higgs boson corresponds to the lightest MSSM Higgs scalar in the $\beta \to \frac{\pi}{2}$ limit ([17], [20],[10]). Therefore we have used the GWS model as an effective theory and computed the $\beta_{\hat{\lambda}}$-function for the quartic Higgs self-coupling λ in order to pull it on the mass shell down from the SUSY-region. The calculation is performed within an R_ξ gauge which provides a generalisation of some earlier computations in Landau-gauge ([6]). This generalisation is not completely straightforward because there are some extra UV-divergent graphs that do not contribute in the Landau Gauge. The on-shell coupling is then used to derive the one-loop leading correction to the tree-level relation $m_h \leq m_Z$. We have improved the results of [20] using a better approximation of the $\beta_{\hat{\lambda}}$-function.

The results of both the diagrammatic and the RGE methods are rather similar: the original unsatisfactory tree-level prediction $m_h \leq m_Z$ receives a large correction which shifts the upper bound above the recently accessible energies.

Appendices

A Dimensional regularization

A.1 General remarks

The main aim of this section is to perform the procedure of dimensional regularization of divergent integrals in all the cases relevant for our purposes and prove the results presented by Aoki et all in [1]. For the sake of brevity we will adopt some formulae from the literature. It is necessary to say that the following derivations will be more intuitive than fully mathematically rigorous and the used scheme *definition-statement-proof* is to be understood in the same manner. We are also going to use the ' $\stackrel{\mathrm{DR}}{\sim}$ ' symbol (which should mean *is after dimensional regularisation equivalent to*) instead of the obvious ' = ' to express this fact explicitly. More information about the mathematical background of the computations can be found for example in [2],[16] or [19].

The philosophy of the dimensional regularisation procedure is quite simple: to try to consider an integral as a generalized function of a parameter d , which denotes the dimension of the integration manifold. Such a function can be well-defined for some integer d and then prolonged to any real dimension using the analytic properties of the resulting d-dependence (usually Γ-function). All the relevant integrals are handled in this way and the resulting higher order correction to some lower order relation is then defined as the limit for $d \to 4$ of the sum of all the contributions, which is often finite.

The results of further computations will be expressed in the usual way

$$\mathit{integral} \stackrel{\mathrm{DR}}{\sim} \alpha\,\mathrm{C}_{\mathrm{UV}} + \mathit{finite}$$

where we used

$$\mathrm{C}_{\mathrm{UV}} \equiv \frac{1}{\varepsilon} - \gamma_{\mathrm{E}} + \ln 4\pi \tag{170}$$

with $2\varepsilon \equiv 4-d$; γ_{E} is the famous Euler-Mascheroni constant (0.577...) and $\alpha \in \mathcal{C}$ depends on the concrete form of the *integral*. The *finite* part generally contains terms of order ε^2 and higher, that we will neglect.

First of all we are going to derive three particular statements that will be useful in subsequent computations:

$$\int \frac{d^4k}{(2\pi)^4}\frac{1}{k^2-m^2} \stackrel{\mathrm{DR}}{\sim} \frac{i}{16\pi^2}m^2\left(\mathrm{C}_{\mathrm{UV}}+1-\ln\frac{m^2}{\mu^2}\right) \tag{171}$$

$$\int \frac{d^4k}{(2\pi)^4}\frac{k^\mu k^\nu}{[k^2-D_q(x)^2]^2} \stackrel{\mathrm{DR}}{\sim} \frac{i}{16\pi^2}\frac{g^{\mu\nu}}{2}D_q(x)\left[\mathrm{C}_{\mathrm{UV}}+1-\ln\frac{D_q(x)}{\mu^2}\right] \tag{172}$$

$$\int \frac{d^4k}{(2\pi)^4}\frac{1}{[k^2-D_q(x)^2]^2} \stackrel{\mathrm{DR}}{\sim} \frac{i}{16\pi^2}\left[\mathrm{C}_{\mathrm{UV}}-\ln\frac{D_q(x)}{\mu^2}\right] \tag{173}$$

The proof is nothing but simple use of the expressions (9A.5) and (9A.7) from [16] (Similar relations can be found also in [2], [19] and many other books) and the Laurent expansion of the Γ function around its poles in $-\mathcal{N}_0$. The first of them, (171) :

$$\int \frac{d^4k}{(2\pi)^4}\frac{1}{k^2-m^2} \quad\to\quad \mu^{2\varepsilon}\int \frac{d^dk}{(2\pi)^d}\frac{1}{k^2-m^2} \stackrel{\mathrm{DR}}{\sim} -\frac{i}{16\pi^2}m^2\Gamma\left(-1+\varepsilon\right)\left(\frac{m^2}{4\pi\mu^2}\right)^{-\varepsilon} =$$

$$= \frac{i}{16\pi^2} m^2 \left[\frac{1}{\varepsilon} - \gamma_{\text{E}} + 1 + O(\varepsilon)\right] \left[1 - \varepsilon \ln \frac{m^2}{4\pi\mu^2} + O(\varepsilon^2)\right] =$$

$$= \frac{i}{16\pi^2} m^2 \left(\text{C}_{\text{UV}} + 1 - \ln \frac{m^2}{\mu^2}\right) + O(\varepsilon^2) \tag{174}$$

The arrow at the beginning comes from the fact that it is necessary to redefine the whole theory into a non-integer dimension. It means first to generalize the 4-dimensional Lagrangian into a dimension d. In order to use the usual techniques to handle such a theory we are forced to keep the original dimensionalities of the couplings. (For example in the $\lambda\phi^4$ theory the dimensionless constant λ serves us as a numerical expansion factor so it is necessary to save this fine property also in the new theory.) This is the reason for introducing a new mass parameter μ into the original Lagrangian to arrange the correct total dimension. The Feynman rules for the relevant vertices then obtain some additional factors proportional to μ. Using these reformulated rules the Feynman diagrams produce expressions which contain different powers of μ. In the computation above we have taken only a part of it proportional to $\mu^{2\varepsilon}$ to simplify the result.

Of course all the (measurable) results of computations should not depend on its particular choice. (Note that the renormalisation parameters in general can be μ-dependent.) In our case the overall μ independence is going to be a trivial consequence of the total cancellation of all the divergences and the special definition of C_{UV} in (170).

In the previous derivation we have used the following expansions ($n \in \mathcal{N}_0$)

$$\Gamma(-n+\varepsilon) = \frac{(-1)^n}{n!} \left[\frac{1}{\varepsilon} + \psi_1(n+1) + O(\varepsilon)\right] \tag{175}$$

where

$$\psi_1(n+1) \equiv \sum_{k=1}^{n} \frac{1}{k} - \gamma_{\text{E}} \tag{176}$$

and

$$a^\varepsilon = 1 + \varepsilon \ln a + O(\varepsilon^2) \qquad \forall a \in \mathcal{R}^+ \tag{177}$$

and neglected the small term proportional to ε^2. (The derivation of (175) can be found for example in [16].)

The second and the third integrals (172),(173) differ by the power of their denominators and the additional momentum components, which complicates their resulting structure; $D_q(x)$ is a real parameter which does not depend on k.

$$\int \frac{d^4k}{(2\pi)^4} \frac{k^\mu k^\nu}{[k^2 - D_q(x)^2]^2} \quad \to \quad \mu^{2\varepsilon} \int \frac{d^dk}{(2\pi)^d} \frac{k^\mu k^\nu}{[k^2 - D_q(x)^2]^2} \overset{\text{DR}}{\sim}$$

$$\overset{\text{DR}}{\sim} \quad \frac{i}{16\pi^2} \frac{g^{\mu\nu}}{2} \Gamma(-1+\varepsilon) D_q(x) \left[\frac{D_q(x)}{4\pi\mu^2}\right]^{-\varepsilon} =$$

$$= \frac{i}{16\pi^2} \frac{g^{\mu\nu}}{2} D_q(x) \left[\frac{1}{\varepsilon} - \gamma_{\text{E}} + 1 + O(\varepsilon)\right] \left[1 - \varepsilon \ln \frac{D_q(x)}{4\pi\mu^2} + O(\varepsilon^2)\right] =$$

$$= \frac{i}{16\pi^2} \frac{g^{\mu\nu}}{2} D_q(x) \left[\text{C}_{\text{UV}} + 1 - \ln \frac{D_q(x)}{\mu^2}\right] + O(\varepsilon^2) \tag{178}$$

And similarly the last one (173):

$$\int \frac{d^4k}{(2\pi)^4} \frac{1}{[k^2 - D_q(x)^2]^2} \quad \rightarrow \quad \mu^{2\varepsilon}\int \frac{d^dk}{(2\pi)^d} \frac{1}{[k^2 - D_q(x)^2]^2} \overset{\text{DR}}{\sim} \frac{i}{16\pi^2}\Gamma(\varepsilon)\left[\frac{D_q(x)}{4\pi\mu^2}\right]^{-\varepsilon} =$$

$$= \frac{i}{16\pi^2}\left[\frac{1}{\varepsilon} - \gamma_{\text{E}} + O(\varepsilon)\right]\left[1 - \varepsilon \ln\frac{D_q(x)}{4\pi\mu^2} + O(\varepsilon^2)\right] =$$

$$= \frac{i}{16\pi^2}\left[\text{C}_{\text{UV}} - \ln\frac{D_q(x)}{\mu^2}\right] + O(\varepsilon^2) \tag{179}$$

A.2 Regularisation of relevant integrals

In the following part of this Appendix we will use the statements above to derive several necessary results relevant for our purposes, i.e. perform the dimensional regularisation procedure in the cases of concrete types of the one-loop Feynman diagrams corresponding to the lowest order corrections to the tree-level relation considered in the first chapter.

I. Integral corresponding to the tadpole and seagull graphs: Neglecting the other structures coming from the external legs and the Lorentz-structure of the vector-boson vertices, all the diagrams from the set

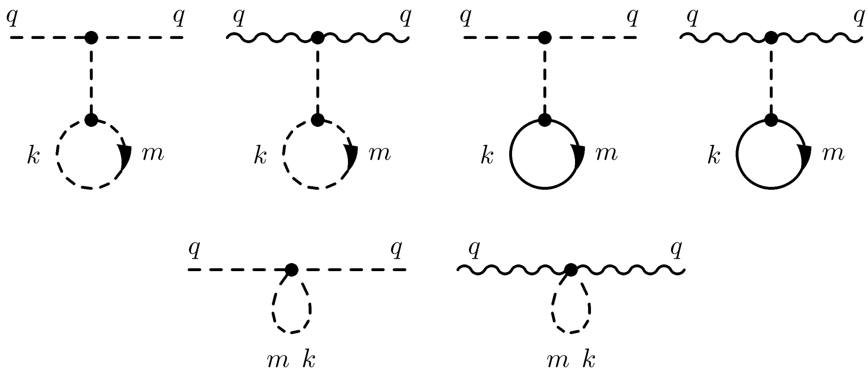

correspond to the already regularized integral (171)

$$\int \frac{d^4k}{(2\pi)^4} \frac{1}{k^2 - m^2} \overset{\text{DR}}{\sim} \frac{i}{16\pi^2} m^2 \left(\text{C}_{\text{UV}} + 1 - \ln\frac{m^2}{\mu^2}\right) \tag{180}$$

II. Integral corresponding to the graphs of the type:

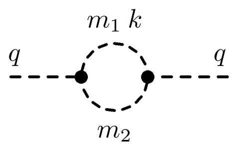

(181)

In this case we are dealing with a contribution of the form (neglecting the couplings)

$$I(q) \equiv \int \frac{d^4k}{(2\pi)^4} \frac{1}{(k^2 - m_1^2)[(k-q)^2 - m_2^2]} \tag{182}$$

To proceed we are going to use the so-called Feynman parameterization

$$\frac{1}{ab} = \int_0^1 dx \frac{1}{[ax + b(1-x)]^2} \tag{183}$$

with a special choice of $a \equiv (k-p)^2 - m_2^2$ and $b \equiv k^2 - m_1^2$. It leads to

$$I(q) = \int \frac{d^4k}{(2\pi)^4} \int_0^1 \mathrm{d}x \frac{1}{\{[(k-p)^2 - m_2^2]x + (k^2 - m_1^2)(1-x)\}^2} \tag{184}$$

which can be easily simplified to the form (considering both the integrations in the Lebesgue sense it is possible to interchange their order without any problems)

$$I(q) = \int_0^1 \mathrm{d}x \int \frac{d^4k}{(2\pi)^4} \frac{1}{[(k-px)^2 - D_q(x)]^2} \tag{185}$$

Here we used the notation of Aoki et all [1]

$$D_q(x) \equiv m_1^2(1-x) + m_2^2 x - q^2 x(1-x) \tag{186}$$

The next step is the substitution $k - qx \to k$ which does not affect the volume element nor the integration domain. After that the momentum integral takes the form of the previously considered expression (173). Using this result we can see that

$$I(q) = \int \frac{d^4k}{(2\pi)^4} \frac{1}{(k^2 - m_1^2)[(k-q)^2 - m_2^2]} \overset{\text{DR}}{\sim} \frac{i}{16\pi^2}\left[\mathrm{C}_{\text{UV}} - \int_0^1 \mathrm{d}x \ln\frac{D_q(x)}{\mu^2}\right] \tag{187}$$

with $D_q(x)$ defined in (186).

III. Integral corresponding to the graph:

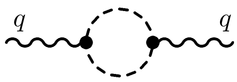

(188)

This kind of diagrams leads to the contribution of the form

$$I(q)^{\mu\nu} \equiv \int \frac{d^4k}{(2\pi)^4} \frac{(2k-q)^\mu(2k-q)^\nu}{(k^2 - m_1^2)[(k-q)^2 - m_2^2]} \tag{189}$$

The complexity of the numerator descents from the nontrivial momentum structure of the *vector-scalar-scalar* vertex. Using the standard Feynman trick (183) we can rewrite the last expression in the form

$$I(q)^{\mu\nu} = \int_0^1 \mathrm{d}x \int \frac{d^4k}{(2\pi)^4} \frac{[2(k-qx) - q(1-2x)]^\mu[2(k-qx) - q(1-2x)]^\nu}{[(k-qx)^2 - D_q(x)]^2} \tag{190}$$

The usual substitution $k - qx \to k$ leads to (neglecting the k-odd terms proportional to $k^\mu q^\nu$ which do not contribute to the integral):

$$I(q)^{\mu\nu} = \int_0^1 \mathrm{d}x \int \frac{d^4k}{(2\pi)^4} \frac{4k^\mu k^\nu + q^\mu q^\nu(1-2x)^2}{[k^2 - D_q(x)]^2} \tag{191}$$

It is now easy to use relations (172) and (173) to perform the regularisation and get

$$\begin{aligned} I(q)^{\mu\nu} \overset{\text{DR}}{\sim} & \int_0^1 \mathrm{d}x \left\{ 4\frac{i}{16\pi^2}\frac{g^{\mu\nu}}{2} D_q(x)\left[\mathrm{C}_{\text{UV}} + 1 - \ln\frac{D_q(x)}{\mu^2}\right] + \right. \\ + & \left. q^\mu q^\nu (1-2x)^2 \frac{i}{16\pi^2}\left[\mathrm{C}_{\text{UV}} - \ln\frac{D_q(x)}{\mu^2}\right]\right\} \end{aligned} \tag{192}$$

Utilising $\int_0^1 \mathrm{d}x(1-2x)^2 = \frac{1}{3}$ we can conclude

$$\begin{aligned} I(q)^{\mu\nu} \overset{\text{DR}}{\sim} & \frac{i}{16\pi^2}\left\{\mathrm{C}_{\text{UV}}\left[\frac{1}{3}\left(q^\mu q^\nu - g^{\mu\nu}q^2\right) + g^{\mu\nu}\left(m_1^2 + m_2^2\right)\right] + \right. \\ + & \left. g^{\mu\nu}\left(m_1^2 + m_2^2 - \frac{q^2}{3}\right) - \int_0^1 \mathrm{d}x \left[q^\mu q^\nu(1-2x)^2 + 2g^{\mu\nu}D_q(x)\right]\ln\frac{D_q(x)}{\mu^2}\right\} \end{aligned} \tag{193}$$

IV. Integral coming from the diagram:

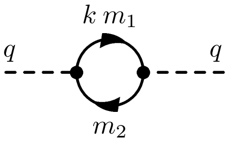

(194)

Thys type of diagrams produce contributions of the general form

$$I(q) \equiv \int \frac{d^4k}{(2\pi)^4} \operatorname{Tr}\left[(A+B\gamma_5)\frac{m_1+\not{k}}{k^2-m_1^2}(C+D\gamma_5)\frac{m_2+\not{k}-\not{q}}{(k-q)^2-m_2^2}\right] \tag{195}$$

(A and B are nonzero for example for pseudoscalars). Let us first calculate the trace :

$$\begin{aligned} &\operatorname{Tr}[(A+B\gamma_5)(m_1+\not{k})(C+D\gamma_5)(m_2+\not{k}-\not{q})] = \\ &= m_1 \operatorname{Tr}[(A+B\gamma_5)(C+D\gamma_5)(m_2+\not{k}-\not{q})] + \\ &\quad + \operatorname{Tr}[(A+B\gamma_5)\not{k}(C+D\gamma_5)(m_2+\not{k}-\not{q})] \end{aligned} \tag{196}$$

Using $\operatorname{Tr}\gamma_5 = 0$, $\operatorname{Tr}\gamma^\mu\gamma^\nu\gamma_5 = 0$ and the fact, that the trace of an odd number of gamma-matrices is zero, we can simplify (196) to the form

$$\begin{aligned} (196) &= m_1 m_2 \operatorname{Tr}[(A+B\gamma_5)(C+D\gamma_5)] + \operatorname{Tr}[(A+B\gamma_5)\not{k}(C+D\gamma_5)(\not{k}-\not{q})] = \\ &= 4m_1m_2(AC+BD) + [(AC-BD)+(BC-AD)\gamma_5] \operatorname{Tr}\not{k}(\not{k}-\not{q}) = \\ &= 4[m_1m_2(AC+BD)+(AC-BD)k(k-q)] \end{aligned} \tag{197}$$

Utilising this result we can rewrite (195) in the form

$$I(q) \equiv 4\int \frac{d^4k}{(2\pi)^4} \frac{m_1m_2(AC+BD)+(AC-BD)k(k-q)}{(k^2-m_1^2)[(k-q)^2-m_2^2]} \tag{198}$$

The first term in numerator corresponds, up to a constant factor, to the already regularized integral (182) so it is easy to write down

$$\begin{aligned} I_1(q) &= 4\int \frac{d^4k}{(2\pi)^4} \frac{m_1m_2(AC+BD)}{(k^2-m_1^2)[(k-q)^2-m_2^2]} \overset{\text{DR}}{\sim} \\ &\overset{\text{DR}}{\sim} \frac{i}{4\pi^2} m_1m_2(AC+BD)\left[\mathrm{C}_{\text{UV}} - \int_0^1 \mathrm{d}x \ln\frac{D_q(x)}{\mu^2}\right] \end{aligned} \tag{199}$$

The rest of (195) must be evaluated by hand: introducing the Feynman parameterization and substituting $k-qx \to k$ gives (in the traditional notation)

$$\begin{aligned} I_2(q) &= 4(AC-BD)\int \frac{d^4k}{(2\pi)^4} \frac{k(k-q)}{(k^2-m_1^2)[(k-q)^2-m_2^2]} = \\ &= 4(AC-BD)\int_0^1 \mathrm{d}x \int \frac{d^4k}{(2\pi)^4} \frac{(k+qx)[k+q(x-1)]}{[k^2-D_q(x)]^2} = \end{aligned} \tag{200}$$

$$= -4(AC-BD)\left\{\int_0^1 \mathrm{d}x \int \frac{d^4k}{(2\pi)^4} \frac{q^2x(1-x)}{[k^2-D_q(x)]^2} - \int_0^1 \mathrm{d}x \int \frac{d^4k}{(2\pi)^4} \frac{k^2+k.q(2x-1)}{[k^2-D_q(x)]^2}\right\}$$

The term proportional to $k.q$ again does not contribute and the rest is already regularized in (171) and (172):

$$\begin{aligned} I_2(q) \overset{\text{DR}}{\sim} & -4(AC-BD)\left\{\int_0^1 \mathrm{d}x q^2 x(1-x)\frac{i}{16\pi^2}\left[\mathrm{C}_{\text{UV}} - \ln\frac{D_q(x)}{\mu^2}\right] - \right. \\ & - \left. \int_0^1 \mathrm{d}x \left[\int \frac{d^4k}{(2\pi)^4}\frac{1}{k^2-D_q(x)} + \int \frac{d^4k}{(2\pi)^4}\frac{D_q(x)}{[k^2-D_q(x)]^2}\right]\right\} \end{aligned} \tag{201}$$

This allows us to conclude

$$I_2(q) \overset{\text{DR}}{\sim} -\frac{i}{4\pi^2}(AC-BD)\left\{\int_0^1 \mathrm{d}x q^2 x(1-x)\left[\mathrm{C}_{\text{UV}} - \ln\frac{D_q(x)}{\mu^2}\right] - \right.$$
$$\left. - \int_0^1 \mathrm{d}x\left[2\mathrm{C}_{\text{UV}} + 1 - 2\ln\frac{D_q(x)}{\mu^2}\right] D_q(x)\right\} \tag{202}$$

Then we obtain the final result

$$I(q) \overset{\text{DR}}{\sim} \frac{i}{4\pi^2}\left\{\mathrm{C}_{\text{UV}}\left[m_1 m_2(AC+BD) - (AC-BD)\left(\frac{q^2}{6} - 2\int_0^1 \mathrm{d}x D_q(x)\right)\right]\right.$$
$$+ \int_0^1 \mathrm{d}x \ln\frac{D_q(x)}{\mu^2}\big\{-m_1 m_2(AC+BD) + (AC-BD)\big[q^2 x(1-x) - 2D_q(x)\big]\big\}$$
$$\left. + (AC-BD)\int_0^1 \mathrm{d}x D_q(x)\right\} \tag{203}$$

In the special case when both the fermions have the same masses $m_1 = m_2 \equiv m$ the previous expression can be simplified into the form:

$$I(q) \overset{\text{DR}}{\sim} \frac{i}{4\pi^2}\left\{\mathrm{C}_{\text{UV}}\left[m^2(3AC-BD) - (AC-BD)\frac{q^2}{2}\right] + \right.$$
$$+ (AC-BD)\left(m^2 - \frac{q^2}{6}\right) +$$
$$\left. + \int_0^1 \mathrm{d}x \ln\frac{D_q(x)}{\mu^2}\left[m^2(BD-3AC) + (AC-BD)3q^2 x(1-x)\right]\right\} \tag{204}$$

(Note that $\int_0^1 \mathrm{d}x D_q(x) = m^2 - \frac{q^2}{6}$)

V. Contributions coming from the graphs:

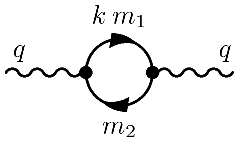

(205)

These graphs lead to the expressions of the form

$$I(q)^{\mu\nu} \equiv \int \frac{d^4k}{(2\pi)^4}\,\mathrm{Tr}\left[\gamma^\mu(1+A\gamma_5)\frac{m_1 + \not{k}}{k^2 - m_1^2}\gamma^\nu(1+B\gamma_5)\frac{m_2 + \not{k} - \not{q}}{(k-q)^2 - m_2^2}\right] \tag{206}$$

First we again calculate the trace:

$$\begin{aligned}
&\mathrm{Tr}\left[\gamma^\mu(1+A\gamma_5)(m_1+\not{k})\gamma^\nu(1+B\gamma_5)(m_2+\not{k}-\not{q})\right] = \\
&= m_1\,\mathrm{Tr}\left[\gamma^\mu(1+A\gamma_5)\gamma^\nu(1+B\gamma_5)(m_2+\not{k}-\not{q})\right] + \\
&+ \mathrm{Tr}\left[\gamma^\mu(1+A\gamma_5)\not{k}\gamma^\nu(1+B\gamma_5)(m_2+\not{k}-\not{q})\right] = \\
&= m_1 m_2\,\mathrm{Tr}\left[\gamma^\mu\gamma^\nu(1-A\gamma_5)(1+B\gamma_5)\right] + \\
&+ \mathrm{Tr}\left[(\not{k}-\not{q})\gamma^\mu\not{k}\gamma^\nu(1+A\gamma_5)(1+B\gamma_5)\right] = \\
&= m_1 m_2\,\mathrm{Tr}\left[\gamma^\mu\gamma^\nu(1-AB+(B-A)\gamma_5)\right] + \\
&+ \mathrm{Tr}\left[(\not{k}-\not{q})\gamma^\mu\not{k}\gamma^\nu(1+AB+(A+B)\gamma_5)\right] =
\end{aligned} \tag{207}$$

Reminding the known identities (see for example [2])

$$\mathrm{Tr}\,\gamma^\mu\gamma^\nu = 4g^{\mu\nu}$$

$$\begin{aligned}
\mathrm{Tr}\,\gamma^\mu\gamma^\nu\gamma_5 &= 0 \\
\mathrm{Tr}\,\gamma^\sigma\gamma^\mu\gamma^\tau\gamma^\nu &= 4\left(g^{\sigma\mu}g^{\tau\nu} + g^{\sigma\nu}g^{\tau\mu} - g^{\mu\nu}g^{\sigma\tau}\right) \\
\mathrm{Tr}\,\gamma^\sigma\gamma^\mu\gamma^\tau\gamma^\nu\gamma_5 &= -4i\varepsilon^{\sigma\mu\tau\nu}
\end{aligned} \tag{208}$$

the trace (207) can be recast

$$\mathrm{Tr}\left[\gamma^\mu(1+A\gamma_5)(m_1+\not{k})\gamma^\nu(1+B\gamma_5)(m_2+\not{k}-\not{q})\right] = 4i\varepsilon^{\sigma\mu\tau\nu}q_\sigma k_\tau + \tag{209}$$
$$+4(1-AB)m_1m_2g^{\mu\nu} + 4(1+AB)\left[(k-q)^\mu k^\nu + (k-q)^\nu k^\mu - g^{\mu\nu}(k-q)k\right]$$

The factor containing $\varepsilon^{\sigma\mu\tau\nu}$ drops out from the integral (206), because of its antisymmetry (which eliminates the part proportional to $q^\sigma q^\tau$) and the fact, that the rest is already k-odd. We then get

$$I(q)^{\mu\nu} = I_1(q)^{\mu\nu} + I_2(q)^{\mu\nu} \tag{210}$$

where

$$\begin{aligned}
I_1(q)^{\mu\nu} &\equiv 4(1-AB)m_1m_2g^{\mu\nu}\int\frac{d^4k}{(2\pi)^4}\frac{1}{(k^2-m_1^2)[(k-q)^2-m_2^2]} \\
I_2(q)^{\mu\nu} &\equiv 4(1+AB)\int\frac{d^4k}{(2\pi)^4}\frac{[(k-q)^\mu k^\nu + (k-q)^\nu k^\mu - g^{\mu\nu}(k-q)k]}{(k^2-m_1^2)[(k-q)^2-m_2^2]}
\end{aligned}$$

An expression similar to $I_1(q)^{\mu\nu}$ is already regularized in (199); we can write immediately

$$I_1(q)^{\mu\nu} \overset{\mathrm{DR}}{\sim} \frac{i}{4\pi^2}m_1m_2(1-AB)g^{\mu\nu}\left[\mathrm{C}_{\mathrm{UV}} - \int_0^1 \mathrm{d}x\ln\frac{D_q(x)}{\mu^2}\right] \tag{211}$$

The first task to be done in the case of $I_2(q)^{\mu\nu}$ is to perform the Feynman trick and the usual substitution $k - qx \to\ k$ to obtain

$$\begin{aligned}
I_2(q)^{\mu\nu} &= 4(1+AB)\int_0^1\mathrm{d}x\int\frac{d^4k}{(2\pi)^4}\frac{2[k^\mu k^\nu - q^\mu q^\nu x(1-x)] - g^{\mu\nu}[k^2 - q^2x(1-x)]}{[k^2 - D_q(x)]^2} \\
&= 4(1+AB)\int_0^1\mathrm{d}x\int\frac{d^4k}{(2\pi)^4}\left\{\frac{-x(1-x)(2q^\mu q^\nu - g^{\mu\nu}q^2)}{[k^2-D_q(x)]^2} + \frac{2k^\mu k^\nu - g^{\mu\nu}k^2}{[k^2-D_q(x)]^2}\right\}
\end{aligned} \tag{212}$$

Let us denote $I_2(q)^{\mu\nu} \equiv I_{2A}(q)^{\mu\nu} + I_{2B}(q)^{\mu\nu}$ where

$$I_{2A}(q)^{\mu\nu} \equiv -4(1+AB)\int_0^1\mathrm{d}x\int\frac{d^4k}{(2\pi)^4}\frac{x(1-x)(2q^\mu q^\nu - g^{\mu\nu}q^2)}{[k^2-D_q(x)]^2} \tag{213}$$

$$I_{2B}(q)^{\mu\nu} \equiv 4(1+AB)\int_0^1\mathrm{d}x\int\frac{d^4k}{(2\pi)^4}\frac{2k^\mu k^\nu - g^{\mu\nu}k^2}{[k^2-D_q(x)]^2} \tag{214}$$

The part $I_{2A}(q)^{\mu\nu}$ is easy to handle:

$$I_{2A}(q)^{\mu\nu} \overset{\mathrm{DR}}{\sim} -\frac{i}{4\pi^2}(1+AB)\int_0^1\mathrm{d}x(2q^\mu q^\nu - g^{\mu\nu}q^2)x(1-x)[\mathrm{C}_{\mathrm{UV}} - \ln\frac{D_q(x)}{\mu^2}] \tag{215}$$

The expression $I_{2B}(q)^{\mu\nu}$ is also not too hard to deal with; recalling the statement (172) and performing similar steps as in (201) we obtain

$$\begin{aligned}
I_{2B}(q)^{\mu\nu} &\overset{\mathrm{DR}}{\sim} -(1+AB)\frac{i}{4\pi^2}g^{\mu\nu}\left\{-\int_0^1\mathrm{d}xD_q(x)\left[\mathrm{C}_{\mathrm{UV}} + 1 - \ln\frac{D_q(x)}{\mu^2}\right] + \right. \\
&+ \left.\int_0^1\mathrm{d}x\left[2\mathrm{C}_{\mathrm{UV}} + 1 - 2\ln\frac{D_q(x)}{\mu^2}\right]D_q(x)\right\} = \\
&= -(1+AB)\frac{i}{4\pi^2}g^{\mu\nu}\int_0^1\mathrm{d}xD_q(x)\left[\mathrm{C}_{\mathrm{UV}} - \ln\frac{D_q(x)}{\mu^2}\right]
\end{aligned} \tag{216}$$

Now we collect all the partial results (211),(215) and (216) built up the total contribution:

$$I(q)^{\mu\nu} = I_1(q)^{\mu\nu} + I_{2A}(q)^{\mu\nu} + I_{2B}(q)^{\mu\nu} \tag{217}$$

After some simple algebraic manipulation we get the final result (reminding that $\int_0^1 \mathrm{d}x D_q(x) = \frac{1}{2}(m_1^2+m_2^2) - \frac{q^2}{6}$):

$$\begin{aligned} I(q)^{\mu\nu} &= \frac{i}{4\pi^2}\mathrm{C}_{\mathrm{UV}}\left\{ g^{\mu\nu}\left[m_1 m_2(1-AB) - \frac{1}{2}(m_1^2+m_2^2)(1+AB)\right] + \right. \\ &+ \left. (1+AB)\frac{1}{3}(g^{\mu\nu}q^2 - q^\mu q^\nu)\right\} - \\ &- \frac{i}{4\pi^2} g^{\mu\nu}\int_0^1 \mathrm{d}x \ln\frac{D_q(x)}{\mu^2}\{(1-AB)m_1 m_2 - (1+AB)[m_1^2(1-x)+m_2^2 x]\} \\ &- \frac{i}{2\pi^2}(1+AB)\int_0^1 \mathrm{d}x\ln\frac{D_q(x)}{\mu^2}(1+AB)(q^\mu q^\nu - g^{\mu\nu}q^2)x(1-x) \end{aligned} \tag{218}$$

The most important is again the case of $m_1 = m_2 \equiv m$; this particular choice allows us to simplify the previous result into the form

$$\begin{aligned} I(q)^{\mu\nu} &= \frac{i}{4\pi^2}\mathrm{C}_{\mathrm{UV}}\left\{ -2m^2 g^{\mu\nu}AB + (1+AB)\frac{1}{3}(g^{\mu\nu}q^2 - q^\mu q^\nu)\right\} - \\ &- \frac{i}{4\pi^2} g^{\mu\nu}\int_0^1 \mathrm{d}x \ln\frac{D_q(x)}{\mu^2}(-2m^2 AB) - \\ &- \frac{i}{2\pi^2}\int_0^1 \mathrm{d}x\ln\frac{D_q(x)}{\mu^2}(1+AB)(q^\mu q^\nu - g^{\mu\nu}q^2)x(1-x) \end{aligned} \tag{219}$$

VI. Regularisation of some special types of integrals:

In this paragraph we are going to regularise integrals appearing mostly in the fourth chapter. They are opticaly worse than the previous types, but the situation is simplified by the fact, that we need their divergent parts only so it will be possible to drop out a lot of terms that do not affect it.

There are two types of integrals that we are going to be interested in. First of them,

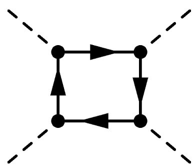

(220)

produces an integral of the type

$$I \equiv \operatorname{Tr}\int\frac{d^d k}{(2\pi)^d}\frac{\mu^{2\varepsilon}}{(\not{k} - m_f)(\not{k} + \not{q}_2 - m_f)(\not{k} + \not{q}_2 + \not{q}_3 - m_f)(\not{k} + \not{q}_2 + \not{q}_3 + \not{q}_4 - m_f)}$$

We would now have to compute a very long trace but the only part that can contribute to the UV-divergence of I is

$$k_\mu k_\nu k_\rho k_\sigma \operatorname{Tr}(\gamma^\mu\gamma^\nu\gamma^\rho\gamma^\sigma) = 4k_\mu k_\nu k_\rho k_\sigma(g^{\mu\nu}g^{\rho\sigma} + g^{\mu\sigma}g^{\nu\rho} - g^{\mu\rho}g^{\nu\sigma}) = 4k^4 \tag{221}$$

because the integrals involving remaining terms are convergent. To handle the denominator of the last expression we have to perform a triple Feynman parametrisation. Because we do not need an explicite form of the finite part, we denote the resulting expression containing all the external momenta $q_1 \dots q_4$ together with the parametrisation variables $x_1 \dots x_3$ by some $C(\vec{x}, q_1 \dots q_4)$. This allows us to write down

$$I = 6 \int_0^1 \mathrm{d}x_1 \int_0^{x_1} \mathrm{d}x_2 \int_0^{x_2} \mathrm{d}x_3 \; 4 g^{\mu\nu} g^{\rho\sigma} \mu^{2\varepsilon} \int \frac{d^d k}{(2\pi)^d} \frac{k_\mu k_\nu k_\rho k_\sigma}{[k^2 - C(\vec{x}, q_1 \dots q_4)]^4} + \text{finite} \tag{222}$$

It is not difficult to show (using the usual technique described for instance in [2]) that the regularisation of this divergent integral has the form

$$\int \frac{d^d k}{(2\pi)^d} \frac{\mu^{2\varepsilon} k_\mu k_\nu k_\rho k_\sigma}{[k^2 - C(\vec{x}, q_1 \dots q_4)]^4} \overset{\text{DR}}{\sim} \frac{i\Gamma(\varepsilon)[C(\vec{x}, q_1 \dots q_4)]^{-\varepsilon}}{4!(4\pi)^{2-\varepsilon}(\mu^2)^{-\varepsilon}} (g_{\mu\nu} g_{\rho\sigma} + g_{\mu\sigma} g_{\nu\rho} + g_{\mu\rho} g_{\nu\sigma})$$

$$= \frac{i}{16\pi^2} \left[\frac{1}{\varepsilon} - \gamma_{\mathrm{E}} - \ln \frac{C(\vec{x}, q_1 \dots q_4)}{4\pi\mu^2} \right] \frac{1}{4!} (g_{\mu\nu} g_{\rho\sigma} + g_{\mu\sigma} g_{\nu\rho} + g_{\mu\rho} g_{\nu\sigma}) \tag{223}$$

Inserting this into (222) and extracting the term proportional to $\frac{1}{\varepsilon}$ we obtain

$$I = \frac{i}{4\pi^2 \varepsilon} + \text{finite} \tag{224}$$

The second integral of this section is the contribution corresponding to the diagram

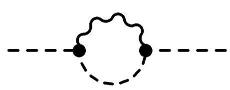

(225)

$$I(q) = \mu^{2\varepsilon} \int \frac{d^d k}{(2\pi)^d} \frac{\left[i D^{\rho\sigma}_{\xi, X}(k - q) \right] (k + q)^\rho (-k - q)^\sigma}{k^2 - \xi m_X^2} \tag{226}$$

Let us again divide this expression into two parts:

$$I(q) = I_1 + I_2$$

where

$$\begin{aligned} I_1 &\equiv -\mu^{2\varepsilon} \int \frac{d^d k}{(2\pi)^d} \frac{(k+q)^2}{(k^2 - \xi m_X^2) \, [(k-q)^2 - m_X^2]} \\ I_2 &\equiv \mu^{2\varepsilon} \, (1 - \xi) \int \frac{d^d k}{(2\pi)^d} \frac{[(k+q).(k-q)]^2}{(k^2 - \xi m_X^2) \, [(k-q)^2 - \xi m_X^2][(k-q)^2 - m_X^2]} \end{aligned} \tag{227}$$

The first of them (performing the usual steps like the Feynman parametrization and the substitution $k \to k + qx$) gives after some algebra:

$$I_1 \overset{\text{DR}}{\sim} -\frac{i}{8\pi^2 \varepsilon} q^2 + \text{stg.} + \text{finite} \tag{228}$$

The term stg. denotes a part of the UV-divergence which is *not* proportional to the external momentum q^2 and therefore does not affect the wave-function renormalisation constant.

The second expression I_2 is much more complicated; performing the whole procedure one can obtain

$$I_2 \overset{\text{DR}}{\sim} -(1 - \xi) \frac{i}{16\pi^2 \varepsilon} q^2 + \text{stg.} + \text{finite} \tag{229}$$

Collecting (228) and (229) we conclude this Appendix by

$$I(q) \overset{\text{DR}}{\sim} -(3 - \xi) \frac{i}{16\pi^2 \varepsilon} q^2 + \text{stg.} + \text{finite} \tag{230}$$

B Feynman rules of the MSSM

Despite the fact that there are several excellent sources of the Feynman rules of MSSM in the literature ([14], [7]) I have decided to include an Appendix containing a brief review of them in this work. The main reasons are two:

- There is a lot of references on the concrete structure of the rules in the computations, so I find it convenient to have them collected at one place
- Many papers containing Feynman rules for superquarks use the 'non-physical' $L-R$ basis, which is advantageous for the formulation of the model but not for our explicit computations, because they do not allow us to use a lot of relations among the MSSM parameters.

Let us start with some comments on the transition from the $L-R$ basis to the 'physical' $1-2$ basis. The Lagrangian describing interactions of the superquarks is diagonal in the $L-R$ basis until the soft-supersymmetry-breaking terms are included. After this step we have to rediagonalise the superquark mass-squared matrix, i.e. find the diagonal basis. This can be done by an orthogonal transformation

$$\begin{pmatrix} \tilde{q}_L \\ \tilde{q}_R \end{pmatrix} \to \begin{pmatrix} \tilde{q}_1 \\ \tilde{q}_2 \end{pmatrix} = A \begin{pmatrix} \tilde{q}_L \\ \tilde{q}_R \end{pmatrix} \tag{231}$$

where the A denotes a real and orthogonal 2×2 matrix. Therefore it can be parametrised by one angle θ_q (in the usual notation)

$$A = \begin{pmatrix} \cos\theta_q & \sin\theta_q \\ -\sin\theta_q & \cos\theta_q \end{pmatrix} \tag{232}$$

To solve the problem of such a rediagonalisation we have to replace all the expressions of the type $\tilde{q}^*_{L,R}\tilde{q}'_{L,R}$ in the original Lagrangian by some relevant combinations of the new fields $\tilde{q}^*_{1,2}\tilde{q}'_{1,2}$. In the next derivations we will focus only on the case $\tilde{q} \equiv \tilde{q}' \equiv \tilde{t}$ (supertop). The generalization for the other flavours is straightforward. The relations among quantities in these two basis can be expressed by

$$\begin{pmatrix} \tilde{t}_L \\ \tilde{t}_R \end{pmatrix}^* \otimes \begin{pmatrix} \tilde{t}_L \\ \tilde{t}_R \end{pmatrix} = (A^{-1} \otimes A^{-1}) \begin{pmatrix} \tilde{t}_1 \\ \tilde{t}_2 \end{pmatrix}^* \otimes \begin{pmatrix} \tilde{t}_1 \\ \tilde{t}_2 \end{pmatrix} \tag{233}$$

which can be translated into the form

$$\begin{pmatrix} \tilde{t}^*_L\tilde{t}_L \\ \tilde{t}^*_L\tilde{t}_R \\ \tilde{t}^*_R\tilde{t}_L \\ \tilde{t}^*_R\tilde{t}_R \end{pmatrix} = \begin{pmatrix} \cos^2\theta_t & -\cos\theta_t\sin\theta_t & -\sin\theta_t\cos\theta_t & \sin^2\theta_t \\ \cos\theta_t\sin\theta_t & \cos^2\theta_t & -\sin^2\theta_t & -\sin\theta_t\cos\theta_t \\ \sin\theta_t\cos\theta_t & -\sin^2\theta_t & \cos^2\theta_t & -\cos\theta_t\sin\theta_t \\ \sin^2\theta_t & \sin\theta_t\cos\theta_t & \cos\theta_t\sin\theta_t & \cos^2\theta_t \end{pmatrix} \begin{pmatrix} \tilde{t}^*_1\tilde{t}_1 \\ \tilde{t}^*_1\tilde{t}_2 \\ \tilde{t}^*_2\tilde{t}_1 \\ \tilde{t}^*_2\tilde{t}_2 \end{pmatrix} \tag{234}$$

In order to obtain the rules in the 'physical' basis we must substitute for all the $L-R$ products in the Lagrangian from the relation (234).

As an example of the above described mechanism we are going to write down several Feynman rules for the trilinear and quartic interactions including supertops, which are necessary for computations within the other chapters.

B.1 Trilinear interactions including supertops

Note first that there are two neutral Higgs scalar and one Higgs and one Goldstone neutral pseudoscalars within the MSSM, but the amount of the possible vertices involving these particles and two supertops is reduced by many conservation laws.

I. Trilinear interactions of supertops with the Higgs scalars: These vertices correspond to the generic picture:

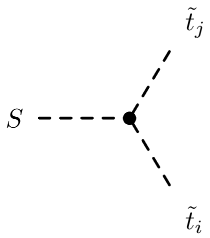

To express the rule for a concrete vertex we will use this shorthanded notation : $\mathbf{S\tilde{t}_i\tilde{t}_j} \sim$ *rule*. (For example the symbolic relation $\mathbf{h\tilde{t}_1\tilde{t}_2} \sim$ *rule* means the expression denoted by *rule* corresponds to the picture above with S replaced by h and i and j by 1 and 2. Note that the rules for $\mathbf{S\tilde{t}_i\tilde{t}_j}$ and $\mathbf{S\tilde{t}_j\tilde{t}_i}$ can be different.

Next, it is often very convenient to divide every rule to a number-like part (without any additional structure) noted by g with the relevant subscripts and a non-number part (i.e. metric tensor, momentum-vector components and matrix structures). For example the interaction of the Z-boson with supertops is described by

$$\mathbf{Z\tilde{t}_1\tilde{t}_1} \sim \frac{ig}{\cos\theta_W}\left(-X\cos^2\theta_t + Y\sin^2\theta_t\right)(k+k')^\mu \tag{235}$$

In this more sophisticated notation it would be rewritten in the form

$$\mathbf{Z\tilde{t}_1\tilde{t}_1} \sim g_{Z\tilde{t}_1\tilde{t}_1}(k+k')^\mu, \qquad \text{where} \qquad g_{Z\tilde{t}_1\tilde{t}_1} \equiv \frac{ig}{\cos\theta_W}\left(-X\cos^2\theta_t + Y\sin^2\theta_t\right) \tag{236}$$

and similarly the other rules.

Using the previous conventions we can start with the exhibition of the rules.To simplify the further relations we use the following notation:

$$X \equiv \frac{1}{2} - e_t\sin^2\theta_W \qquad \text{and} \qquad Y \equiv e_t\sin^2\theta_W \tag{237}$$

(θ_W is the Weinberg angle, e_t is the charge of the top-quark in the units the positron charge and the factor $\frac{1}{2}$ comes from the weak isospin of $\tilde{t}_L$.) Then rules for the interactions of the Higgs scalars h and H with the supertops sound:

$$\mathbf{h\tilde{t}_1\tilde{t}_1} \quad \sim \quad \frac{igm_Z}{\cos\theta_W}\sin(\alpha+\beta)\left(X\cos^2\theta_t + Y\sin^2\theta_t\right) - \frac{igm_t^2\cos\alpha}{m_W\sin\beta} \tag{238}$$

$$-\frac{igm_t\sin2\theta_t}{2m_W\sin\beta}\left(A_tm_6\cos\alpha - \mu\sin\alpha\right) \tag{239}$$

$$\mathbf{h\tilde{t}_2\tilde{t}_2} \quad \sim \quad \frac{igm_Z}{\cos\theta_W}\sin(\alpha+\beta)\left(X\sin^2\theta_t + Y\cos^2\theta_t\right) - \frac{igm_t^2\cos\alpha}{m_W\sin\beta}$$

$$+\frac{igm_t\sin2\theta_t}{2m_W\sin\beta}\left(A_tm_6\cos\alpha - \mu\sin\alpha\right) \tag{240}$$

$$\mathbf{h\tilde{t}_1\tilde{t}_2} \quad \sim \quad \frac{igm_Z}{\cos\theta_W}\sin(\alpha+\beta)\left(-X\sin\theta_t\cos\theta_t + Y\sin\theta_t\cos\theta_t\right)$$

$$-\frac{igm_t\cos2\theta_t}{2m_W\sin\beta}\left(A_tm_6\cos\alpha - \mu\sin\alpha\right) \tag{241}$$

$$\begin{aligned}
\mathbf{H\tilde{t}_1\tilde{t}_1} \quad \sim \quad & -\frac{igm_Z}{\cos\theta_W}\cos(\alpha+\beta)\,\left(X\cos^2\theta_t\,+Y\sin^2\theta_t\,\right)-\frac{igm_t^2\sin\alpha}{m_W\sin\beta} \\
& -\frac{igm_t\sin2\theta_t}{2m_W\sin\beta}\left(A_t m_6\sin\alpha\,+\mu\cos\alpha\,\right)
\end{aligned} \tag{242}$$

$$\mathbf{H\tilde{t}_2\tilde{t}_2} \quad \sim \quad -\frac{igm_Z}{\cos\theta_W}\cos(\alpha+\beta)\,\left(X\sin^2\theta_t\, + Y\cos^2\theta_t\,\right) - \frac{igm_t^2\sin\alpha}{m_W\sin\beta} \tag{243}$$

$$+\frac{igm_t\sin2\theta_t}{2m_W\sin\beta}\,(A_t m_6\sin\alpha\, + \mu\cos\alpha\,) \tag{244}$$

$$\mathbf{H\tilde{t}_1\tilde{t}_2} \quad \sim \quad -\frac{igm_Z}{\cos\theta_W}\cos(\alpha+\beta)\,(-X\sin\theta_t\cos\theta_t\, + Y\sin\theta_t\cos\theta_t\,)$$

$$-\frac{igm_t\sin2\theta_t}{2m_W\sin\beta}\,(A_t m_6\sin\alpha\, + \mu\cos\alpha\,) \tag{245}$$

II. Trilinear interactions of supertops with the pseudoscalars: The graphs corresponding to these vertices generally look like

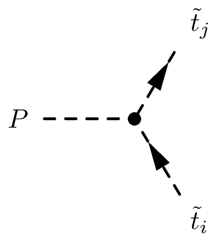

The arrows are necessary because the A and G are pseudoscalars. This feature causes the antisymmetry of the corresponding vertex; we can immediately see it from the Lagrangian, for instance the $A\tilde{t}_1\tilde{t}_2$ vertex:

$$\mathcal{L}_{A\tilde{t}_i\tilde{t}_j} = \frac{igm_t}{2m_W\sin\beta}\,(A_t m_6\cos\beta\, - \mu\sin\beta\,)\left(\tilde{t}_1^*\tilde{t}_2 - \tilde{t}_2^*\tilde{t}_1\right)A \tag{246}$$

The Feynman rules have the following form:

$$\mathbf{A\tilde{t}_1\tilde{t}_2} \sim \quad -A\tilde{t}_2\tilde{t}_1 \quad \sim \quad \frac{gm_t}{2m_W\sin\beta}\,(A_t m_6\cos\beta\, - \mu\sin\beta\,) \tag{247}$$

$$\mathbf{G\tilde{t}_1\tilde{t}_2} \sim \quad -G\tilde{t}_2\tilde{t}_1 \quad \sim \quad \frac{gm_t}{2m_W\sin\beta}\,(A_t m_6\sin\beta\, + \mu\cos\beta\,) \tag{248}$$

Note that there are no $\mathbf{A\tilde{t}_1\tilde{t}_1}$, $\mathbf{A\tilde{t}_2\tilde{t}_2}$, $\mathbf{G\tilde{t}_1\tilde{t}_1}$ and $\mathbf{G\tilde{t}_2\tilde{t}_2}$ vertices in the theory.

III. Trilinear interactions of supertops with the gauge bosons: As in the previous cases, the general scheme

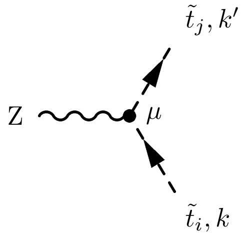

corresponds to the rules

$$\mathbf{Z\tilde{t}_1\tilde{t}_1} \quad \sim \quad \frac{ig}{\cos\theta_W}\left(-X\cos^2\theta_t\, + Y\sin^2\theta_t\,\right)(k+k')^\mu \tag{249}$$

$$\mathbf{Z\tilde{t}_2\tilde{t}_2} \quad \sim \quad \frac{ig}{\cos\theta_W}\left(-X\sin^2\theta_t\, + Y\cos^2\theta_t\,\right)(k+k')^\mu \tag{250}$$

$$\mathbf{Z\tilde{t}_1\tilde{t}_2} \quad \sim \quad \frac{ig}{\cos\theta_W}\,(X\sin\theta_t\cos\theta_t\, + Y\sin\theta_t\cos\theta_t\,)\,(k+k')^\mu \sim -Z\tilde{t}_2\tilde{t}_1 \tag{251}$$

B.2 Quartic vertices including supertops

I. Interactions of two supertops with two scalars: The general picture looks like

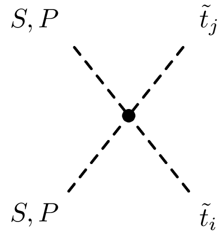

Using the notation defined in the previous section the Feynman rules can be written in the form

$$\mathbf{hh\tilde{t}_1\tilde{t}_1} \sim \frac{ig^2}{2\cos^2\theta_W}\cos 2\alpha \left(X\cos^2\theta_t + Y\sin^2\theta_t\right) - \frac{ig^2 m_t^2 \cos^2\alpha}{2m_W^2 \sin^2\beta} \tag{252}$$

$$\mathbf{hh\tilde{t}_2\tilde{t}_2} \sim \frac{ig^2}{2\cos^2\theta_W}\cos 2\alpha \left(X\sin^2\theta_t + Y\cos^2\theta_t\right) - \frac{ig^2 m_t^2 \cos^2\alpha}{2m_W^2 \sin^2\beta} \tag{253}$$

$$\mathbf{HH\tilde{t}_1\tilde{t}_1} \sim -\frac{ig^2}{2\cos^2\theta_W}\cos 2\alpha \left(X\cos^2\theta_t + Y\sin^2\theta_t\right) - \frac{ig^2 m_t^2 \sin^2\alpha}{2m_W^2 \sin^2\beta} \tag{254}$$

$$\mathbf{HH\tilde{t}_2\tilde{t}_2} \sim -\frac{ig^2}{2\cos^2\theta_W}\cos 2\alpha \left(X\sin^2\theta_t + Y\cos^2\theta_t\right) - \frac{ig^2 m_t^2 \sin^2\alpha}{2m_W^2 \sin^2\beta} \tag{255}$$

II. Interactions of two supertops with two pseudoscalars: The rules for the quartic interactions of supertops with the pseudoscalars A and G are

$$\mathbf{AA\tilde{t}_1\tilde{t}_1} \sim \frac{ig^2}{2\cos^2\theta_W}\cos 2\beta \left(X\cos^2\theta_t + Y\sin^2\theta_t\right) - \frac{ig^2 m_t^2}{2m_W^2}\tan^2\beta \tag{256}$$

$$\mathbf{AA\tilde{t}_2\tilde{t}_2} \sim \frac{ig^2}{2\cos^2\theta_W}\cos 2\beta \left(X\sin^2\theta_t + Y\cos^2\theta_t\right) - \frac{ig^2 m_t^2}{2m_W^2}\tan^2\beta \tag{257}$$

$$\mathbf{GG\tilde{t}_1\tilde{t}_1} \sim -\frac{ig^2}{2\cos^2\theta_W}\cos 2\beta \left(X\cos^2\theta_t + Y\sin^2\theta_t\right) - \frac{ig^2 m_t^2}{2m_W^2} \tag{258}$$

$$\mathbf{GG\tilde{t}_2\tilde{t}_2} \sim -\frac{ig^2}{2\cos^2\theta_W}\cos 2\beta \left(X\sin^2\theta_t + Y\cos^2\theta_t\right) - \frac{ig^2 m_t^2}{2m_W^2} \tag{259}$$

III. Interactions of two supertops with two gauge bosons: The vertices of the considered type correspond to the generic picture

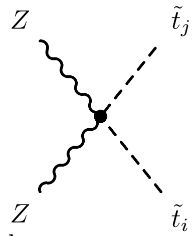

and the relevant Feynman rules sound

$$\mathbf{ZZ\tilde{t}_1\tilde{t}_1} \sim \frac{2ig^2}{\cos^2\theta_W}\left(X^2\cos^2\theta_t + Y^2\sin^2\theta_t\right) g^{\mu\nu} \tag{260}$$

$$\mathbf{ZZ\tilde{t}_2\tilde{t}_2} \sim \frac{2ig^2}{\cos^2\theta_W}\left(X^2\sin^2\theta_t + Y^2\cos^2\theta_t\right) g^{\mu\nu} \tag{261}$$

Note that the previous expressions fulfill the following relation (written in the traditional notation):

$$g_{hh\tilde{t}_1\tilde{t}_1} + g_{HH\tilde{t}_1\tilde{t}_1} + g_{hh\tilde{t}_2\tilde{t}_2} + g_{HH\tilde{t}_2\tilde{t}_2} - g_{AA\tilde{t}_1\tilde{t}_1} - g_{GG\tilde{t}_1\tilde{t}_1} - g_{AA\tilde{t}_2\tilde{t}_2} - g_{GG\tilde{t}_2\tilde{t}_2} = 0 \quad (262)$$

B.3 Trilinear vertices including top quark

The diagrams relevant here are the following:

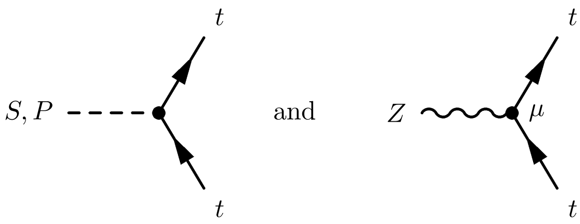

(263)

The corresponding Feynman rules sound

$$\mathbf{htt} \sim -\frac{igm_t\cos\alpha}{2m_W\sin\beta} \quad (264)$$

$$\mathbf{Htt} \sim -\frac{igm_t\sin\alpha}{2m_W\sin\beta} \quad (265)$$

$$\mathbf{Att} \sim -\frac{gm_t}{2m_W}\cot\beta\,\gamma_5 \quad (266)$$

$$\mathbf{Gtt} \sim -\frac{gm_t}{2m_W}\gamma_5 \quad (267)$$

$$\mathbf{Ztt} \sim -\frac{ig}{2\cos\theta_W}\gamma^\mu\left[X(1-\gamma_5) - Y(1+\gamma_5)\right] \quad (268)$$

B.4 Trilinear interactions of the Higgs bosons

The last part of this Appendix contains the Feynman rules for the trilinear HZZ and HHH vertices related to the pictures

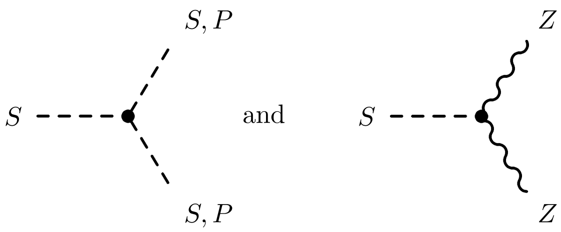

(269)

I. Vertices involving three Higgs particles: There are eight relevant Feynman rules in this cathegory:

$$\mathbf{hhh} \sim -\frac{igm_Z}{2\cos\theta_W}3\cos2\alpha\sin(\alpha+\beta) \quad (270)$$

$$\mathbf{hHH} \sim \frac{igm_Z}{2\cos\theta_W}\left[2\sin2\alpha\cos(\alpha+\beta) + \cos2\alpha\sin(\alpha+\beta)\right] \quad (271)$$

$$\mathbf{hAA} \sim -\frac{igm_Z}{2\cos\theta_W}\cos2\beta\sin(\alpha+\beta) \quad (272)$$

$$\mathbf{hGG} \sim \frac{igm_Z}{2\cos\theta_W}\cos2\beta\sin(\alpha+\beta) \quad (273)$$

$$\begin{aligned}
\mathbf{Hhh} &\sim -\frac{igm_Z}{2\cos\theta_W}\left[2\sin 2\alpha\sin(\alpha+\beta) - \cos 2\alpha\cos(\alpha+\beta)\right] &(274)\\
\mathbf{HHH} &\sim -\frac{igm_Z}{2\cos\theta_W}3\cos 2\alpha\cos(\alpha+\beta) &(275)\\
\mathbf{HAA} &\sim \frac{igm_Z}{2\cos\theta_W}\cos 2\beta\cos(\alpha+\beta) &(276)\\
\mathbf{HGG} &\sim -\frac{igm_Z}{2\cos\theta_W}\cos 2\beta\cos(\alpha+\beta) &(277)
\end{aligned}$$

II. Vertices involving one Higgs scalar and two Z bosons: These vertices contain two intermediate bosons so the corresponding Feynman rules involve metric tensors:

$$\begin{aligned}
\mathbf{hZZ} &\sim \frac{igm_Z}{\cos\theta_W}\sin(\beta-\alpha)\, g^{\mu\nu} &(278)\\
\mathbf{HZZ} &\sim \frac{igm_Z}{\cos\theta_W}\cos(\beta-\alpha)\, g^{\mu\nu} &(279)
\end{aligned}$$

As in the previous section there are several very important relations among the couplings

$$\begin{aligned}
g_{hhh} + g_{hHH} + g_{hZZ} &= 0\\
g_{Hhh} + g_{HHH} + g_{HZZ} &= 0 \qquad (280)\\
g_{hAA} + g_{hGG} &= 0\\
g_{HAA} + g_{HGG} &= 0
\end{aligned}$$

These relations ensure a great simplification of the total contribution (to tree-relation considered in chapter 2) coming from the tadpole sector of the theory.

C Computation of relevant diagrams

In this Appendix I would like to present an explicit computation of the (one-loop) two-particle OPI-Feynman graphs that are necessary in the previous sections. We will need the Feynman rules and the regularisation prescriptions that are written in the Appendices A and B. The main aim of this section is to catalogize the graphs and their contributions so the comments will be brief.

We will use the usual generic notation $\Pi(q)$ for the self-energies corresponding to scalars and $\Pi(q)^{\mu\nu}$ for the IVB polarisation tensors. Both these quantities will be equiped by a set of indeces to distinguish among them; the same holds also for the functions $D_q(x)$ from the appendix B (see [1]):

$$D_q^{XY}(x) \equiv m_X^2(1-x) + m_Y^2 x - q^2 x(1-x) \tag{281}$$

C.1 Diagrams involving one top quark loop

This subsection is devoted to the diagrams involving one top-quark loop. The reason of neglecting the other flavours is simple: the contributions of the considered graphs are typically proportional to the quark masses, which are hidden in the Yukawa coupling constants. This means that the contributions of the graphs including quarks of other flavours are suppressed by the factor $\frac{m_f^2}{m_t^2}$ which is very small. Moreover the mechanism of the ultraviolet divergences compensation does not mix different quark flavours so the top-sector is 'self-contained' also in this sense. For better orientation we are going to divide the whole set of considered graphs into two parts:

I. Graphs dependent on the external momenta

Working in the unitary gauge there are only four diagrams of this type; in R_ξ-gauges one more diagram corresponding to Goldstone boson propagator must be taken into account.

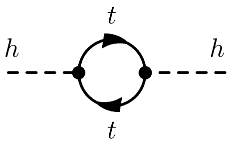

$$\equiv \quad -g_{htt}^2 \,\mathrm{Tr} \int \frac{d^4k}{(2\pi)^4} \frac{i}{\not{k} - m_t} \frac{i}{\not{k} - \not{q} - m_t} =$$

$$= \quad g_{htt}^2 \int \frac{d^4k}{(2\pi)^4} \,\mathrm{Tr} \frac{(\not{k} + m_t)(\not{k} - \not{q} + m_t)}{(k^2 - m_t^2)[(k-q)^2 - m_t^2]} \tag{282}$$

This integral is regularised in (204) with the particular choice $A = C = 1$ and $B = D = 0$ so we can write

$$-i\Pi_h^{tt}(q) \overset{\text{DR}}{\sim} -i\frac{g^2 m_t^2 \cos^2\alpha}{16\pi^2 m_W^2 \sin^2\beta} \left\{ \mathrm{C_{UV}} \left(3m_t^2 - \frac{q^2}{2}\right) + \left(m_t^2 - \frac{q^2}{6}\right) + \right.$$
$$\left. + \int_0^1 \mathrm{d}x \ln \frac{D_q^{tt}(x)}{\mu^2} \left[-3m_t^2 + 3q^2 x(1-x)\right] \right\} \tag{283}$$

Similarly in the case of H instead of h:

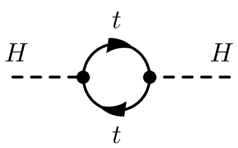

$$\equiv \quad -g_{Htt}^2 \,\mathrm{Tr} \int \frac{d^4k}{(2\pi)^4} \frac{i}{\not{k} - m_t} \frac{i}{\not{k} - \not{q} - m_t} =$$

$$= \quad g_{Htt}^2 \int \frac{d^4k}{(2\pi)^4} \,\mathrm{Tr} \frac{(\not{k} + m_t)(\not{k} - \not{q} + m_t)}{(k^2 - m_t^2)[(k-q)^2 - m_t^2]} \tag{284}$$

which gives

$$-i\Pi_H^{tt}(q) \overset{\text{DR}}{\sim} -i\frac{g^2 m_t^2 \sin^2\alpha}{16\pi^2 m_W^2 \sin^2\beta}\left\{\mathrm{C}_{\text{UV}}\left(3m_t^2-\frac{q^2}{2}\right)+\left(m_t^2-\frac{q^2}{6}\right)+\right.$$
$$\left.+\int_0^1 \mathrm{d}x \ln\frac{D_q^{tt}(x)}{\mu^2}\left[-3m_t^2+3q^2x(1-x)\right]\right\} \tag{285}$$

A different situation occurs in the case of the pseudoscalar A:

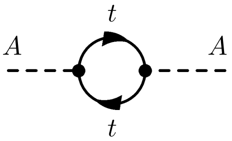

$$\equiv -g_{Att}^2\int\frac{d^4k}{(2\pi)^4}\,\mathrm{Tr}\gamma_5\frac{i}{\not k-m_t}\gamma_5\frac{i}{\not k-\not q-m_t}=$$
$$= g_{Att}^2\int\frac{d^4k}{(2\pi)^4}\,\mathrm{Tr}\left[\gamma_5\frac{m_t+\not k}{k^2-m_t^2}\gamma_5\frac{m_t+\not k-\not q}{(k-q)^2-m_t^2}\right] \tag{286}$$

which corresponds to the integral (204) choosing $A=C=0$ and $B=D=1$

$$-i\Pi_A^{tt}(q) \overset{\text{DR}}{\sim} i\frac{g^2 m_t^2 \cos^2\beta}{16\pi^2 m_W^2 \sin^2\beta}\left\{\mathrm{C}_{\text{UV}}\left(-m_t^2+\frac{q^2}{2}\right)-\left(m_t^2-\frac{q^2}{6}\right)+\right.$$
$$\left.+\int_0^1 \mathrm{d}x \ln\frac{D_q^{tt}(x)}{\mu^2}\left[m_t^2-3q^2x(1-x)\right]\right\} \tag{287}$$

The next investigated graph is

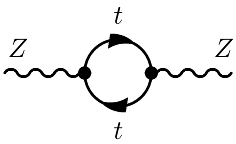

$$\equiv \tag{288}$$

$$\equiv -g_{Ztt}^2\,\mathrm{Tr}\int\frac{d^4k}{(2\pi)^4}\frac{i\gamma^\mu\left[X(1-\gamma_5)-Y(1+\gamma_5)\right]}{\not k-m_t}\frac{i\gamma^\nu\left[X(1-\gamma_5)-Y(1+\gamma_5)\right]}{\not k-\not q-m_t}= \tag{289}$$

$$=-g_{Ztt}^2(X-Y)^2\,\mathrm{Tr}\int\frac{d^4k}{(2\pi)^4}\frac{i\gamma^\mu\left[1-\frac{(X+Y)}{(X-Y)}\gamma_5)\right]}{\not k-m_t}\frac{i\gamma^\nu\left[1-\frac{(X+Y)}{(X-Y)}\gamma_5)\right]}{\not k-\not q-m_t}= \tag{290}$$

$$=g_{Ztt}^2(X-Y)^2\int\frac{d^4k}{(2\pi)^4}\,\mathrm{Tr}\left[\gamma^\mu(1+A\gamma_5)\frac{m_t+\not k}{k^2-m_t^2}\gamma^\nu(1+B\gamma_5)\frac{m_t+\not k-\not q}{(k-q)^2-m_t^2}\right] \tag{291}$$

here we have denoted

$$A=B\equiv-\frac{(X+Y)}{(X-Y)} \tag{292}$$

(note that $X-Y\neq 0$). This integral is already prepared in (219) so it is easy to obtain

$$-i\Pi_Z^{tt}(q)^{\mu\nu} \overset{\text{DR}}{\sim} g_{Ztt}^2(X-Y)^2\left\{-\frac{i}{4\pi^2}g^{\mu\nu}\int_0^1\mathrm{d}x\ln\frac{D_q^{tt}(x)}{\mu^2}(-2m_t^2AB)\right. \tag{293}$$
$$+\frac{i}{4\pi^2}\mathrm{C}_{\text{UV}}\left[-2m_t^2g^{\mu\nu}AB+(1+AB)\frac{1}{3}(g^{\mu\nu}q^2-q^\mu q^\nu)\right]+$$
$$\left.-\frac{i}{2\pi^2}\int_0^1\mathrm{d}x\ln\frac{D_q^{tt}(x)}{\mu^2}(1+AB)(q^\mu q^\nu-g^{\mu\nu}q^2)x(1-x)\right\}$$

Note that from (292) and (237) follows

$$(1+AB)=\frac{2(X^2+Y^2)}{(X-Y)^2}\qquad\text{and}\qquad AB(X-Y)^2=\frac{1}{4} \tag{294}$$

Moreover, looking at the coupling (268) we can conclude

$$
\begin{aligned}
-i\Pi_Z^{tt}(q)^{\mu\nu} \overset{\text{DR}}{\sim} & -\frac{g^2 m_Z^2}{4m_W^2}\left\{-\frac{i}{4\pi^2}g^{\mu\nu}\int_0^1 \mathrm{d}x \ln\frac{D_q^{tt}(x)}{\mu^2}\left(-\frac{m_t^2}{2}\right)\right. \\
& + \frac{i}{4\pi^2}\mathrm{C_{UV}}\left[-\frac{m_t^2}{2}g^{\mu\nu} + \frac{2}{3}(X^2+Y^2)(g^{\mu\nu}q^2 - q^\mu q^\nu)\right] + \\
& \left. - \frac{i}{2\pi^2}\int_0^1 \mathrm{d}x \ln\frac{D_q^{tt}(x)}{\mu^2} 2(X^2+Y^2)(q^\mu q^\nu - g^{\mu\nu}q^2)x(1-x)\right\}
\end{aligned}
\tag{295}
$$

In the R_ξ gauges there is one more graph to be considered because of presence of the Goldstone boson in the theory [4].

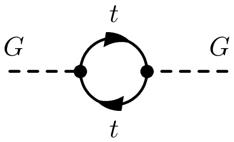

$$
\equiv -g_{Gtt}^2 \int \frac{d^4k}{(2\pi)^4}\,\mathrm{Tr}\gamma_5 \frac{i}{\not{k} - m_t}\gamma_5 \frac{i}{\not{k} - \not{q} - m_t} \tag{296}
$$

The situation is similar to the case of the pseudoscalar A in (286). This leads to the result

$$
\begin{aligned}
-i\Pi_G^{tt}(q) \overset{\text{DR}}{\sim} & \; i\frac{g^2 m_t^2}{16\pi^2 m_W^2}\left\{\mathrm{C_{UV}}\left(-m_t^2 + \frac{q^2}{2}\right) - \left(m_t^2 - \frac{q^2}{6}\right) + \right. \\
& \left. + \int_0^1 \mathrm{d}x \ln\frac{D_q^{tt}(x)}{\mu^2}\left[m_t^2 - 3q^2 x(1-x)\right]\right\}
\end{aligned}
\tag{297}
$$

II. Tadpole diagrams

Working in the unitary gauge there are eight diagrams of this type (and two with the Goldstones in the R_ξ-gauges). We will not show all of them because they are similar one to another. Moreover their total contribution to the tree relation $m_h^2 + m_H^2 = m_A^2 + m_Z^2$ (i.e. both the divergent and the finite part) in R_ξ-gauges exactly cancel (see [4]). The only graphs that are not cancelled in the unitary gauge are the tadpoles including the pseudoscalar A. We include also the tadpoles contributiong to the Goldstone boson propagator to use them in the third chapter. Let us first deal with

II.a. Tadpoles containing A: There are two such graphs:

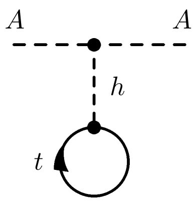

$$
\begin{aligned}
& \equiv -(-1)g_{AAh}\frac{i}{m_h^2}g_{htt}\,\mathrm{Tr}\int\frac{d^4k}{(2\pi)^4}\frac{i}{\not{k} - m_t} \\
& = -g_{AAh}g_{htt}\frac{1}{m_h^2}\,\mathrm{Tr}\int\frac{d^4k}{(2\pi)^4}\frac{\not{k} + m_t}{k^2 - m_t^2}
\end{aligned}
\tag{298}
$$

The only thing to be done is to recall the relation (180) and the couplings (272) and (264) to get the regularized contribution of this graph:

$$
-i\Pi_A^{ht} \overset{\text{DR}}{\sim} \frac{g^2 m_Z m_t \cos\alpha}{\cos\theta_W\, m_W \sin\beta}\frac{1}{m_h^2}\cos 2\beta \sin(\alpha+\beta)\frac{i}{16\pi^2}m_t^3\left(\mathrm{C_{UV}} + 1 - \ln\frac{m_t^2}{\mu^2}\right) \tag{299}
$$

Then we use the relation

$$
m_Z^2 \cos 2\beta \sin(\alpha+\beta) = m_h^2 \sin(\alpha-\beta) \tag{300}
$$

which allows us to simplify the last result to the form

$$-i\Pi_A^{ht} \overset{\text{DR}}{\sim} \frac{g^2 m_t^4}{m_W^2 \sin\beta} \cos\alpha \sin(\alpha-\beta) \frac{i}{16\pi^2} \left(\mathrm{C}_{\text{UV}} + 1 - \ln\frac{m_t^2}{\mu^2} \right) \tag{301}$$

Similarly the next graph:

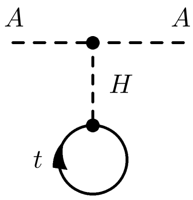

$$\equiv \quad (-1) g_{AAH} \frac{i}{0 - m_H^2} g_{Htt} \, \mathrm{Tr} \int \frac{d^4k}{(2\pi)^4} \frac{i}{\not{k} - m_t}$$

$$= \quad -g_{AAH} g_{Htt} \frac{1}{m_H^2} \, \mathrm{Tr} \int \frac{d^4k}{(2\pi)^4} \frac{\not{k} + m_t}{k^2 - m_t^2} \tag{302}$$

Utilising again (180),(276) and (265) we obtain

$$-i\Pi_A^{Ht} \overset{\text{DR}}{\sim} -\frac{g^2 m_Z m_t \sin\alpha}{\cos\theta_W \, m_W \sin\beta} \frac{1}{m_H^2} \cos 2\beta \cos(\alpha+\beta) \frac{i}{16\pi^2} m_t^3 \left(\mathrm{C}_{\text{UV}} + 1 - \ln\frac{m_t^2}{\mu^2} \right) \tag{303}$$

The relation

$$m_Z^2 \cos 2\beta \cos(\alpha+\beta) = m_H^2 \cos(\alpha-\beta) \tag{304}$$

simplifies (303) to the form

$$-i\Pi_A^{Ht} \overset{\text{DR}}{\sim} -\frac{g^2 m_t^4}{m_W^2 \sin\beta} \sin\alpha \cos(\alpha-\beta) \frac{i}{16\pi^2} \left(\mathrm{C}_{\text{UV}} + 1 - \ln\frac{m_t^2}{\mu^2} \right) \tag{305}$$

II.b. Tadpoles including Goldstone bosons:

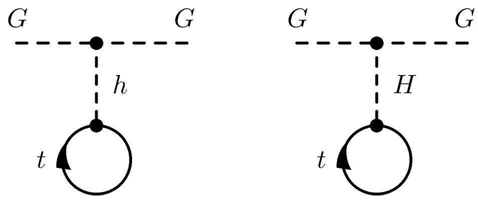

(306)

The contributions of these graphs can be obtained immediately from the results for A. Recalling relations (280)

$$g_{GGh} + g_{AAh} = 0 \qquad \text{and} \qquad g_{GGH} + g_{AAH} = 0 \tag{307}$$

we get

$$-i\Pi_G^{ht} \overset{\text{DR}}{\sim} -\frac{g^2 m_t^4}{m_W^2 \sin\beta} \cos\alpha \sin(\alpha-\beta) \frac{i}{16\pi^2} \left(\mathrm{C}_{\text{UV}} + 1 - \ln\frac{m_t^2}{\mu^2} \right) \tag{308}$$

$$-i\Pi_G^{Ht} \overset{\text{DR}}{\sim} \frac{g^2 m_t^4}{m_W^2 \sin\beta} \sin\alpha \cos(\alpha-\beta) \frac{i}{16\pi^2} \left(\mathrm{C}_{\text{UV}} + 1 - \ln\frac{m_t^2}{\mu^2} \right) \tag{309}$$

C.2 Diagrams involving one supertop loop

The topic of this subsection is to write down all the necessary graphs involving one supertop loop and their regularized contributions. The structure of the expressions coming from scalar loops is much more simple than the same graph with top-quark loop, but the couplings are very complicated due to the presence of the soft-supersymmetry breaking terms.

I. Graphs dependent on the external momenta

There are 10 graphs to be investigated in the unitary gauge.(In the R_ξ-gauges there is one additional graph containing Goldstone boson in this category.)

I.a. Diagrams involving h:

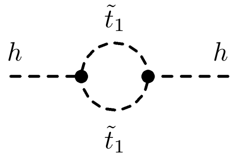

$$\equiv g^2_{h\tilde{t}_1\tilde{t}_1}\int\frac{d^4k}{(2\pi)^4}\frac{i}{k^2-m^2_{\tilde{t}_1}}\frac{i}{(k-q)^2-m^2_{\tilde{t}_1}} \tag{310}$$

We use (173) and (238) to get

$$-i\Pi_h^{\tilde{t}_1\tilde{t}_1}(q) \overset{\text{DR}}{\sim} \left[\frac{gm_Z}{\cos\theta_W}\sin(\alpha+\beta)\,\left(X\cos^2\theta_t\,+Y\sin^2\theta_t\,\right)-\frac{gm_t^2\cos\alpha}{m_W\sin\beta}-\right. \tag{311}$$

$$\left.-\frac{gm_t\sin2\theta_t}{2m_W\sin\beta}\,(A_tm_6\cos\alpha\,-\mu\sin\alpha\,)\right]^2\frac{i}{16\pi^2}\left[\mathrm{C_{UV}}-\int_0^1\mathrm{d}x\ln\frac{D_q^{\tilde{t}_1\tilde{t}_1}(x)}{\mu^2}\right]$$

And similarly the other graphs:

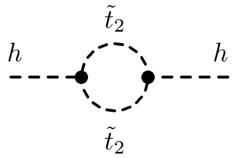

$$\equiv g^2_{h\tilde{t}_2\tilde{t}_2}\int\frac{d^4k}{(2\pi)^4}\frac{i}{k^2-m^2_{\tilde{t}_2}}\frac{i}{(k-q)^2-m^2_{\tilde{t}_2}} \tag{312}$$

$$-i\Pi_h^{\tilde{t}_2\tilde{t}_2}(q) \overset{\text{DR}}{\sim} \left[\frac{gm_Z}{\cos\theta_W}\sin(\alpha+\beta)\,\left(X\sin^2\theta_t\,+Y\cos^2\theta_t\,\right)-\frac{gm_t^2\cos\alpha}{m_W\sin\beta}+\right. \tag{313}$$

$$\left.+\frac{gm_t\sin2\theta_t}{2m_W\sin\beta}\,(A_tm_6\cos\alpha\,-\mu\sin\alpha\,)\right]^2\frac{i}{16\pi^2}\left[\mathrm{C_{UV}}-\int_0^1\mathrm{d}x\ln\frac{D_q^{\tilde{t}_2\tilde{t}_2}(x)}{\mu^2}\right]$$

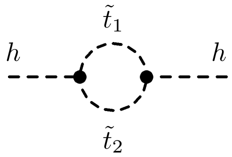

$$\equiv 2g^2_{h\tilde{t}_1\tilde{t}_2}\int\frac{d^4k}{(2\pi)^4}\frac{i}{k^2-m^2_{\tilde{t}_1}}\frac{i}{(k-q)^2-m^2_{\tilde{t}_2}} \tag{314}$$

$$-i\Pi_h^{\tilde{t}_1\tilde{t}_2}(q) \overset{\text{DR}}{\sim} 2\left[\frac{gm_Z}{\cos\theta_W}\sin(\alpha+\beta)\,\left(-X\sin\theta_t\cos\theta_t\,+Y\sin\theta_t\cos\theta_t\,\right)-\right. \tag{315}$$

$$\left.-\frac{gm_t\cos2\theta_t}{2m_W\sin\beta}\,(A_tm_6\cos\alpha\,-\mu\sin\alpha\,)\right]^2\frac{i}{16\pi^2}\left[\mathrm{C_{UV}}-\int_0^1\mathrm{d}x\ln\frac{D_q^{\tilde{t}_1\tilde{t}_1}(x)}{\mu^2}\right]$$

I.b. Diagrams involving H: The computation is straightforward - the only differences come from the corresponding couplings.

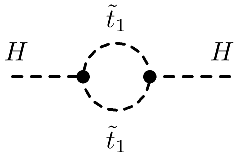

$$\equiv g^2_{H\tilde{t}_1\tilde{t}_1}\int\frac{d^4k}{(2\pi)^4}\frac{i}{k^2-m^2_{\tilde{t}_1}}\frac{i}{(k-q)^2-m^2_{\tilde{t}_1}} \tag{316}$$

$$-i\Pi_H^{\tilde{t}_1\tilde{t}_1}(q) \overset{\text{DR}}{\sim} \left[-\frac{gm_Z}{\cos\theta_W}\cos(\alpha+\beta)\,\left(X\cos^2\theta_t\,+Y\sin^2\theta_t\,\right)-\frac{gm_t^2\sin\alpha}{m_W\sin\beta}-\right. \tag{317}$$

$$-\frac{gm_t\sin 2\theta_t}{2m_W\sin\beta}\left(A_t m_6 \sin\alpha + \mu\cos\alpha\right)\Big]^2 \frac{i}{16\pi^2}\left[\mathrm{C_{UV}} - \int_0^1 \mathrm{d}x \ln\frac{D_q^{\tilde{t}_1\tilde{t}_1}(x)}{\mu^2}\right]$$

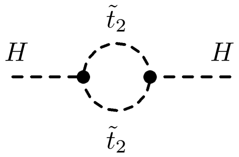

$$\equiv g^2_{H\tilde{t}_2\tilde{t}_2}\int\frac{d^4k}{(2\pi)^4}\frac{i}{k^2-m^2_{\tilde{t}_2}}\frac{i}{(k-q)^2-m^2_{\tilde{t}_2}} \tag{318}$$

$$-i\Pi_H^{\tilde{t}_2\tilde{t}_2}(q) \overset{\mathrm{DR}}{\sim} \Big[-\frac{gm_Z}{\cos\theta_W}\cos(\alpha+\beta)\left(X\sin^2\theta_t + Y\cos^2\theta_t\right) - \frac{gm_t^2\sin\alpha}{m_W\sin\beta} + \tag{319}$$

$$+\frac{gm_t\sin 2\theta_t}{2m_W\sin\beta}\left(A_t m_6 \sin\alpha + \mu\cos\alpha\right)\Big]^2 \frac{i}{16\pi^2}\left[\mathrm{C_{UV}} - \int_0^1 \mathrm{d}x \ln\frac{D_q^{\tilde{t}_2\tilde{t}_2}(x)}{\mu^2}\right]$$

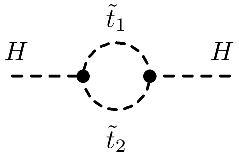

$$\equiv g^2_{H\tilde{t}_1\tilde{t}_2}\int\frac{d^4k}{(2\pi)^4}\frac{i}{k^2-m^2_{\tilde{t}_1}}\frac{i}{(k-q)^2-m^2_{\tilde{t}_2}} \tag{320}$$

$$-i\Pi_H^{\tilde{t}_1\tilde{t}_2}(q) \overset{\mathrm{DR}}{\sim} 2\Big[-\frac{gm_Z}{\cos\theta_W}\cos(\alpha+\beta)\left(-X\sin\theta_t\cos\theta_t + Y\sin\theta_t\cos\theta_t\right) - \tag{321}$$

$$-\frac{gm_t\sin 2\theta_t}{2m_W\sin\beta}\left(A_t m_6 \sin\alpha + \mu\cos\alpha\right)\Big]^2 \frac{i}{16\pi^2}\left[\mathrm{C_{UV}} - \int_0^1 \mathrm{d}x \ln\frac{D_q^{\tilde{t}_1\tilde{t}_2}(x)}{\mu^2}\right]$$

I.c. Diagrams involving A: There is only one graph of this type because of absence of the $A\tilde{t}_1\tilde{t}_1$ and $A\tilde{t}_2\tilde{t}_2$ vertices in the theory.

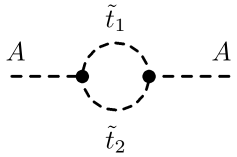

$$\equiv -g^2_{A\tilde{t}_1\tilde{t}_2}\int\frac{d^4k}{(2\pi)^4}\frac{i}{k^2-m^2_{\tilde{t}_1}}\frac{i}{(k-q)^2-m^2_{\tilde{t}_2}} \tag{322}$$

$$-i\Pi_A^{\tilde{t}_1\tilde{t}_2}(q) \overset{\mathrm{DR}}{\sim} 2\left[\frac{gm_t}{2m_W\sin\beta}\left(A_t m_6\cos\beta - \mu\sin\beta\right)\right]^2 \times \tag{323}$$

$$\times\frac{i}{16\pi^2}\left[\mathrm{C_{UV}} - \int_0^1 \mathrm{d}x \ln\frac{D_q^{\tilde{t}_1\tilde{t}_2}(x)}{\mu^2}\right]$$

Note that the overall minus sign in (322) comes from the antisymmetry of the $A\tilde{t}_1\tilde{t}_2$ vertex.

I.d. Diagrams involving Goldstone boson G: Working in the R_ξ gauges we have to investigate graphs containing Goldstone bosons. There is only one of them in this category. The neutral Goldstone boson G is a pseudoscalar like the A so the results are similar:

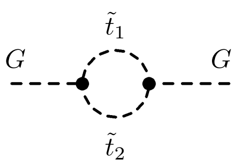

$$\equiv -g^2_{G\tilde{t}_1\tilde{t}_2}\int\frac{d^4k}{(2\pi)^4}\frac{i}{k^2-m^2_{\tilde{t}_1}}\frac{i}{(k-q)^2-m^2_{\tilde{t}_2}} \tag{324}$$

$$-i\Pi_G^{\tilde{t}_1\tilde{t}_2}(q) \overset{\mathrm{DR}}{\sim} 2\left[\frac{gm_t}{2m_W\sin\beta}\left(A_t m_6\sin\beta + \mu\cos\beta\right)\right]^2 \times \tag{325}$$

$$\times\frac{i}{16\pi^2}\left[\mathrm{C_{UV}} - \int_0^1 \mathrm{d}x \ln\frac{D_q^{\tilde{t}_1\tilde{t}_2}(x)}{\mu^2}\right]$$

I.e. Diagrams containing the intermediate Z boson: There are three of these graphs used in the text. Having prepared (193) the regularisation is straightforward and gives:

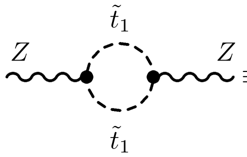

$$\equiv g^2_{Z\tilde{t}_1\tilde{t}_1}\int\frac{d^4k}{(2\pi)^4}\frac{i(2k-p)^\mu}{k^2-m^2_{\tilde{t}_1}}\frac{i(2k-p)^\nu}{(k-q)^2-m^2_{\tilde{t}_1}} \tag{326}$$

We use expresions (193) and (249) to get

$$-i\Pi_Z^{\tilde{t}_1\tilde{t}_1}(q)^{\mu\nu}\overset{\text{DR}}{\sim}\left[\frac{g}{\cos\theta_W}\left(-X\cos^2\theta_t\,+Y\sin^2\theta_t\,\right)\right]^2\times \tag{327}$$

$$\times\frac{i}{16\pi^2}\left\{\mathrm{C_{UV}}\left[\frac{1}{3}\left(q^\mu q^\nu-g^{\mu\nu}q^2\right)+2m^2_{\tilde{t}_1}g^{\mu\nu}\right]+\right.$$

$$\left.+g^{\mu\nu}\left(2m^2_{\tilde{t}_1}-\frac{q^2}{3}\right)-\int_0^1\mathrm{d}x\left[q^\mu q^\nu(1-2x)^2+2g^{\mu\nu}D_q^{\tilde{t}_1\tilde{t}_1}(x)\right]\ln\frac{D_q^{\tilde{t}_1\tilde{t}_1}(x)}{\mu^2}\right\}$$

Similarly the next two diagrams:

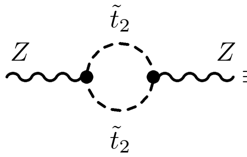

$$\equiv g^2_{Z\tilde{t}_2\tilde{t}_2}\int\frac{d^4k}{(2\pi)^4}\frac{i(2k-p)^\mu}{k^2-m^2_{\tilde{t}_2}}\frac{i(2k-p)^\nu}{(k-q)^2-m^2_{\tilde{t}_2}} \tag{328}$$

$$-i\Pi_Z^{\tilde{t}_2\tilde{t}_2}(q)^{\mu\nu}\overset{\text{DR}}{\sim}\left[\frac{g}{\cos\theta_W}\left(-X\sin^2\theta_t\,+Y\cos^2\theta_t\,\right)\right]^2\times \tag{329}$$

$$\times\frac{i}{16\pi^2}\left\{\mathrm{C_{UV}}\left[\frac{1}{3}\left(q^\mu q^\nu-g^{\mu\nu}q^2\right)+2m^2_{\tilde{t}_2}g^{\mu\nu}\right]+\right.$$

$$\left.+g^{\mu\nu}\left(2m^2_{\tilde{t}_2}-\frac{q^2}{3}\right)-\int_0^1\mathrm{d}x\left[q^\mu q^\nu(1-2x)^2+2g^{\mu\nu}D_q^{\tilde{t}_2\tilde{t}_2}(x)\right]\ln\frac{D_q^{\tilde{t}_2\tilde{t}_2}(x)}{\mu^2}\right\}$$

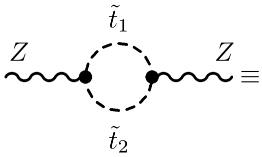

$$\equiv 2g^2_{Z\tilde{t}_1\tilde{t}_2}\int\frac{d^4k}{(2\pi)^4}\frac{i(2k-p)^\mu}{k^2-m^2_{\tilde{t}_1}}\frac{i(2k-p)^\nu}{(k-q)^2-m^2_{\tilde{t}_2}} \tag{330}$$

$$-i\Pi_Z^{\tilde{t}_1\tilde{t}_2}(q)^{\mu\nu}\overset{\text{DR}}{\sim}2\left[\frac{g}{\cos\theta_W}\left(X\sin\theta_t\cos\theta_t\,+Y\sin\theta_t\cos\theta_t\,\right)\right]^2\times \tag{331}$$

$$\times\frac{i}{16\pi^2}\left\{\mathrm{C_{UV}}\left[\frac{1}{3}\left(q^\mu q^\nu-g^{\mu\nu}q^2\right)+(m^2_{\tilde{t}_1}+m^2_{\tilde{t}_2})g^{\mu\nu}\right]+\right.$$

$$\left.+g^{\mu\nu}\left(m^2_{\tilde{t}_1}+m^2_{\tilde{t}_2}-\frac{q^2}{3}\right)-\int_0^1\mathrm{d}x\left[q^\mu q^\nu(1-2x)^2+2g^{\mu\nu}D_q^{\tilde{t}_1\tilde{t}_2}(x)\right]\ln\frac{D_q^{\tilde{t}_1\tilde{t}_2}(x)}{\mu^2}\right\}$$

II. The tadpole graphs

The situation in the sector of the tadpole-graphs containing one supertop loop is similar to the top-quark tadpoles, i.e. large cancellation of contributions occur. The rest of them (there are 4 graphs involving the pseudoscalar A in the unitary gauge and 4 more graphs involving Goldstones must be taken into account in R_ξ-gauges) will be discussed in this paragraph. The regularisation is easy (see top-quark loops) with the results:

II.a. Tadpoles containing A: As we have already said there are four graphs of this type:

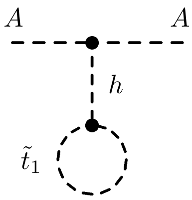

$$\equiv -g_{AAh}\frac{i}{m_h^2}g_{h\tilde{t}_1\tilde{t}_1}\int\frac{d^4k}{(2\pi)^4}\frac{i}{k^2-m_{\tilde{t}_1}^2} \tag{332}$$

Recalling relations (180), (300), (272) and (238) we obtain the result :

$$-i\Pi_A^{h\tilde{t}_1} \stackrel{\text{DR}}{\simeq} \frac{g}{2m_W}\left[\frac{gm_Z}{\cos\theta_W}\sin(\alpha+\beta)\left(X\cos^2\theta_t+Y\sin^2\theta_t\right)-\frac{gm_t^2\cos\alpha}{m_W\sin\beta}-\right. \tag{333}$$

$$\left.-\frac{gm_t\sin2\theta_t}{2m_W\sin\beta}\left(A_tm_6\cos\alpha-\mu\sin\alpha\right)\right]\sin(\alpha-\beta)\,\frac{i}{16\pi^2}m_{\tilde{t}_1}^2\left(\mathrm{C}_{\mathrm{UV}}+1-\ln\frac{m_{\tilde{t}_1}^2}{\mu^2}\right)$$

The next graphs are evaluated in a similar way.

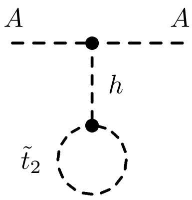

$$\equiv -g_{AAh}\frac{i}{m_h^2}g_{h\tilde{t}_2\tilde{t}_2}\int\frac{d^4k}{(2\pi)^4}\frac{i}{k^2-m_{\tilde{t}_2}^2} \tag{334}$$

with the result

$$-i\Pi_A^{h\tilde{t}_2} \stackrel{\text{DR}}{\simeq} \frac{g}{2m_W}\left[\frac{gm_Z}{\cos\theta_W}\sin(\alpha+\beta)\left(X\sin^2\theta_t+Y\cos^2\theta_t\right)-\frac{gm_t^2\cos\alpha}{m_W\sin\beta}+\right. \tag{335}$$

$$\left.+\frac{gm_t\sin2\theta_t}{2m_W\sin\beta}\left(A_tm_6\cos\alpha-\mu\sin\alpha\right)\right]\sin(\alpha-\beta)\,\frac{i}{16\pi^2}m_{\tilde{t}_2}^2\left(\mathrm{C}_{\mathrm{UV}}+1-\ln\frac{m_{\tilde{t}_2}^2}{\mu^2}\right)$$

The same can be done for the graphs with H instead of h:

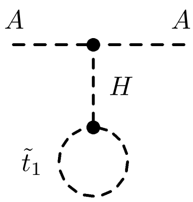

$$\equiv -g_{AAH}\frac{i}{m_H^2}g_{h\tilde{t}_1\tilde{t}_1}\int\frac{d^4k}{(2\pi)^4}\frac{i}{k^2-m_{\tilde{t}_1}^2} \tag{336}$$

$$-i\Pi_A^{H\tilde{t}_1} \stackrel{\text{DR}}{\simeq} \frac{g}{2m_W}\left[\frac{gm_Z}{\cos\theta_W}\cos(\alpha+\beta)\left(X\cos^2\theta_t+Y\sin^2\theta_t\right)+\frac{gm_t^2\sin\alpha}{m_W\sin\beta}+\right. \tag{337}$$

$$\left.+\frac{gm_t\sin2\theta_t}{2m_W\sin\beta}\left(A_tm_6\sin\alpha+\mu\cos\alpha\right)\right]\cos(\alpha-\beta)\,\frac{i}{16\pi^2}m_{\tilde{t}_1}^2\left(\mathrm{C}_{\mathrm{UV}}+1-\ln\frac{m_{\tilde{t}_1}^2}{\mu^2}\right)$$

Here we have used the relation (304).And the last diagram:

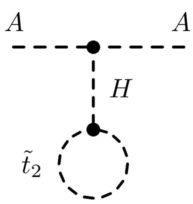

$$\equiv -g_{AAH}\frac{i}{m_H^2}g_{h\tilde{t}_2\tilde{t}_2}\int\frac{d^4k}{(2\pi)^4}\frac{i}{k^2-m_{\tilde{t}_2}^2} \tag{338}$$

$$-i\Pi_A^{H\tilde{t}_2} \stackrel{\text{DR}}{\simeq} \frac{g}{2m_W}\left[\frac{gm_Z}{\cos\theta_W}\cos(\alpha+\beta)\left(X\sin^2\theta_t+Y\cos^2\theta_t\right)+\frac{gm_t^2\sin\alpha}{m_W\sin\beta}-\right. \tag{339}$$

$$\left.-\frac{gm_t\sin2\theta_t}{2m_W\sin\beta}\left(A_tm_6\sin\alpha+\mu\cos\alpha\right)\right]\cos(\alpha-\beta)\,\frac{i}{16\pi^2}m_{\tilde{t}_2}^2\left(\mathrm{C}_{\mathrm{UV}}+1-\ln\frac{m_{\tilde{t}_2}^2}{\mu^2}\right)$$

II.b. Tadpoles containing G: The contributions of the graphs

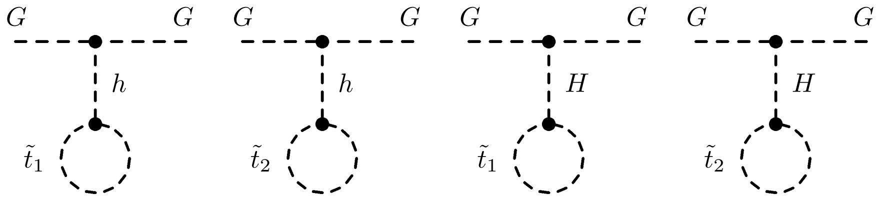

(340)

can be easily obtained from the previous results for A recalling the relations $g_{GGh}+g_{AAh}=0$ and $g_{GGH}+g_{AAH}=0$. The final results sound:

$$-i\Pi_G^{h\tilde{t}_1} \overset{\mathrm{DR}}{\sim} -\frac{g}{2m_W}\left[\frac{gm_Z}{\cos\theta_W}\sin(\alpha+\beta)\left(X\cos^2\theta_t + Y\sin^2\theta_t\right) - \frac{gm_t^2\cos\alpha}{m_W\sin\beta} - \right. \tag{341}$$
$$\left. -\frac{gm_t\sin2\theta_t}{2m_W\sin\beta}\left(A_t m_6\cos\alpha - \mu\sin\alpha\right)\right]\sin(\alpha-\beta)\,\frac{i}{16\pi^2}m_{\tilde{t}_1}^2\left(\mathrm{C_{UV}}+1-\ln\frac{m_{\tilde{t}_1}^2}{\mu^2}\right)$$

$$-i\Pi_G^{h\tilde{t}_2} \overset{\mathrm{DR}}{\sim} -\frac{g}{2m_W}\left[\frac{gm_Z}{\cos\theta_W}\sin(\alpha+\beta)\left(X\sin^2\theta_t + Y\cos^2\theta_t\right) - \frac{gm_t^2\cos\alpha}{m_W\sin\beta} + \right. \tag{342}$$
$$\left. +\frac{gm_t\sin2\theta_t}{2m_W\sin\beta}\left(A_t m_6\cos\alpha - \mu\sin\alpha\right)\right]\sin(\alpha-\beta)\,\frac{i}{16\pi^2}m_{\tilde{t}_2}^2\left(\mathrm{C_{UV}}+1-\ln\frac{m_{\tilde{t}_2}^2}{\mu^2}\right)$$

$$-i\Pi_G^{H\tilde{t}_1} \overset{\mathrm{DR}}{\sim} -\frac{g}{2m_W}\left[\frac{gm_Z}{\cos\theta_W}\cos(\alpha+\beta)\left(X\cos^2\theta_t + Y\sin^2\theta_t\right) + \frac{gm_t^2\sin\alpha}{m_W\sin\beta} + \right. \tag{343}$$
$$\left. +\frac{gm_t\sin2\theta_t}{2m_W\sin\beta}\left(A_t m_6\sin\alpha + \mu\cos\alpha\right)\right]\cos(\alpha-\beta)\,\frac{i}{16\pi^2}m_{\tilde{t}_1}^2\left(\mathrm{C_{UV}}+1-\ln\frac{m_{\tilde{t}_1}^2}{\mu^2}\right)$$

$$-i\Pi_G^{H\tilde{t}_2} \overset{\mathrm{DR}}{\sim} -\frac{g}{2m_W}\left[\frac{gm_Z}{\cos\theta_W}\cos(\alpha+\beta)\left(X\sin^2\theta_t + Y\cos^2\theta_t\right) + \frac{gm_t^2\sin\alpha}{m_W\sin\beta} - \right. \tag{344}$$
$$\left. -\frac{gm_t\sin2\theta_t}{2m_W\sin\beta}\left(A_t m_6\sin\alpha + \mu\cos\alpha\right)\right]\cos(\alpha-\beta)\,\frac{i}{16\pi^2}m_{\tilde{t}_2}^2\left(\mathrm{C_{UV}}+1-\ln\frac{m_{\tilde{t}_2}^2}{\mu^2}\right)$$

III. The seagull graphs

The so-called seagull diagrams appear through the fact that there exists also a quartic interaction among the scalars in the theory. In the fermionic sector this possibility is forbidden by the fact, that the vertices describing direct interactions of two fermions with two scalars would cause a nonrenormalizability of the theory. (The mass-dimension of such terms would be 5, which implies a negative dimension of relevant coupling and problems with the so-called tree-unitarity of the theory; see for example [13].)

There are ten seagull diagrams to be considered in this paragraph (two of them involving Goldstone boson). Their structure is practically the same as the structure of the tadpole diagrams investigated above so the comments will be brief. The first of them:

III.a. Seagulls including h: The regularisation is straightforward. Reminding (180) and the cuplings (252) - (257) we can write

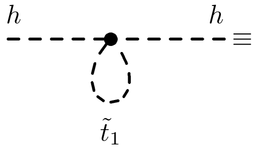

$$\equiv g_{hh\tilde{t}_1\tilde{t}_1} \int \frac{d^4k}{(2\pi)^4} \frac{i}{k^2 - m^2_{\tilde{t}_1}} \tag{345}$$

$$-i\Pi_h^{\tilde{t}_1} \overset{\text{DR}}{\sim} -\left[\frac{g^2}{2\cos^2\theta_W}\cos 2\alpha \left(X\cos^2\theta_t + Y\sin^2\theta_t\right) - \frac{g^2 m_t^2 \cos^2\alpha}{2m_W^2 \sin^2\beta}\right] \times$$
$$\times \frac{i}{16\pi^2} m^2_{\tilde{t}_1} \left(\mathrm{C}_{\mathrm{UV}} + 1 - \ln\frac{m^2_{\tilde{t}_1}}{\mu^2}\right) \tag{346}$$

Similarly for $\tilde{t}_2$:

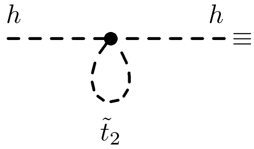

$$\equiv g_{hh\tilde{t}_2\tilde{t}_2} \int \frac{d^4k}{(2\pi)^4} \frac{i}{k^2 - m^2_{\tilde{t}_2}}$$

$$-i\Pi_h^{\tilde{t}_2} \overset{\text{DR}}{\sim} -\left[\frac{g^2}{2\cos^2\theta_W}\cos 2\alpha \left(X\sin^2\theta_t + Y\cos^2\theta_t\right) - \frac{g^2 m_t^2 \cos^2\alpha}{2m_W^2 \sin^2\beta}\right] \times$$
$$\times \frac{i}{16\pi^2} m^2_{\tilde{t}_2} \left(\mathrm{C}_{\mathrm{UV}} + 1 - \ln\frac{m^2_{\tilde{t}_2}}{\mu^2}\right) \tag{347}$$

III.b. Seagulls including H: The situation is similar to the case of the h scalar above:

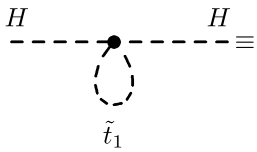

$$\equiv g_{HH\tilde{t}_1\tilde{t}_1} \int \frac{d^4k}{(2\pi)^4} \frac{i}{k^2 - m^2_{\tilde{t}_1}}$$

$$-i\Pi_H^{\tilde{t}_1} \overset{\text{DR}}{\sim} \left[\frac{g^2}{2\cos^2\theta_W}\cos 2\alpha \left(X\cos^2\theta_t + Y\sin^2\theta_t\right) + \frac{g^2 m_t^2 \sin^2\alpha}{2m_W^2 \sin^2\beta}\right] \times$$
$$\times \frac{i}{16\pi^2} m^2_{\tilde{t}_1} \left(\mathrm{C}_{\mathrm{UV}} + 1 - \ln\frac{m^2_{\tilde{t}_1}}{\mu^2}\right) \tag{348}$$

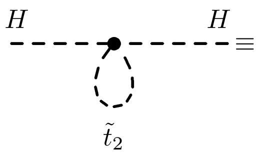

$$\equiv g_{HH\tilde{t}_2\tilde{t}_2} \int \frac{d^4k}{(2\pi)^4} \frac{i}{k^2 - m^2_{\tilde{t}_2}}$$

$$-i\Pi_H^{\tilde{t}_2} \overset{\text{DR}}{\sim} \left[\frac{g^2}{2\cos^2\theta_W}\cos 2\alpha \left(X\sin^2\theta_t + Y\cos^2\theta_t\right) + \frac{g^2 m_t^2 \sin^2\alpha}{2m_W^2 \sin^2\beta}\right] \times$$
$$\times \frac{i}{16\pi^2} m^2_{\tilde{t}_2} \left(\mathrm{C}_{\mathrm{UV}} + 1 - \ln\frac{m^2_{\tilde{t}_2}}{\mu^2}\right) \tag{349}$$

III.c. Seagulls including A: There are two graphs belonging to this cathegory:

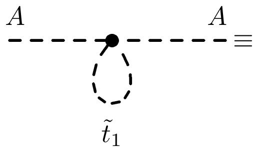

$$\equiv g_{AA\tilde{t}_1\tilde{t}_1}\int\frac{d^4k}{(2\pi)^4}\frac{i}{k^2-m_{\tilde{t}_1}^2}$$

$$\begin{aligned}-i\Pi_A^{\tilde{t}_1} \overset{\mathrm{DR}}{\sim} & -\left[\frac{g^2}{2\cos^2\theta_W}\cos 2\beta\left(X\cos^2\theta_t+Y\sin^2\theta_t\right)-\frac{g^2m_t^2}{2m_W^2}\tan^2\beta\right]\times\\ & \times\frac{i}{16\pi^2}m_{\tilde{t}_1}^2\left(\mathrm{C_{UV}}+1-\ln\frac{m_{\tilde{t}_1}^2}{\mu^2}\right)\end{aligned}\tag{350}$$

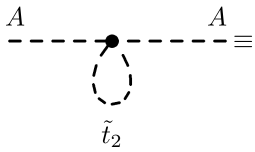

$$\equiv g_{AA\tilde{t}_2\tilde{t}_2}\int\frac{d^4k}{(2\pi)^4}\frac{i}{k^2-m_{\tilde{t}_2}^2}$$

$$\begin{aligned}-i\Pi_A^{\tilde{t}_2} \overset{\mathrm{DR}}{\sim} & -\left[\frac{g^2}{2\cos^2\theta_W}\cos 2\beta\left(X\sin^2\theta_t+Y\cos^2\theta_t\right)-\frac{g^2m_t^2}{2m_W^2}\tan^2\beta\right]\times\\ & \times\frac{i}{16\pi^2}m_{\tilde{t}_2}^2\left(\mathrm{C_{UV}}+1-\ln\frac{m_{\tilde{t}_2}^2}{\mu^2}\right)\end{aligned}\tag{351}$$

III.d. Seagulls including Z boson: We will also need contributions of two seagull graphs with Z boson. These graphs are in fact the only seagulls diagrams that contribute nontrivially to the computations performed in the second chapter.

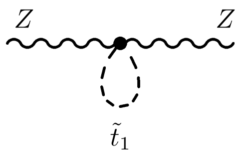

$$\equiv g_{GG\tilde{t}_1\tilde{t}_1}\int\frac{d^4k}{(2\pi)^4}\frac{ig^{\mu\nu}}{k^2-m_{\tilde{t}_1}^2}$$

$$\begin{aligned}-i(\Pi_Z^{\tilde{t}_1})^{\mu\nu} \overset{\mathrm{DR}}{\sim} & -g^{\mu\nu}\left[\frac{2g^2}{\cos^2\theta_W}\left(X^2\cos^2\theta_t+Y^2\sin^2\theta_t\right)\right]\times\\ & \times\frac{i}{16\pi^2}m_{\tilde{t}_1}^2\left(\mathrm{C_{UV}}+1-\ln\frac{m_{\tilde{t}_1}^2}{\mu^2}\right)\end{aligned}\tag{352}$$

and

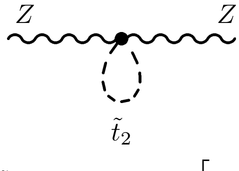

$$\equiv g_{ZZ\tilde{t}_2\tilde{t}_2}\int\frac{d^4k}{(2\pi)^4}\frac{ig^{\mu\nu}}{k^2-m_{\tilde{t}_2}^2}$$

$$\begin{aligned}-i(\Pi_Z^{\tilde{t}_2})^{\mu\nu} \overset{\mathrm{DR}}{\sim} & -g^{\mu\nu}\left[\frac{2g^2}{\cos^2\theta_W}\left(X^2\sin^2\theta_t+Y^2\cos^2\theta_t\right)\right]\times\\ & \times\frac{i}{16\pi^2}m_{\tilde{t}_2}^2\left(\mathrm{C_{UV}}+1-\ln\frac{m_{\tilde{t}_2}^2}{\mu^2}\right)\end{aligned}\tag{353}$$

III.e. Seagulls including Goldstone boson G: There are two more graphs to be considered in the case that we are not working in the unitary gauge:

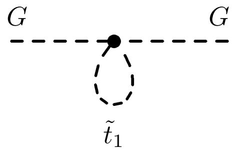

$$\equiv g_{GG\tilde{t}_1\tilde{t}_1} \int \frac{d^4k}{(2\pi)^4} \frac{i}{k^2 - m^2_{\tilde{t}_1}}$$

$$\begin{aligned} -i\Pi_G^{\tilde{t}_1} \overset{\text{DR}}{\sim} & \left[\frac{g^2}{2\cos^2\theta_W} \cos 2\beta \left(X\cos^2\theta_t + Y\sin^2\theta_t \right) + \frac{g^2 m_t^2}{2m_W^2} \right] \times \\ & \times \frac{i}{16\pi^2} m^2_{\tilde{t}_1} \left(\mathrm{C}_{\mathrm{UV}} + 1 - \ln \frac{m^2_{\tilde{t}_1}}{\mu^2} \right) \end{aligned} \tag{354}$$

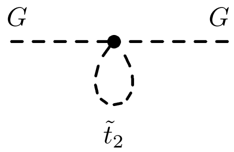

$$\equiv g_{GG\tilde{t}_2\tilde{t}_2} \int \frac{d^4k}{(2\pi)^4} \frac{i}{k^2 - m^2_{\tilde{t}_2}}$$

$$\begin{aligned} -i\Pi_G^{\tilde{t}_2} \overset{\text{DR}}{\sim} & \left[\frac{g^2}{2\cos^2\theta_W} \cos 2\beta \left(X\sin^2\theta_t + Y\cos^2\theta_t \right) + \frac{g^2 m_t^2}{2m_W^2} \right] \times \\ & \times \frac{i}{16\pi^2} m^2_{\tilde{t}_2} \left(\mathrm{C}_{\mathrm{UV}} + 1 - \ln \frac{m^2_{\tilde{t}_2}}{\mu^2} \right) \end{aligned} \tag{355}$$

The set of the necessary Feynman graphs is now complete so we can finish this Appendix.

D The Minimal Supersymmetric Standard Model (MSSM)

The main topic of this Appendix is to recall the basic structure of the Minimal Supersymmetric (extension of the) Standard Model which is investigated in this work. More precisely, we will deal with the electroweak part of the full MSSM (generally containing $SU(3)$ chromodynamic). There are several excellent information sources in the literature (for example the 'classical' SUSY book of J.Wess [18] and monographies [17],[11],[7]) so this review will be very brief. In the second part of it we focus on the Higgs sector of this model to derive the explicit form of the Higgs potential.

We are going to work in the *superspace* formulation which provides the most elegant way how to express the Lagrangian of the theory. The basics of this formalism can be found for example in [18] or [17] .

D.1 Definition of the MSSM

D.1.1 Superfields and particle content

The (electroweak) MSSM can be generally defined as an $N = 1$ supersymmetric (SUSY) nonabelian $SU(2)_{\text{L}} \otimes U(1)$ R-parity conserving gauge field theory with a softly broken global supersymmetry and a minimal particle content. This quite abstract definition need some comments:

- The term $N = 1$ supersymmetry means that there is only one supersymetry generator in the super-Poincaré algebra (see [16],[3]).
- The gauge group is the same as in the case of the original GSW Standard model, i.e. $SU(2)_{\text{L}} \otimes U(1)$.
- The requirement of the exact R-parity conserving prevents the theory from some physically unacceptable results like a fast nucleon decay rates, because it forbids several types of interactions responsible for that.
- The soft SUSY-breaking is a mechanism which is used to shift the masses of the superpartners above the experimentally observable region (note that up to now no superparticle was observed). A good review of the SUSY-breaking sector can be found for example in [14] or [17]. Being very accurate the presence of the soft-SUSY breaking terms causes that the MSSM is *not* supersymmetric, but it can be viewed as a low energy limit of a SUGRA theory [18].
- The term 'minimal particle content' means tree generations of quarks and leptons, four gauge bosons, two Higgs doublets and the superpartners of all these particles.

Detailed discussions of these properties can be found in the literature [17] so we omit any further comments. Let us now start with the explicit formulation of the model. We follow the construction written in the monography [17].

The first thing to be done is to built up the superfields necessary to describe all the known electroweakly interacting particles in the nature. All the ordinary matter fields are contained in the so called *chiral* superfields. Any chiral superfield can be written in the form

(using the superspace formalism)

$$\begin{aligned}\hat{S}(x,\theta,\bar{\theta}) &= \tilde{S}(x) + i\theta^{\alpha}\sigma^{\mu}_{\alpha\dot{\alpha}}\bar{\theta}^{\dot{\alpha}}\partial_{\mu}\tilde{S}(x) - \frac{1}{4}\theta^{\alpha}\theta_{\alpha}\bar{\theta}_{\dot{\alpha}}\bar{\theta}^{\dot{\alpha}}\partial^{\mu}\partial_{\mu}\tilde{S}(x) + \\ &\quad + \sqrt{2}\theta^{\alpha}S_{\alpha}(x) + \frac{i}{\sqrt{2}}\theta^{\alpha}\theta_{\alpha}\bar{\theta}_{\dot{\alpha}}\bar{\sigma}^{\mu\beta\dot{\alpha}}\partial_{\mu}S_{\beta}(x) + \theta^{\alpha}\theta_{\alpha}F_S(x) \end{aligned} \tag{356}$$

For example the (left-handed) lepton chiral superfield describing the left-handed leptons and their superpartners can be obtained via identification $S \equiv L_f$, (i.e. $\hat{S} \equiv \hat{L}_f$, $\tilde{S} \equiv \tilde{L}_f$ and $F_S \equiv F_{L_f}$) which gives

$$\begin{aligned}\hat{L}(x,\theta,\bar{\theta}) &= \tilde{L}_f(x) + i\theta^{\alpha}\sigma^{\mu}_{\alpha\dot{\alpha}}\bar{\theta}^{\dot{\alpha}}\partial_{\mu}\tilde{L}_f(x) - \frac{1}{4}\theta^{\alpha}\theta_{\alpha}\bar{\theta}_{\dot{\alpha}}\bar{\theta}^{\dot{\alpha}}\partial^{\mu}\partial_{\mu}\tilde{L}_f(x) + \\ &\quad + \sqrt{2}\theta^{\alpha}L_{f\alpha}(x) + \frac{i}{\sqrt{2}}\theta^{\alpha}\theta_{\alpha}\bar{\theta}_{\dot{\alpha}}\bar{\sigma}^{\mu\beta\dot{\alpha}}\partial_{\mu}L_{f\beta}(x) + \theta^{\alpha}\theta_{\alpha}F_{L_f}(x) \end{aligned} \tag{357}$$

where

$$\tilde{L}_f \equiv \begin{pmatrix} \tilde{\nu}_f \\ \tilde{f}_{\rm L} \end{pmatrix} \quad , \qquad L_f \equiv \begin{pmatrix} \nu_f \\ f_{\rm L} \end{pmatrix} \qquad \text{and} \qquad F_{L_f} \equiv \begin{pmatrix} F^{\nu} \\ F^f_{\rm L} \end{pmatrix} \tag{358}$$

(note that the left-handed leptons are arranged into dublets). The entries of the vectors above are identified with the physical fields in the following way: scalars $\tilde{\nu}_f$ and $\tilde{f}_{\rm L}$ are the so-called *neutralinos* and the (left) *sleptons* which are the superpartners of the leptons ν and $f_{\rm L}$ (described by two-component Weyl spinors). F^{ν} and $F^f_{\rm L}$ are auxiliary fields.

The same identification can be done for all the chiral matter superfields of the theory. We write down only the component form of the multiplets corresponding to the following assignements: $S \equiv R_f$ for the right-handed lepton supersinglet, $S \equiv Q_f$ for the left-handed quark superdublet, $S \equiv U$ for the right handed up-quark supersinglet, $S \equiv D_f$ for the right-handed down-quark supersinglet and $S \equiv H_{1,2}$ for both the Higghs supermultiplets. In component notation this corresponds to

$$\tilde{R}_f \equiv \tilde{f}^c_{\rm R} \quad , \qquad R_f = f_{\rm R} \qquad \text{and} \qquad F_{R_f} \equiv F^f_{\rm R} \tag{359}$$

(Note that we assume the purely left-handed neutrino so the right-handed leptons are singlets as in the GWS model. The superpartner $\tilde{\nu}_f$ of the neutrino is called *neutralino*.)

$$\tilde{Q}_f \equiv \begin{pmatrix} \tilde{u}^c_f \\ \tilde{d}^c_f \end{pmatrix}_{\rm L} \quad , \qquad Q_f \equiv \begin{pmatrix} u_f \\ d_f \end{pmatrix}_{\rm L} \qquad \text{and} \qquad F_{Q_f} \equiv \begin{pmatrix} F^{u_f} \\ F^{d_f} \end{pmatrix}_{\rm L} \tag{360}$$

(all the left-handed quarks belong to dublets, right-handed quarks are singlets; the up quarks are massive so we have to insert the up right-handed component which causes (optical) asymetry between the quarks and leptons)

$$\tilde{U}_f \equiv \tilde{u}^c_{f\rm R} \quad , \qquad U_f = u_{f\rm R} \qquad \text{and} \qquad F_{U_f} \equiv F^{u_f}_{\rm R} \tag{361}$$

$$\tilde{D}_f \equiv \tilde{d}^c_{f\rm R} \quad , \qquad D_f = d_{f\rm R} \qquad \text{and} \qquad F_{D_f} \equiv F^{d_f}_{\rm R} \tag{362}$$

(the quarks are denoted by u_f and d_f and their superpartners - *squarks* by $\tilde{u}_f$ and $\tilde{d}_f$; the superscript c means the charge conjugation [3])

$$\tilde{H}_1 \equiv \begin{pmatrix} H^1_1 \\ H^2_1 \end{pmatrix} \quad , \qquad \tilde{H}_1 \equiv \begin{pmatrix} \psi^1_{H_1} \\ \psi^2_{H_1} \end{pmatrix} \qquad \text{and} \qquad F_{H_1} \equiv \begin{pmatrix} F^1_{H_1} \\ F^2_{H_1} \end{pmatrix} \tag{363}$$

$$\tilde{H}_2 \equiv \begin{pmatrix} H_2^1 \\ H_2^2 \end{pmatrix}, \qquad \tilde{H}_2 \equiv \begin{pmatrix} \psi_{H_2}^1 \\ \psi_{H_2}^2 \end{pmatrix} \qquad \text{and} \qquad F_{H_2} \equiv \begin{pmatrix} F_{H_2}^1 \\ F_{H_2}^2 \end{pmatrix} \tag{364}$$

The fields H_j^i correspond to the Higgs bosons and $\psi_{H_j}^i$ denote their superpartners called *higgsinos*. As usual the F fields are auxiliary.

The next ingredience of the model are the so called gauge superfields which contain the usual gauge bosons and their superpartners - *gauginos*. A general gauge superfield can be written in the form

$$\hat{X}(x,\theta,\bar{\theta}) = -\theta^\alpha \sigma^\mu_{\alpha\dot{\alpha}} \bar{\theta}^{\dot{\alpha}} X_\mu(x) + i\theta^\alpha\theta_\alpha\bar{\theta}_{\dot{\alpha}}\bar{\lambda}^{\dot{\alpha}}(x) - i\bar{\theta}_{\dot{\alpha}}\bar{\theta}^{\dot{\alpha}}\theta^\alpha\lambda_\alpha(x) + \frac{1}{2}\theta^\alpha\theta_\alpha\bar{\theta}_{\dot{\alpha}}\bar{\theta}^{\dot{\alpha}}D(x) \tag{365}$$

The gauge superfields are some Lie-algebra valued functions; this can be expressed by the identifications $\hat{A} = \hat{A}^a T^a$ (for the $SU(2)_{\mathrm{L}}$ gauge superfield) and $\hat{B} = \hat{B}' Y_{\mathrm{W}}$ (in the case of the $U(1)$ gauge superfield). T^a and Y_{W} are generators of the corresponding representations of the gauge groups and $\hat{A}^a$ and $\hat{B}'$ are some ordinary superfields. Thus the $SU(2)_{\mathrm{L}}$ and $U(1)$ gauge superfields can be recast

$$\begin{aligned} \hat{A}(x,\theta,\bar{\theta}) &= -\theta^\alpha \sigma^\mu_{\alpha\dot{\alpha}} \bar{\theta}^{\dot{\alpha}} A^a_\mu(x) T^a + i\theta^\alpha\theta_\alpha\bar{\theta}_{\dot{\alpha}}\bar{\lambda}^{a\dot{\alpha}}(x) T^a - i\bar{\theta}_{\dot{\alpha}}\bar{\theta}^{\dot{\alpha}}\theta^\alpha\lambda^a_\alpha(x) T^a + \\ &\quad + \frac{1}{2}\theta^\alpha\theta_\alpha\bar{\theta}_{\dot{\alpha}}\bar{\theta}^{\dot{\alpha}} D^a(x) T^a \end{aligned} \tag{366}$$

$$\begin{aligned} \hat{B}(x,\theta,\bar{\theta}) &= -\theta^\alpha \sigma^\mu_{\alpha\dot{\alpha}} \bar{\theta}^{\dot{\alpha}} B_\mu(x) Y_{\mathrm{W}} + i\theta^\alpha\theta_\alpha\bar{\theta}_{\dot{\alpha}}\bar{\lambda}'^{\dot{\alpha}}(x) Y_{\mathrm{W}} - i\bar{\theta}_{\dot{\alpha}}\bar{\theta}^{\dot{\alpha}}\theta^\alpha\lambda'_\alpha(x) Y_{\mathrm{W}} + \\ &\quad + \frac{1}{2}\theta^\alpha\theta_\alpha\bar{\theta}_{\dot{\alpha}}\bar{\theta}^{\dot{\alpha}} D'(x) Y_{\mathrm{W}} \end{aligned} \tag{367}$$

The fields A^a_μ and B_μ correspond to the usual SM gauge fields 'responsible' for the Z, $W^\pm$ bosons and photon, while the (spinor) fields λ^a and λ' correspond to their superpartners called gauginos (zino, winos and photino). D^a and D' are some nonphysical auxiliary fields.

D.1.2 Lagrangian of the MSSM

The Lagrangian of the (electroweak) MSSM can be written in the form [17]

$$\mathcal{L}_{\mathrm{MSSM}} = \mathcal{L}_{\mathrm{SUSY}} + \mathcal{L}_{\mathrm{SOFT}} \tag{368}$$

where the term $\mathcal{L}_{\mathrm{SUSY}}$ is the SUSY-invariant part and the $\mathcal{L}_{\mathrm{SOFT}}$ is the so-called soft supersymmetry breaking term. The part $\mathcal{L}_{\mathrm{SUSY}}$ can be expanded in the form

$$\mathcal{L}_{\mathrm{SUSY}} = \mathcal{L}_{\mathrm{LEPTON}} + \mathcal{L}_{\mathrm{QUARK}} + \mathcal{L}_{\mathrm{HIGGS}} + \mathcal{L}_{\mathrm{GAUGE}} + \mathcal{L}_{\mathrm{SUPERPOT}} \tag{369}$$

The terms $\mathcal{L}_{\mathrm{LEPTON}}$, $\mathcal{L}_{\mathrm{QUARK}}$ and $\mathcal{L}_{\mathrm{HIGGS}}$ contain the lepton, quark and Higgs chiral superfields, $\mathcal{L}_{\mathrm{GAUGE}}$ corresponds to the gauge-boson vector superfield and the term $\mathcal{L}_{\mathrm{SUPERPOT}}$ contains the so called superpotential. In the superspace formalism these terms can be written in the form:

$$\mathcal{L}_{\mathrm{LEPTON}} = \int \mathrm{d}^4\theta \sum_f \left[\hat{L}^\dagger_f G(\hat{L}_f)\hat{L}_f + \hat{R}^\dagger_f G(\hat{R}_f)\hat{R}_f\right] \tag{370}$$

$$\mathcal{L}_{\mathrm{QUARK}} = \int \mathrm{d}^4\theta \sum_f \left[\hat{Q}^\dagger_f G(\hat{Q}_f)\hat{Q}_f + \hat{U}^\dagger_f G(\hat{U}_f)\hat{U}_f + \hat{D}^\dagger_f G(\hat{D}_f)\hat{D}_f\right] \tag{371}$$

$$\mathcal{L}_{\mathrm{HIGGS}} = \int \mathrm{d}^4\theta \left[\hat{H}^\dagger_1 G(\hat{H}_1)\hat{H}_1 + \hat{H}^\dagger_2 G(\hat{H}_2)\hat{H}_2\right] \tag{372}$$

$$\mathcal{L}_{\text{GAUGE}} = \frac{1}{4}\int \mathrm{d}^4\theta \left[\left(W^{a\alpha}W^a_\alpha + W'^{\alpha}W'_\alpha\right)\delta^2(\bar\theta) + \left(\bar W^a_{\dot\alpha}\bar W^{a\dot\alpha} + \bar W'_{\dot\alpha}W'^{\dot\alpha}\right)\delta^2(\theta)\right] \tag{373}$$

$$\mathcal{L}_{\text{SUPERPOT}} = \int \mathrm{d}^4\theta \left[W\delta^2(\bar\theta) + \bar W\delta^2(\theta)\right] \tag{374}$$

Here we have used the following notation: Hatted quantities denote the chiral or gauge superfields defined above. W^α and $\bar W_{\dot\alpha}$ are some auxiliary (spinorial) quantities which will be defined below and W is the superpotential. Next, the operator

$$G(\hat S) \equiv \exp\left(2g\hat A(\hat S) + 2g'\hat B(\hat S)\right) = \exp\left(2g\hat A^a T^a(\hat S) + 2g'\hat B' Y_{\text{W}}(\hat S)\right) \tag{375}$$

corresponds to the gauge transformation. $\hat A^a$ and $\hat B'$ are the gauge-boson vector superfields defined above , $T^a(\hat S)$ and $Y_{\text{W}}(\hat S)$ are the generators of the corresponding $SU(2)_{\text{L}}$ and $U(1)$ representations and constants g and g' are the usual gauge coupling constants. The eigenvalues of the weak hypercharge operator are defined in the usual way [13]

$$Y_{\text{W}} = Q - T^3 \tag{376}$$

The hypercharges Y_{W} and isospins T of all the relevant superfields are written in the table

Superfield	Y_{W}	T	
$\hat L$	$-\frac{1}{2}$	$\frac{1}{2}$	dublet
$\hat R$	1	0	singlet
$\hat Q$	$\frac{1}{6}$	$\frac{1}{2}$	dublet
$\hat U$	$-\frac{2}{3}$	0	singlet
$\hat D$	$\frac{1}{3}$	0	singlet
$\hat H_1$	$-\frac{1}{2}$	$\frac{1}{2}$	dublet
$\hat H_2$	$\frac{1}{2}$	$\frac{1}{2}$	dublet

Table 1: Superfield isospins and weak hypercharges

The remaining quantities are defined as follows: The auxiliary spinors:

$$W^a_\alpha = -\frac{1}{8g}\bar D_{\dot\alpha}\bar D^{\dot\alpha}\exp(-2g\hat A^a T^a)D_\alpha \exp(2g\hat A^a T^a) \tag{377}$$

$$W'_\alpha = -\frac{1}{8g'}\bar D_{\dot\alpha}\bar D^{\dot\alpha}\exp(-2g'\hat B' Y_{\text{W}})D_\alpha \exp(2g'\hat B' Y) \tag{378}$$

The D symbols here are the so-called *fermionic* derivatives [18] defined in the way

$$D_\alpha = \frac{\partial}{\partial\theta^\alpha} + i\sigma^\mu_{\alpha\dot\alpha}\bar\theta^{\dot\alpha}\frac{\partial}{\partial x^\mu} \qquad \bar D^{\dot\alpha} = \frac{\partial}{\partial\bar\theta^{\dot\alpha}} - i\varepsilon^{\dot\alpha\dot\beta}\theta^\beta\sigma^\mu_{\beta\dot\beta}\frac{\partial}{\partial x^\mu} \tag{379}$$

Note that the diagonality of Y_{W} allows us to simplify (378) into the form

$$W'_\alpha = -\frac{1}{4}\bar D_{\dot\alpha}\bar D^{\dot\alpha}D_\alpha\hat B' Y_{\text{W}} \tag{380}$$

The superpotential W is defined by ([17],[14],[3])

$$W = \varepsilon^{ij}\left(f\hat H^i_1\hat L^j\hat R + f_1\hat H^i_1\hat Q^j\hat D + f_2\hat H^j_2\hat Q^i\hat U + \mu\hat H^i_1\hat H^j_2\right) \tag{381}$$

This quantity corresponds to the SM Yukawa Lagrangian (the three first terms) and the Higgs mass term. (In fact, this is not the most general SUSY and gauge invariant superpotential. There are four additional possible terms: $\alpha_1^{ijk} Q^i L^j \bar{D}^k$, $\alpha_2^{ijk} L^i L^j \bar{R}^k$, $\alpha_3^i L^i H_2$ and $\alpha_4^{ijk} \bar{D}^i \bar{D}^j \bar{U}^k$. However these terms break the baryon and lepton number conservation. They are removed by the requirement of exact R-symmetry.) Note that the constants f are connected with the corresponding fermion masses by the relations $f = \sqrt{2} m_l v_1^{-1}$, $f_1 = \sqrt{2} m_d v_1^{-1}$ and $f = \sqrt{2} m_u v_2^{-1}$.

To proceed, we have to write down the explicit form of the soft-SUSY breaking terms contained in $\mathcal{L}_{\text{SOFT}}$ (see [17],[14]):

$$\mathcal{L}_{\text{SOFT}} = \mathcal{L}_{\text{SM}} + \mathcal{L}_{\text{GM}} \tag{382}$$

where the part

$$\begin{aligned}\mathcal{L}_{\text{SM}} = -\int \mathrm{d}^4\theta \Big[& M_{\text{L}}^2 \hat{L}^\dagger \hat{L} + M_{\text{R}}^2 \hat{R}^\dagger \hat{R} + M_{\text{Q}}^2 \hat{Q}^\dagger \hat{Q} + M_{\text{U}}^2 \hat{U}^\dagger \hat{U} + M_{\text{D}}^2 \hat{D}^\dagger \hat{D} + \\ & + m_6 \varepsilon^{ij} \left(f A_l \hat{H}_1^i \hat{L}^j \hat{R} + f_1 A_d \hat{H}_1^i \hat{Q}^j \hat{D} + f_2 A_u \hat{H}_2^j \hat{Q}^i \hat{U} \right) + \\ & + m_1^2 \hat{H}_1^\dagger \hat{H}_1 + m_2^2 \hat{H}_2^\dagger \hat{H}_2 - m_3^2 \varepsilon^{ij} \left(\hat{H}_2^i \hat{H}_2^j + h.c. \right) \Big] \, \delta^4(\theta, \bar{\theta})\end{aligned} \tag{383}$$

is the so-called scalar mass term and

$$\mathcal{L}_{\text{GM}} = \frac{1}{2} \int \mathrm{d}^4\theta \left[\left(M W^{a\alpha} W_\alpha^a + M' W'^\alpha W'_\alpha \right) + \left(M \bar{W}_{\dot{\alpha}}^a \bar{W}^{a\dot{\alpha}} + M' \bar{W}'_{\dot{\alpha}} W'^{\dot{\alpha}} \right) \right] \delta^4(\theta, \bar{\theta}) \tag{384}$$

is the gauge mass term. The definition of the MSSM in the superspace formalism is now complete. But this is not the end of the story. To use the standard quantisation techniques we have to transform the whole theory into the ordinary Minkowski-space formulation. This procedure consists of several steps:

- calculation of the necessary superfield products arising from the Lagrangian
- Berezin integration (see [17]); performing this operation the theory is contracted from the superspace to the ordinary Minkowski space
- elimination of all the auxiliary F and D fields using the Euler-Lagrange equations of motion
- transformation of the Lagrangian into the four-component (bispinor) formalism
- rediagonalisation of the kinetic terms in order to reformulate the theory into the physical basis

D.2 Derivation of the Higgs potential V_{HIGGS}

In this section we are going to derive the component form of the MSSM Higgs potential; we use it in the first chapter to investigate the Higgs sector mass-squared matrix. Moreover it is an example how to use the list above to convert the part of the theory from the superformalism to the usual component form. Of course we are forced to omit a lot of details; the explicit discussion of the following calculation can be found for example in [17].

The terms contributing to the Higgs potential come from four sources: $\mathcal{L}_{\text{HIGGS}}$, $\mathcal{L}_{\text{GAUGE}}$, $\mathcal{L}_{\text{SUPERPOT}}$ and $\mathcal{L}_{\text{SM}}$. Let us first investigate the term $\mathcal{L}_{\text{HIGGS}}$:

$$\mathcal{L}_{\text{HIGGS}} = \int \mathrm{d}^4\theta \left[\hat{H}_1^\dagger \exp\left(2g\hat{A}^a T^a + 2g'\hat{B}Y_{\text{W}}\right)\hat{H}_1 + \hat{H}_2^\dagger \exp\left(2g\hat{A}^a T^a + 2g'\hat{B}Y_{\text{W}}\right)\hat{H}_2 \right] \quad (385)$$

The only relevant contribution to the Higgs potential V_{HIGGS} descents from the expression

$$\hat{H}_1^\dagger \left(1 + 2g\hat{A}^a T^a + 2g'\hat{B}'Y_{\text{W}}\right)\hat{H}_1 + \hat{H}_2^\dagger \left(1 + 2g\hat{A}^a T^a + 2g'\hat{B}'Y_{\text{W}}\right)\hat{H}_2$$

obtained from the Taylor expansion of the exp; it generates (after some algebra)

$$F_{H_1}^\dagger F_{H_1} + F_{H_2}^\dagger F_{H_2} + H_1^\dagger (gD^a T^a + g'D'Y_{\text{W}})H_1 + H_2^\dagger (gD^a T^a + g'D'Y_{\text{W}})H_2 \quad (386)$$

The other terms are not important because they contain non-Higgs fields and do not affect V_{HIGGS}. The auxiliary fields $F_{H_1}^i$ and $F_{H_2}^i$ are connected to the Higgs fields H_1^k and H_2^k in the way

$$\begin{aligned} F_{H_1}^i &= -\mu\varepsilon^{ij} H_2^{*j} + \ldots \\ F_{H_2}^i &= \mu\varepsilon^{ij} H_1^{*j} + \ldots \end{aligned} \quad (387)$$

Similarly the (vector) auxiliary fields D^a and D':

$$\begin{aligned} D^a &= -g(H_1^\dagger T^a H_1 + H_2^\dagger T^a H_2) + \ldots \\ D' &= -g'(H_1^\dagger Y_{\text{W}} H_1 + H_2^\dagger Y_{\text{W}} H_2) + \ldots \end{aligned} \quad (388)$$

These statements can be derived from the sum of all the auxiliary fields in $\mathcal{L}_{\text{MSSM}}$ using the Euler-Lagrange equations. With the help of the table (1) we can rewrite (386) to the form

$$V_{\text{HIGGS}}^{(1)} = \mu^2 \left(H_1^\dagger H_1 + H_2^\dagger H_2\right) + g^2 (H_1^\dagger T^a H_1 + H_2^\dagger T^a H_2)^2 + \frac{g'^2}{4} \left(H_1^\dagger H_1 - H_2^\dagger H_2\right)^2 \quad (389)$$

(The minus sign was droped because of the conventional $-V$ in the Lagrangian.)

Next, let us investigate the $\mathcal{L}_{\text{GAUGE}}$ term. It can be proven (see for example [17]) that the only terms relevant for the Higgs potential construction are again only these involving auxiliary fields D^a and D':

$$\mathcal{L}_{\text{GAUGE}} = \frac{1}{2}\left(D^a D^a + D'^2\right) + \ldots \quad (390)$$

The bracket can be transformed using (387) and (388) into the second part of V_{HIGGS}

$$V_{\text{HIGGS}}^{(2)} = -\frac{g^2}{2}(H_1^\dagger T^a H_1 + H_2^\dagger T^a H_2)^2 - \frac{g'^2}{8}\left(H_1^\dagger H_1 - H_2^\dagger H_2\right)^2 \quad (391)$$

Next, the Lagrangian part $\mathcal{L}_{\text{SUPERPOT}}$ gives [14],[17]

$$\mathcal{L}_{\text{SUPERPOT}} = \mu\varepsilon^{ij}\left[H_1^i F_{H_2}^j + H_1^{i*} F_{H_2}^{*j} + H_2^j F_{H_1}^i + H_2^{j*} F_{H_1}^{*i}\right] + \ldots \quad (392)$$

Utilising (387) this contribution turns to be zero.

The last thing to be done is to calculate the part of the potential coming from the soft supersymmetry breaking term $\mathcal{L}_{\text{SM}}$. It is not so hard to obtain the three relevant terms:

$$\mathcal{L}_{\text{SM}} = -m_1^2 H_1^\dagger H_1 - m_2^2 H_2^\dagger H_2 + m_3^2 \varepsilon^{ij}\left(H_1^i H_2^j + h.c.\right) + \ldots \equiv -V_{\text{HIGGS}}^{(3)} + \ldots \quad (393)$$

Collecting the partial results (389),(391) and (393) we can conclude

$$\begin{aligned} V_{\text{HIGGS}} &= (m_1^2+\mu^2)H_1^\dagger H_1 + (m_2^2+\mu^2)H_2^\dagger H_2 - m_3^2\varepsilon^{ij}\left(H_1^i H_2^j + h.c.\right) + \\ &+ \frac{g^2}{2}(H_1^\dagger T^a H_1 + H_2^\dagger T^a H_2)^2 + \frac{g'^2}{8}\left(H_1^\dagger H_1 - H_2^\dagger H_2\right)^2 \end{aligned} \tag{394}$$

In the last step we can simplify this result using the explicit form of the T^a generators in the relevant two-dimensional representation of the $SU(2)_{\text{L}}$; these operators are proportional to the Pauli-matrices: $T^a = \frac{1}{2}\sigma^a$. Following [17] it is easy to obtain

$$\begin{aligned} V_{\text{HIGGS}} &= (m_1^2+\mu^2)H_1^\dagger H_1 + (m_2^2+\mu^2)H_2^\dagger H_2 - m_3^2\varepsilon^{ij}\left(H_1^i H_2^j + h.c.\right) + \\ &+ \frac{g^2}{2}\left|H_1^\dagger H_2\right|^2 + \frac{1}{8}\left(g^2+g'^2\right)\left(H_1^\dagger H_1 - H_2^\dagger H_2\right)^2 \end{aligned} \tag{395}$$

which concludes this Appendix.

References

[1] Aoki, K. et all , Supplement of the Progres of Theoretical Physics, **73**,1982.

[2] Bailin, D. and Love, A.: *Introduction to Gauge Field Theory*, IOP Publishing Ltd., Bristol 1986.

[3] Bailin D. and Love, A. : *Supersymmetric Gauge Field Theories*, IOP Publishing Ltd., Bristol 1986.

[4] Berger, Michael S.: *Radiative corrections to Higgs-boson-mass sum rules in the minimal supersymmetric extension to the standard model*, Physical Review D **41**,225.

[5] Cheng, T.P. and Li, L.F.: *Gauge Theory of Elementary Particle Physics*, Clarendon Press, Oxford 1991.

[6] Cheng, T.P., Eichten, E. and Li, L.F.: *Higgs phenomena in asymptotically free gauge theories*, Physical Review D**9**, 225 9 (1974).

[7] Gunion, J.F. and Haber, Howard E.: *Higgs bosons in supersymmetric models*, Nuclear Physics **B272**, 1-76 (1986).

[8] Gunion, J.F. and Turski, A.: *Renormalisation of Higgs-boson-mass sum rules and screening*, Physical Review **D39**, 2701 (1989).

[9] Gunion, John F. and Turski, A.: *Corrections to Higgs-boson-mass sum rules from the sfermion sector of a supersymmetric model*, Physical Review **D40**, 2333(1989).

[10] Haber, Howard E. :*How well can we predict the mass of the Higgs boson of the MSSM ?*, hep-ph/9901365.

[11] Haber, Howard E. and Kane, G.L.: *The search for supersymmetry: probing physics beyond the standard model*, Physics Reports **117**, 75 (1985).

[12] Heinimeyer, S., Hollik, W. and Weiglein, G.: *Precise prediction for the mass of the lightest Higgs boson in the MSSM*, hep-ph/9807423

[13] Hořejší, Jiří: *Introduction to Electroweak Unification*, World Scientific, Singapore 1994.

[14] Kuroda,M.: *Complete Lagrangian of the MSSM*, hep-ph/9902340

[15] Review of Particle Properties, Physical Review **D54**, 1 (1996)

[16] Ryder, Lewis H.: *Quantum Field Theory*, 2nd edition. Cambridge Unversity Press, 1996.

[17] Simonsen, I. : *A review of the MSSM*, hep-ph/9506369.

[18] Wess, J., Bagger, J.: *Supersymmetry and Supergravity*, 2nd edition, Princeton University Press, Princeton, New Jersey 1992.

[19] Weinberg, Stephen: *The Quantum Theory of Fields*, Cambridge University Press, Cambridge 1995.

[20] Okada, Y., Yamaguchi, M. and Yanagida, T.: *Renormalisation group analysis of the Higgs mass in the softly broken supersymmetric SM*; Physics Letters **B262**, 54 (1991).

[21] DELPHI Collaboration; *Search for neutral Higgs bosons in* e^+e^- *collisions at* $\sqrt{s} = 183\ GeV$, CERN-EP/99-06.